ABSTRACT

Title of Dissertation:	ANTAGONIZING JAK-STAT SIGNALING BY PORCINE REPRODUCTIVE AND RESPIRATORY SYNDROME VIRUS
	Liping Yang, Doctor of Philosophy, 2018
Dissertation directed by:	Associate Professor Yanjin Zhang Department of Veterinary Medicine

The Janus kinase (JAK)-signal transducer and activator of transcription (STAT) signaling pathway is activated by numerous cytokines. JAK-STAT pathways involve in regulation of cell growth, proliferation, differentiation, apoptosis, angiogenesis, immunity and inflammatory response. Because of their significance in immune response, they are often targeted by pathogens, including porcine reproductive and respiratory syndrome virus (PRRSV). PRRSV causes reproductive failure in sows and severe respiratory disease in pigs of all ages. A typical feature of the immune response to PRRSV infection in pigs is delayed production and low titer of virus neutralizing antibodies, and weak cell-mediated immune response. One possible reason for the weak protective immune response is that PRRSV interferes with innate immunity and modulates cytokine signaling, including JAK-STAT pathways. The objective of this project was to elucidate the mechanisms of PRRSV interference with JAK-STAT2 and JAK-STAT3 signaling. This study demonstrates that PRRSV

antagonizes interferon (IFN)-activated JAK-STAT2 signaling and oncostatin M (OSM)-activated JAK-STAT3 pathway via inducing STAT2 and STAT3 degradation. Mechanistically, PRRSV non-structural protein 11 (nsp11) and nsp5 induce the degradation of STAT2 and STAT3, respectively, via the ubiquitin-proteasome pathway. Notably, PRRSV manipulates karyopherin alpha 6 (KPNA6), an importin that is responsible for STAT3 nuclear translocation in the JAK-STAT signaling, to facilitate viral replication. Knockdown of KPNA6 expression led to significant reduction in PRRSV replication. These data demonstrate that PRRSV interferes with different JAK-STAT pathways to evade host antiviral response while harnessing cellular factors for its own replication. These findings provide new insights into PRRSV-cell interactions and its molecular pathogenesis in interference with the host immune response, and facilitate the development of novel antiviral therapeutics.

ANTAGONIZING JAK-STAT SIGNALING BY PORCINE REPRODUCTIVE AND RESPIRATORY SYNDROME VIRUS

by

Liping Yang

Dissertation submitted to the Faculty of the Graduate School of the
University of Maryland, College Park, in partial fulfillment
of the requirements for the degree of
Doctor of Philosophy
2018

Advisory Committee:
Associate Professor Yanjin Zhang, Chair
Professor Jeffrey DeStefano
Professor Siba K. Samal
Associate Professor Georgiy A. Belov
Assistant Professor Shin-Hee Kim

Preface

This dissertation is original and based on independent work conducted by the author Liping Yang under the supervision of Dr. Yanjin Zhang at the University of Maryland, College Park, MD from 2013 to 2018.

There are seven chapters in the dissertation. The first three chapters focus on literature review of PRRSV, JAK-STAT signaling and nucleocytoplasmic trafficking system, respectively. The next three chapters present research results on PRRSV interference with JAK-STAT signaling and manipulation of KPNA6 for its own replication. The last chapter is conclusion and future perspectives. Other research has also been done during my Ph.D. studies but not included in this dissertation due to scope. Readers interested can follow my publications.

Dedication

To my father Zhonghua Yang and my mother Suorong Meng, who raise me up and help me shape my personality and establish right outlook on life and values. During the past five years, my parents encouraged me to overcome difficulties and move forward towards my goal. They provided support whenever I need.

To my advisor, Dr. Yanjin Zhang, who not only instructs me how to do research and think logically, but also teaches me to face obstacles and solve problems imperturbably.

Acknowledgements

I express my sincere gratitude to my advisor Dr. Yanjin Zhang for his continuous support to my Ph.D. study and related research, for his patience, motivation, and immense knowledge. He is a wonderful mentor, collaborator, and friend. His guidance helped me in all the research and writing of this thesis. I could not imagine having a better advisor and mentor for my Ph.D. study.

Besides my advisor, I thank my committee members: Drs. DeStefano, Samal, Belov, and Kim for their insightful advice and help.

My sincere thanks also go to Drs. Frank Li, Qiyi Tang, and Ying Fang for their gifts of some research materials used in this project. I thank Drs. David Mosser, Jonathan Dinman, Xiaoping Zhu, Meiqing Shi, Utpal Pal, Daniel Nelson and John Patton for teaching me valuable knowledge to broaden my horizon.

Furthermore, I thank all the faculty and staff members in the Department of Veterinary Medicine.

Last but not least, I am grateful to my family and friends. My parents, my grandma, my elder sister, and my aunt have given me immense help and encouragement, especially when I have difficulties. With the company of my boyfriend Mengfei Peng, I get over challenges and live happily. I thank my friend Jia He for her help in both life and work.

Table of Contents

List of Tables

List of Figures

List of Abbreviations

3CLSP, 3C-like serine protease

3-MA, 3-methyladenine

ADCC, antibody-dependent cell-mediated cytotoxicity

AP-1, activation protein 1

Arm, armadillo

BIR, baculovirus inhibitor repeat

BM-imDC, bone marrow-derived immature dendritic cell

CARD, caspase-recruiting domain

CAS, cellular apoptosis susceptibility

CBP, CREB-binding protein

CCD, coil-coil domain

CHX, cycloheximide

cNLS, classical NLS

CTD, C-terminal domain

CTL, cytotoxic T cell

CVB3, coxsackievirus B3 virus

DAPI, 4’6’-diamidino-2-phenylindole

DC, dendritic cell

DDX, DEAD box helicase

DENV, Dengue virus

DMEM, Dulbecco’s Modified Eagle Medium

DMV, double-membrane vesicles

DUB, deubiquitinating enzyme

EAV, equine viral arteritis

EBV, Epstein-Barr virus

EM, electron microscopic

ER, endoplasmic reticulum

FADD, Fas-associated-death-domain

FBS, fetal bovine serum

GBS, Guillain-Barre syndrome

GM-CSF, granulocyte macrophage colony-stimulating factor

Gp130, glycoprotein 130

gRNA, guide RNA

HA, hemagglutinin

HBV, hepatitis B virus

HCV, hepatitis C virus

HEL, helicase

HMGB1, high mobility group box 1

hpi, hours post infection

hpt, hours post transfection

HPAI, Highly pathogenic avian influenza

HSV-1, herpes simplex virus-1

HV, hypervariable

IBB, importin β-binding

IFA, immunofluorescence assay

IFN, interferon

IKKε, IκB kinase epsilon

IN, integrase

IL, interleukin

IP, immunoprecipitation

IRF, interferon regulatory factor

ISG, interferon-stimulated genes

ISGF3, interferon-stimulated gene factor 3

ISRE, interferon-stimulated response element

JAK, janus kinase

K63, lysine 63

keap1, Kelch-like ECH-associated protein 1

KPNA, karyopherin α

KPNB, karyopherin β

KV, killed virus

L-DC, lung dendritic cells

LCTD, linker domain with C-terminal domain

LDV, lactate dehydrogenase elevating virus

LGP2, laboratory of genetics and physiology 2

LIF, leukemia inhibitory factor

LPS, lipopolysaccharide

LRR, leucine-rich repeat

MA, matrix

MAPK, mitogen-activated protein kinase

MAVS, mitochondrial antiviral signaling protein

MDa, megadaltons

MDA5, melanoma differentiation-associated gene 5

MDDC, monocyte-derived dendritic cell

MEM, Minimum Essential Media

MHC, Major histocompatibility complex

MLV, modified-live virus

MOI, multiplicities of infection

Nab, neutralizing antibody

NAP1, NAK-associated protein 1

NEMO, NF-κB essential modulator

NendoU, nidovirus uridylate-specific endoribonuclease

NES, nuclear export signal

NF-κB, nuclear factor κB

NK, natural killer

NLR, nucleotide oligomerization domain-containing protein-like receptor

NLS, nuclear localization signals

NOD, nucleotide oligomerization domain

NoRS/-LS, nucleolar retention/localization signal

NP, nucleoprotein

NPC, nuclear pore complex

NPI, nucleoprotein interact

NPM, nucleoplasmin

Nrf2, nuclear factor erythroid 2-related factor 2

Nsp, non-structural protein

NTD, N-terminal domain

NTDL, NTD with linker domain

Nup, nucleoporins

ORF, open reading frames

OSM, oncostatin M

OUT, ovarian tumor domain

PAM, pulmonary alveolar macrophages

PAMP, pathogen-associated molecular patterns

PBMC, peripheral blood mononuclear cell

PCD, programmed cell death

PCP, papain-like cysteine protease

PEDV, porcine epidemic diarrhea virus

PI3K, phosphatidylinositol-3-kinase

PKCδ, protein kinase δ

PKR, protein kinase R

PLP2, putative cysteine protease domain

PRF, programmed ribosomal frameshift

PRR, pattern-recognition receptors

PRRS, porcine reproductive and respiratory syndrome

PRRSV, porcine reproductive and respiratory syndrome virus

pSTAT1, phosphorylated STAT1

PYD, pyrin domain

Ran, Ras-related GTPase

RB, retinoblastoma

RCC, regulator of chromosome condensation

Rch1, Rag cohort 1

RdRp, RNA-dependent RNA polymerase

RIG-G, retinoic acid-induced gene G

RIG-I, retinoic acid–inducible gene I

RIP1, receptor interacting protein 1

RNP, ribonucleoprotein

ROS, reactive oxygen species

RPL32, ribosomal protein L32

RT, reverse transcriptase

RT-qPCR, reverse transcription and real-time PCR

RTC, replication and transcription complex

sgRNA, sub-genomic RNA

SH2, Src homology 2

SHFV, simian hemorrhagic fever virus

SLA-I, swine leukocyte antigen class I

SOCS, suppressor of cytokine signaling

SRP1, serine-rich protein 1

ssRNA, single-stranded viral RNA

STAT, signal transducer and activator of transcription

STING, stimulator of interferon genes

TANK, TRAF family member-associated NF-κB activator

TBK1, TANK-binding kinase 1

TCID50, the median tissue culture infectious dose

Th17, T helper 17

TIR, Toll/interleukin-1 receptor

TLR, Toll-like receptor

TNF, tumor necrosis factor

TRAF, tumor necrosis factor receptor-associated factor

Treg, regulatory T cell

TRS, transcription-regulatory sequences

TYK, tyrosine kinase

UTR, untranslated region

WB, western blot

ZF, zinc finger

ZIKV, Zika virus

+ssRNA, positive-sense single-stranded RNA

Chapter 1: Porcine reproductive and respiratory syndrome virus

Introduction

Porcine reproductive and respiratory syndrome (PPRS) is a contagious disease, which leads to severe respiratory disorder, poor growth condition with weight loss in pigs of all ages, and reproductive failure in sows (1). PRRS has been the most costly viral disease for swine industry with an estimated annual loss of $664 million in the United States (2), and an average loss of 126 €/sow in Europe (3). The disease was first reported in 1987 in North America and soon recognized in Europe and other regions. The causative agent, PRRS virus (PRRSV), was first isolated and characterized in Europe in 1991, recently reclassified as species *PRRSV-1*, followed by successful isolation of a *PRRSV-2* strain in the United States (4, 5). PRRSV remains highly prevalent in swine farms across the globe with a few exceptions like Australia and New Zealand, although PRRS vaccines have been widely used since the mid-1990s. Highly effective vaccines or antiviral drugs against PRRSV are still not available due to the meager protective immune response induced by PRRSV infection and the large genetic and antigenic variations among PRRSV strains. Therefore, more studies are needed to further characterize PRRSV biology, virus-cell interactions, pathogenesis and mechanisms of PRRSV evasion of the host immune response as well as interference with cell signaling to facilitate the development of improved vaccines or therapeutics for PRRS control.

PRRSV classification

PRRSV is a small, enveloped single-stranded positive-sense RNA virus with a particle size ranging from 50-80 nm. It belongs to the genus *Porartevirus*, the family *Arteriviridae*, the order *Nidovirales* (6). The *Arteriviridae* is composed of five genera: *Dipartevirus, Equartevirus, Nesartevirus, Porartevirus*, and *Simartevirus* (7). The other previously known members of the *Arteriviridae* are simian

hemorrhagic fever virus (SHFV, a member of *Simartevirus*), equine viral arteritis (EAV, a member of *Equartevirus*), and lactate dehydrogenase elevating virus (LDV, a member of *Porartevirus*). PRRSV strains are highly divergent. PRRSV has been well known to have two genotypes: Type 1 (European PRRSV, the prototype is Lelystad virus) and Type 2 (North American PRRSV, the prototype is VR-2332). Recently, the two genotypes are reclassified into two species: *PRRSV-1* and *PRRSV-2* in the genus *Porartevirus*. The overall clinical signs, disease phenotype, virion structure, genomic organization, genetic elements, and replication cycle of *PRRSV-1* and *PRRSV-2* strains are all similar though they only share less than 60% genomic nucleotide identity (8).

PRRSV morphology

Electron microscopic (EM) studies show that purified extracellular PRRSV virions are mostly spherical or oval-shaped particles with smooth outer appearance, which are similar to other arteriviruses (9). The virion contains an isometric core with a mean diameter of 39 nm. Inside the core is PRRSV genomic RNA capsulated by nucleocapsid proteins with asymmetric and linear arrangement (10). Cryo-

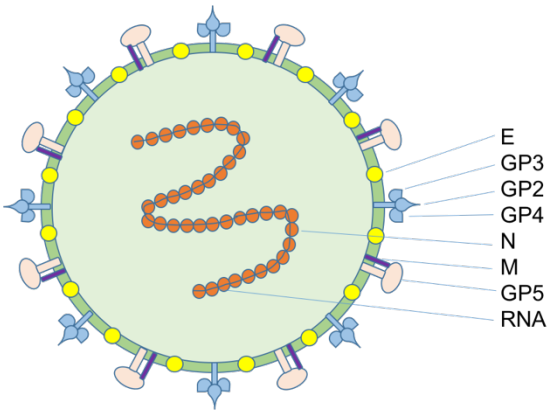

Fig. 1.1 Schematic illustration of PRRSV virion. Seven virion-associated proteins and genomic RNA in PRRSV are depicted: E, minor non-glycosylated membrane protein; GP2, GP3, and GP4, minor envelope glycoproteins; N: nucleocapsid protein; M: matrix protein; GP5, major envelope glycoprotein.

EM displays the visible lipid bilayer of the envelope and shows its thickness is 4.5 nm, which may include the endodomains of envelope proteins and other membrane proteins, especially M and GP5

proteins. Moreover, there are 10-15 nm protrusions on the envelope. Based on the shape and size, the heterotrimer formed by GP2, GP3, and GP4 may account for the protrusions. The heterotrimer complex in the virion may play a critical role in the PRRSV binding and entry of target cells. The structure of PRRSV virion is schematically illustrated in Fig. 1.1.

PRRSV genome

PRRSV virion contains a linear, non-segmented single-stranded positive-sense RNA genome with a size of approximately 15 kb. The RNA genome carries a methylated cap at the 5' end and a polyadenylated tail at the 3' end. Over ten open reading frames (ORFs) have been identified in the PRRSV genome, illustrated in Fig. 1.2. About 80% of the PRRSV genome is composed of ORF1a and

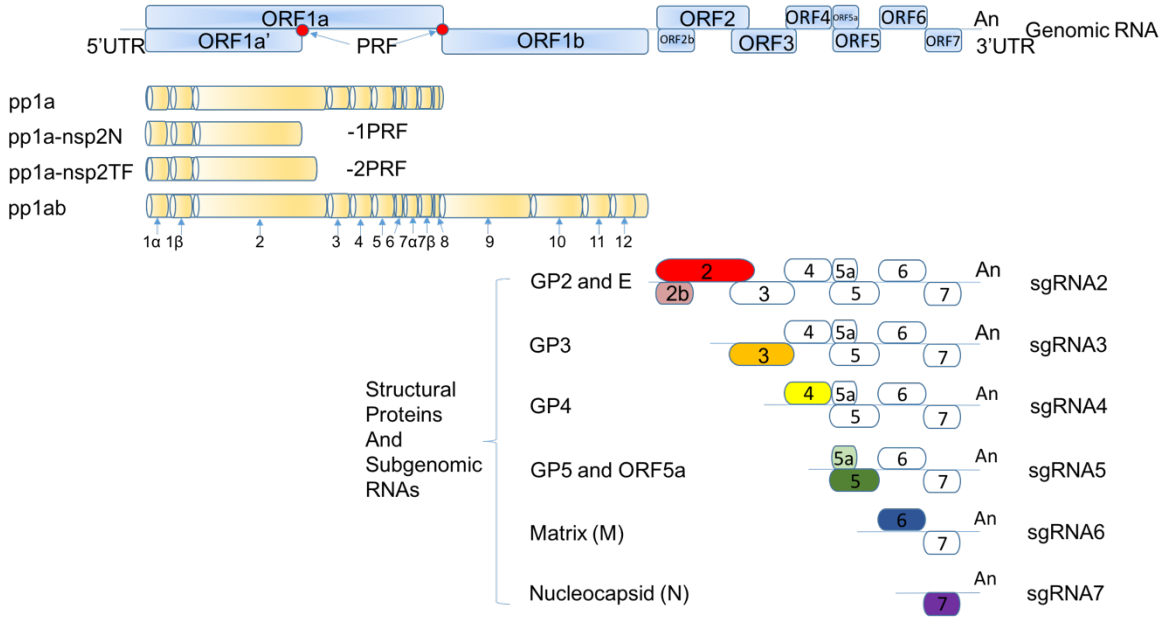

Fig. 1.2 Schematic illustration of PRRSV genome, transcription and translation. The open reading frames (ORFs), 5′ UTR, 3′ poly A tail (An), programmed ribosomal frameshift (PRF) of the ORF1a/1b are indicated on top row. Replicase polyproteins pp1a and pp1ab are translated from ORF1a and 1ab, respectively. The pp1a-nsp2N and pp1a-nsp2TF are generated transcripts by -1 and -2 PRF, respectively. These polyproteins are cleaved to generate at least 14 nonstructural proteins (indicated by arrows) by viral proteinases. Structural proteins and subgenomic RNAs are also depicted.

ORF1b encoding two replicase polyproteins pp1a and pp1ab, translated by a -1 programmed ribosomal

frameshift (PRF) signal in the ORF1a/ORF1b overlap area. Then they are proteolytically cleaved into 14 nonstructural proteins (nsps) from nsp1α to nsp12 by viral proteases (11). Nsp1, nsp2, and nsp4 are three different proteases. Both nsp1 and nsp2 contain a papain-like cysteine protease domain, and nsp4 is a 3C-like serine protease. Nsp3 and nsp5 are transmembrane proteins. It has been demonstrated that nsp9 encodes the viral RNA-dependent RNA polymerase (RdRp) and nsp10 is a helicase, which are responsible for the viral genome replication and transcription (11). Nsp11 has been shown to play a critical role in the replication cycle of all arteriviruses due to its endoribonuclease domain (12). In addition, nsp1β is a transactivator to induce -2/-1 PRF in nsp2, leading to the expression of two novel proteins: nsp2TF and nsp2N (13, 14). These two proteins have been demonstrated to be important in inhibiting the host innate immune response (15).

Structural proteins are encoded by ORFs 2-7 located at the 3' end of the PRRSV genome (16-18). ORFs 2, 3, and 4 encode minor membrane-associated proteins GP2, GP3, and GP4, respectively. These proteins interact with each other to assemble as a heterotrimeric complex, which plays a role in viral entry (19). ORF2b, a small ORF embedded in ORF2 sequence in a different reading frame, encodes a 10-kDa, non-glycosylated protein named E (18). ORF5 encodes the major envelope glycoprotein (GP5), which interacts with the matrix protein (M) encoded by ORF6, forming a heterodimer. It is believed that the heterodimer is critical in PRRSV attachment and internalization (11). ORF7 encodes N protein that is associated with PRRSV genomic RNA to form the nucleocapsid (16). GP5, M, and N are the major components of the viral particles. Furthermore, a polypeptide of 51 amino acids encoded by ORF5a is referred as the ORF5a protein, which is highly conserved among diverse PRRSV strains (20).

PRRSV tropism

Pig is the only known natural host for PRRSV infection. PRRSV has a very restricted cell tropism both *in vivo* and *in vitro*. *In vivo*, PRRSV targets certain subpopulations of swine

monocyte/macrophage lineage, mainly pulmonary alveolar macrophages (PAMs) (21). PAMs are important effector immune cells of the innate immune system against invading pathogens in lung (22).

Some studies show that monocyte-derived dendritic cells (MDDCs) and bone marrow-derived immature dendritic cells (BM-imDCs) are susceptible to PRRSV infection (23, 24). However, the primary lung dendritic cells (L-DCs) are not permissive to PRRSV (25). Even though MDDCs share many common features of primary DCs, they still preserve certain original characteristics of monocytes which contribute to their susceptibility to PRRSV (26). Therefore, further studies are required to investigate the permissibility of DCs on PRRSV infection. Moreover, during the persistence of PRRSV infection, tonsils, lungs, and lymphoid organs are the major source of viral RNA in pigs (27).

In vitro, the African green monkey kidney cell MA-104 and its derivatives MARC-145, CL-2621, and CRL11171 are used to propagate PRRSV and explore the interaction between PRRSV and host cells (5, 28, 29). Immortalized PAMs and other porcine-derived cells such as PK15 with overexpression of CD163, the main PRRSV receptor, have been used for PRRSV propagation. BHK21 with overexpression of CD163 has been used for PRRSV proliferation and vaccine production (30).

PRRSV replication cycle

PRRSV entry

The restricted cell tropism of PRRSV is attributed to some entry factors in the host cells, because some non-permissive cell lines could support the replication of PRRSV once they are transfected with the infectious cDNA clone (31). Several cellular proteins that play roles in PRRSV entry have been identified.

The first identified entry factor for PRRSV is heparin-like molecules (32). Incubation of PRRSV with heparin prior to infecting the cells inhibits the viral infection. Moreover, treating the host cells with heparinase I before inoculation with PRRSV reduces the infection rate. Both results indicate the critical

role of heparin-like molecules on PRRSV entry. In 2002, heparan sulfate proteoglycans were identified in binding with M/GP5 protein complex of PRRSV to mediate PRRSV entry into PAM cells (33).

However, heparan sulfate proteoglycans are present on the surface of most mammalian cells, including monocytes/macrophages. Moreover, incubation of PRRSV with heparin or heparan sulphate could not completely block PRRSV infection. These findings indicate that other host factors are associated with facilitating PRRSV attachment and entry into the host cells (34).

Sialoadhesin (CD169) was then identified by immunoprecipitation using the antibody that could block PRRSV infection (35-37). Sialoadhesin is a transmembrane glycoprotein on the surface of macrophages, and belongs to the siglecs family of sialic acid-binding lectins (38). Sialoadhesin was demonstrated to promote the internalization of PRRSV by interacting with M/GP5 complex (39), followed by clathrin-mediated endocytosis (40). However, overexpression of porcine sialoadhesin in unsusceptible cells does not support uncoating, genomic RNA release, and efficient infection, which suggests additional macrophage-specific entry factors are required for PRRSV infection (37).

Other critical entry mediators were not reported until 2007 (30). The overexpression of transmembrane glycoprotein CD163 makes the non-permissive cells be susceptible to PRRSV. Incubation of host cells with CD163-specific antibody at 37 °C, but not at 4 °C, inhibits PRRSV infection dramatically, indicating that CD163 is not involved in the attachment of PRRSV on the cell surface but later steps (41). The experiment with the presence or absence of sialoadhesin demonstrated that sialoadhesin is responsible for the attachment and internalization of PRRSV virions, while CD163 is critical for the capsid uncoating and genomic RNA release, both of which are crucial for the productive infection of PRRSV. However, the mechanism of CD163 promoting the uncoating still remains unknown (26).

PRRSV replication

After entering the cells via clathrin-mediated endocytosis, PRRSV releases the viral genomic RNA into the cytoplasm following the fusion of viral envelope with the endosomal membrane and uncoating of nucleocapsid by endosome acidification. The genomic RNA is directly translated into the

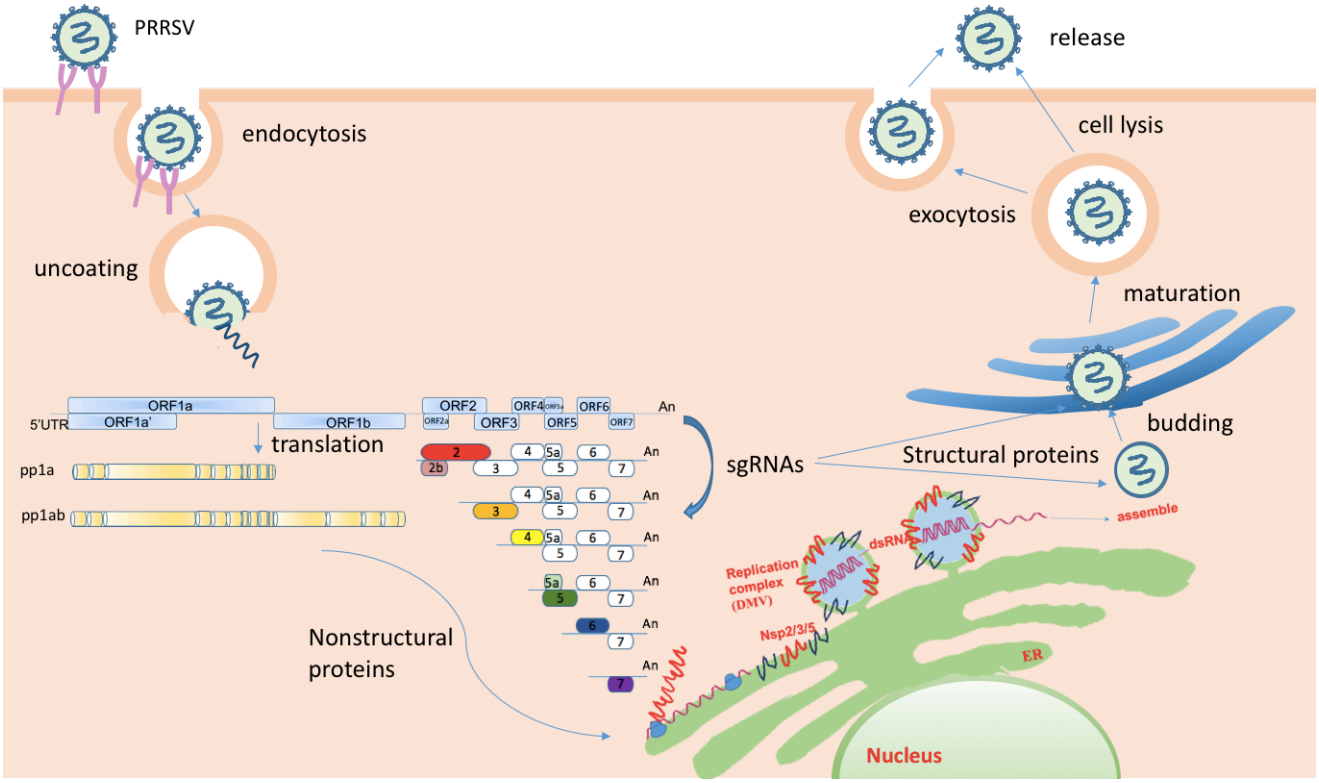

Fig. 1.3 Schematic illustration of PRRSV replication cycle. PRRSV enters cells by receptor-mediated endocytosis and releases its genomic RNA into the cytoplasm by endosome acidification. After translation and cleavage, nsp2, nsp3 and nsp5 induce ER membrane rearrangement to form double-membrane vesicles (DMV) for double-stranded (ds) RNA synthesis. The newly synthesized viral genome and structural proteins encoded by sub-genomic RNAs assemble into new virions, followed by budding, and maturation, and release via exocytosis or cell lysis.

replicase polyproteins pp1a and pp1ab, generating individual non-structural proteins by proteolytic cleavage. The membrane-associated nsps including nsp2, nsp3, and nsp5 induce the membrane rearrangement of endoplasmic reticulum (ER) to form double-membrane vesicles (DMV), which is also known as the replication and transcription complex (RTC) (12, 42, 43). The RTC formation ensures the

efficiency of viral replication and evades the cellular pattern recognition receptors and consequent antiviral response.

The RTC allows the synthesis of new genomic RNA and minus-strand RNA, which is used as the template for the generation of sub-genomic RNAs (sgRNAs) to express structural proteins. The sgRNAs are composed of the identical 5′ leader sequence derived from the 5′ untranslated region (UTR) of viral genomic RNA, and a common 3′-poly(A) tail, to form a 5′- and 3′-coterminal nested set of transcripts (44). The individual ORFs that encode the viral structural proteins have partially overlapping sequences in different frames and located at the 3′ end of the PRRSV genome. It has been demonstrated that the nested set sgRNAs are generated by discontinuous transcription during the synthesis of minus-strand RNAs, mediated by specific RNA signals, transcription-regulatory sequences (TRS) (45). Each sgRNA expresses at least the first ORF for a structural protein (Fig. 1.2). The newly synthesized viral genome and structural proteins assemble into new virions through encapsidation, budding, and maturation before released via exocytosis or cell lysis (46). The replication cycle of PRRSV is illustrated in Fig. 1.3.

PRRSV pathogenesis

PRRS causes reproductive disease manifested as a high abortion rate, premature or delayed farrowing, and the increasing number of mummified, stillborn and weak-born piglets. Inappetence, reluctance to drink and agalactia occurring during the farrowing and lactating period, resulting in increased mortality of suckling piglets. PRRSV infection also causes postweaning respiratory disease. The infected suckling piglets develop severe macroscopic lung lesions. Histopathologic examination and microscopic lesions analysis show necrotizing interstitial pneumonia, arteritis, encephalitis, and myocarditis (47, 48).

PRRSV infection is also characterized by prolonged viremia up to one month followed by persistent viral replication in regional lymph nodes for as long as 250 days (49). Experimental studies

have shown that subclinical PRRSV infection persists in pigs (50). PRRSV uses a variety of strategies to antagonize the host immune responses, which results in the prolonged viremia and persistent infection. Therefore, persistent infection of PRRSV plays a critical role in PRRSV survival and transmission, and becomes a big challenge in PRRS control. Typical features of the immune responses to PRRSV infection in pigs include delayed production and low titer of virus neutralizing antibodies and weak cell-mediated immune response (51, 52).

PRRSV effect on apoptosis and autophagy

Programmed cell death (PCD) is considered as one of the first line host defense strategies against viral infection. Different from the innate and adaptive immunity effectors, PCD is cellular-based and its effectors are generally expressed constitutively, not relying on virus-stimulated signaling (53).

Apoptosis is a well-known form of PCD mediated by intracellular programs. It is a highly regulated and controlled process during growth and development for maintenance of a homeostatic condition in tissues. Apoptosis occurs once cells are damaged by pathogens or toxins in order to eliminate the unhealthy cells and the invasive pathogens (54).

During the early phase of apoptosis, cell shrinkage is visible under microscope, followed by pyknosis resulting from chromatin condensation which is the most typical feature of apoptosis. The shrank cells are divided into apoptotic bodies by the blebbing of the plasma membrane during a process named “budding” (54). Phagocytic cells then phagocytose the apoptotic bodies to avoid the unnecessary damage of surrounding cells.

Autophagy is a conserved, regulated, and destructive metabolic process to maintain cellular homeostasis by disassembling, degrading, and recycling dysfunctional, damaged, or unnecessary cellular components, such as damaged organelles and protein aggregates (55). Autophagy has distinct roles under various cellular conditions. In response to nutrient deficiency, autophagy is induced to ensure cell survival. Xenophagy is a form of autophagic degradation of infectious particles such as *Mycobacterium*

tuberculosis. Stimulation of autophagy could defeat the pathogen by inducing the maturation of phagolysosome (56). However, excessive autophagy can cause cell death morphologically different from apoptosis.

Since apoptosis can eliminate virus or limit viral infection by destructing viral infected cells, and autophagy can devastate the intracellular pathogens, many pathogens especially viruses including PRRSV have evolved to evade or even take advantage of these processes for their survival and infection.

In its initial phase of infection, PRRSV has been reported to induce anti-apoptotic activity. GP2 protein has been shown to delay the process of apoptosis by modulating transcription factors nuclear factor κB (NF-κB) and activation protein 1 (AP-1) (57). On the other hand, PRRSV activates phosphatidylinositol-3-kinase (PI3K)/Akt1 signaling for the phosphorylation of BAD, a pro-apoptotic protein, in order to delay apoptosis (58). Moreover, inhibition of autophagy by 3-methyladenine (3-MA) resulted in a significant increase of apoptosis induced by PRRSV, indicating a potential link between autophagy and apoptosis (59). PRRSV also facilitates the interaction between BAD and Beclin1, an autophagy regulator, to postpone apoptosis. In summary, inhibition of apoptotic cell death provides PRRSV enough time for replication, assembly and the generation of large quantities of progeny virions.

Nuclear condensation, DNA fragmentation, and PARP cleavage normally occur in PRRSV-infected cells between 36 to 48 hours post infection (hpi) *in vitro*, indicating that PRRSV can induce apoptosis at late stage (60). Furthermore, both intrinsic and extrinsic pathways are involved in the apoptotic activity induced by PRRSV. The inhibition of reactive oxygen species (ROS) has been shown to suppress the cleavage of PRRSV infection-induced PARP, which indicates that ROS could serve as an inducer of apoptosis through the intrinsic pathway during PRRSV infection (61). PRRSV infection disrupts the membrane of mitochondria by upregulating Bax protein to release cytochrome *c*, followed by caspase-9 activation. In addition, tumor necrosis factor (TNF)-α (62) and GP5 (63) released from PRRSV-infected cells have been implicated to be associated with apoptotic activity of "bystander cells"

in vivo. GP5 can enhance caspase 3 activity to induce apoptosis *in vitro* (64). E protein has been demonstrated to induce apoptosis through interacting with mitochondrial proteins ATP5A to suppress the production of ATP (65). Moreover, nsp4 and nsp10 are capable of triggering apoptotic process by activating the pro-apoptotic proteins Bim and Bid, respectively (66). In addition, nsp5 has been shown to induce autophagy by some unknown mechanism (67).

In conclusion, PRRSV is able to manipulate and take advantage of the host machineries for its own replication and survival through inducing anti-apoptotic, autophagic, and pro-apoptotic activities in different context. However, the interplay between PRRSV and apoptosis/autophagy is so complicated that more studies are needed to examine the mechanisms in whole virus infection *in vivo* and *in vitro*.

PRRSV inhibits the host innate immune response

The innate immunity is the early line host defense to prevent, control, and eliminate infections by pathogens. Innate immune responses are immediate and do not require prior exposure to the pathogens. The host innate immune system consists of three major components: (1) physical and chemical barriers such as skin and the gastrointestinal and respiratory tracts; (2) phagocytic cells, dendritic cells (DCs), natural killer (NK) cells, and other innate lymphoid cells; and (3) cell-free soluble factors, including the inflammatory cytokines and the complement system (68). Cytokines are a broad and loose category of small secreted proteins with a variety of structures and functions. Cytokines that are produced at the site of infection stimulate and coordinate the innate and adaptive immunity against invading pathogens. They act through their specific receptors on the surface of target cells, followed by cascades of intracellular signaling.

The innate immunity protects the host against viruses through two major types of responses: antiviral defense and inflammation, initiated by host pattern-recognition receptors (PRRs). PRRs are expressed in innate immune cells, such as DCs and macrophages, and other types of cells (69). PRRs recognize pathogen-associated molecular patterns (PAMP), such as viral genomic DNA and RNA,

distinct from cellular nucleic acids. Upon interaction with the viral PAMPs, PRRs initiate signal transduction pathways to activate the production of interferons and proinflammatory cytokines (70, 71).

Toll-like receptors

In mammalian cells, there are several distinct classes of cellular PRRs that differ in their structure, specificity for different PAMPs, and functions. Among the PRRs, Toll-like receptors (TLRs) are the best characterized. TLRs are type I integral transmembrane glycoproteins and expressed on many cell types. TLRs contain leucine-rich repeats (LRR) and cysteine-rich motifs in their extracellular portion for ligand binding, and a Toll/interleukin-1 receptor (TIR) homology domain in the cytoplasmic regions involved in intracellular signaling cascades (72). More than ten different functional TLRs in human and murine cells have been reported and are named as TLR1 through TLR10 (73-77). Different TLRs recognize distinct ligands with diverse structures covering all molecules derived from microorganisms. For virus recognition, TLRs 3, 7, 8, and 9 play critical roles, which are expressed on the membrane of intracellular compartments, such as endosomes, where they detect nucleic acids from microbial source. TLR3 interacts with dsRNA (78), whereas, TLR7 and TLR8 recognizes single-stranded viral RNA (ssRNA) (79). TLR9 detects the unmethylated CpG DNA of bacterial or viral genomes (75).

The recognition of PAMPs leads to the dimerization of TLRs, followed by recruitment of TIR domain-containing adaptor proteins including MYD88, TRIF, TIRAP, and TRAM (80). Then the complexes further recruit and activate multiple protein kinases to induce the activation of various transcription factors such as NF-κB, AP1, interferon regulatory factor 3 (IRF3), and IRF7 (81, 82). The activated transcription factors translocate into the nucleus to promote the transcription of genes for antiviral and inflammatory response. NF-κB and AP-1 control the expression of inflammatory cytokines, chemokines, and genes related to adaptive immunity, for example, interleukin (IL)-1β, IL-6, TNF,

CCL2, and CD80 (81). IRF3 and IRF7 are critical factors in producing type I interferons (IFN-α and IFN-β), the key mediators in host immune response against viral infection (83).

RIG-I-like receptors

Besides TLR3, 7, 8, and 9 who are membrane-associated receptors, RIG-I-like receptors (RLRs) also recognize virus nucleic acids but by acting as the cytosolic sensors. RLRs recognize dsRNA and ssRNA of RNA viruses. RIG-I (retinoic acid–inducible gene I) and MDA5 (melanoma differentiation-associated gene 5) are two of the well-studied RLRs (84, 85). Both RIG-I and MDA-5 contain two tandem N-terminal caspase-recruiting domains (CARDs), a DExD/H-box helicase domain, and a C-terminal domain (CTD). The CARDs are required for interacting and activating downstream signaling proteins, and the helicase domain is responsible for recognizing viral nucleic acids (86). RIG-I and MDA5 recognize complementary sets of viral ribonucleic acids. RIG-I typically recognizes short 5′-triphosphorylated or 5′-diphosphorylated blunt ends of viral ssRNA or dsRNA, whereas MDA5 is activated by long dsRNA with no end specificity (87). Laboratory of genetics and physiology 2 (LGP2), another member of RLR family, also binds with dsRNA but lacks CARD for signaling transduction. Therefore, LGP2 is suggested to be a negative regulator by sequestering dsRNA from RLRs (88).

After recognition of the ligands, RIG-I and MDA5 are ubiquitinated with lysine 63 (K63)-linked polyubiquitin chains to the CARDs via the E3 ubiquitin ligases (89). This modification leads to their homotetramerization and activating mitochondrial antiviral signaling protein (MAVS) on the mitochondrial membrane (90). MAVS is then dimerized and associated with multiple adaptor proteins such as TRADD, Tumor Necrosis Factor Receptor-associated Factor (TRAF)-2, TRAF-6, and TRAF-3 (91), followed by recruiting TRAF family member-associated NF-κB activator (TANK) and NAK-associated protein 1 (NAP1) (92) to induce the activation of TANK-binding kinase 1 (TBK1), IκB kinase epsilon (IKKε), and a DEAD box helicase DDX3 (93). These kinases phosphorylate IRF3 and IRF7, followed by the homodimerization and translocation of IRF3 and IRF7 into the nucleus to induce

the production of type I IFNs. MAVS also interacts with Fas-associated-death-domain (FADD) and receptor interacting protein 1 (RIP1) to activate the NF-κB pathway for expression of pro-inflammatory cytokines (94).

Nod-like receptors

NOD (nucleotide oligomerization domain-containing protein)-like receptors (NLRs) are a specialized group of cytosolic receptors recognizing PAMPs and other danger signals for activation of inflammatory signaling pathways (95).

The NLR family consists of 22 different proteins in human and at least 33 genes in mice. Typical NLR proteins are defined by a tripartite structure composed of three different domains with distinct functions. The sensor domain is a C-terminal LRR similar with TLR, which is responsible for sensing and interacting with the ligands. NOD domain locates in the middle and mediates oligomerization with another NLR during activation. There are four different NLR subfamilies named NLRA, NLRB, NLRC, and NLRP, based on their different N-terminal effector domains: acidic transactivating domain, baculovirus inhibitor repeat (BIR) domain, CARD, and pyrin domain (PYD), respectively (96). NOD9, localizing in the mitochondria, is called NLRX1 due to its weak homology to any of the four effector domains (97).

Among NLRs, NLRP3 is the best-characterized sensor for viral nucleic acids including viral RNA, dsRNA, and viral DNA (98-100). Once binding with a ligand, multiple identical NLRP3 proteins could undergo self-oligomerization, followed by recruitment of an adaptor protein called ASC (adaptor protein apoptosis speck protein with caspase recruitment) (101). ASC in turn interacts with an inactive precursor form of the enzyme caspase-1 (pro-caspase-1) via the CARD on both proteins. After recruitment to the inflammasome complex formed by NLRs, caspase-1 becomes active and further cleaves pro-IL-1β and pro-IL-18 into their active and mature forms for stimulating various pro-inflammatory response (102).

Type I IFNs

IFNs are major components of the antiviral innate immunity and have diverse biological functions including antiviral activity, anti-proliferative activity, stimulation of T cell cytotoxic activity, and modulation of the immune response. There are three types of interferons. Type I IFNs include IFN-α, IFN-β, IFN-ε, IFN-κ, and IFN-ω in humans. IFN-δ, IFN-τ and IFN-ζ (or Limitin) have been identified as type I IFNs in swine, ruminant and mice, respectively. IFN-γ produced by activated T-cells and natural killer cells is the only member of Type II IFN. IFN-γ not only enhances the effects of type I IFNs, but also involves in the regulation of the immune and inflammatory responses. The recently discovered type III IFNs are composed of four IFN-λ molecules called IFN-λ1, IFN-λ2, IFN-λ3 (103) and IFN-λ4 (104). It has been demonstrated that IFN-λ can be induced by viruses (105) and stimulates a type I IFN-like response through JAK-STAT pathway (106).

The induction of type I IFNs is the major approach by which the innate immune system defends against viral infection through the signaling of TLRs, RLRs, and DNA sensors. Type I IFNs are the largest IFN class, in which IFN-α and IFN-β are the most important factors in antiviral defense. The specific binding of IFN-α and IFN-β to IFN-α receptor (IFNAR), consisting of IFNAR1 and IFNAR2 chains on cell surface, triggers phosphorylation of JAK1 and tyrosine kinase 2 (TYK2), which are pre-associated with the cytoplasmic tails of the receptors. Activated JAK1 and TYK2 in turn phosphorylate the specific intracellular tyrosine residues of the receptors, creating docking sites for STAT1 and STAT2 for further activation. Phosphorylated STAT1 and STAT2 form a heterodimer, followed by interacting with interferon regulatory factor 9 (IRF9) to form a complex known as interferon-stimulated gene factor 3 (ISGF3) (107). The ISGF3 complex translocate into the nucleus to induce the transcription of genes regulated by interferon-stimulated response element (ISRE), followed by the expression of interferon-stimulated genes (ISGs), such as PKR (dsRNA-activated protein kinase) and RNase L. The induction of

type I IFNs stimulated by +ssRNA virus and type I IFN-stimulated JAK-STAT signaling is illustrated in Fig. 1.4.

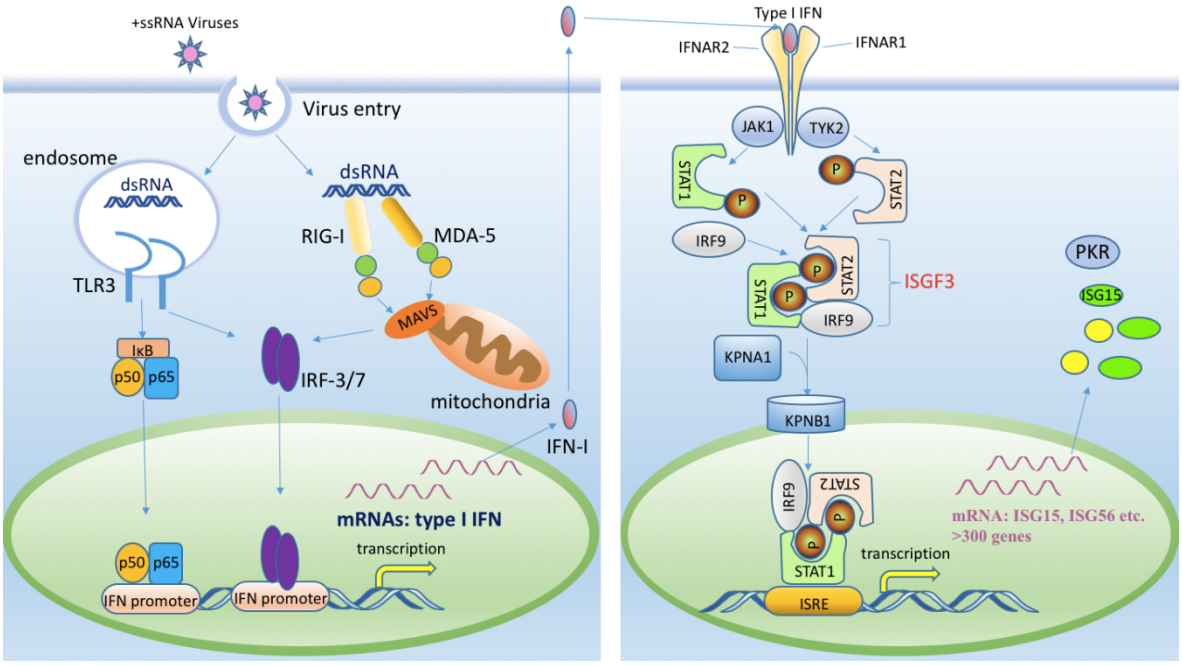

Fig. 1.4 Schematic illustration of type I IFN induction and signaling. Once +ssRNA virus enters into the host cells, viral-derived dsRNAs are recognized by pattern-recognition receptors, including TLR3 in the endosome, and RIG-I/MDA5 in the cytosol, resulting in activation and nuclear translocation of IRF3, IRF7, and NF-κB. Then type I IFNs are synthesized and released. They bind to the type I IFN receptor IFNAR-1 and IFNAR-2 on the cell membrane and activate the JAK-STAT1/STAT2 pathway. The phosphorylated STAT1 and STAT2 form heterodimer, followed by interaction with IRF9 to form interferon-stimulated gene factor 3 (ISGF3). Karyopherin α1 (KPNA1), an adaptor protein binding ISGF3, is essential to mediate the nuclear import of ISGF3 via interaction with karyopherin β1 (KPNB1). The ISGF3 binds to interferon-stimulated response element (ISRE) in DNA to activate transcription of interferon-stimulated genes (ISGs). "P" besides STATs indicates phosphorylation.

PRRSV evasion of innate immunity

PRRSV has developed multiple strategies to evade immunological surveillance, especially by disturbing host innate immune response through different viral proteins.

Nsp1: an antagonist of type I IFN production and signaling

Located in the amino (N)-terminal of pp1a, nsp1 is the first PRRSV protein synthesized in PRRSV-infected cells. Nsp1 has 382 amino acids and is proteolytically cleaved into two proteins, nsp1α

and nsp1β. Both of them contain a papain-like cysteine protease (PCP) domain (PCPα and PCPβ) indispensable for their self-cleavage. PCPα by nsp1α is responsible for releasing itself from nsp1β at the site of 180M↓A181, while PCPβ allows the cleavage at 383G↓A384 between nsp1β and its neighbor nsp2 to generate nsp1β (108). It has been reported that PCPα activity is required for PRRSV sgRNA synthesis but not related to genome replication (109). In contrast, inactivation of PCPβ blocks viral RNA synthesis completely. For EAV, controlling the abundance of mRNAs to balance the genome replication and sgRNA synthesis involves all domains of nsp1 (110). Moreover, some arterivirus nsp1 mutations independent from either genome replication or sgRNA transcription inhibit the generation of infectious progeny virions (111). In this case, nsp1 plays key roles in multiple steps in the arterivirus life cycle including polyprotein cleavage, sgRNA transcription, and virion biogenesis.

The crystal structure of nsp1α shows that it also contains an N-terminal zinc finger (ZF) domain (amino acids (aa) 1-65) and a C-terminal extension (CTE) (aa 167-180), with PCPα domain in the middle (aa 66-166) containing a ZF motif (112). The ZF domain is critical for viral replication through combining the sgRNA synthesis together with replicase expression during nidovirus replication (113). Moreover, the DNA-binding ability of the ZF domain in nsp1α also facilitates the inhibition of IFN-β production (114). In addition, the ZF domain might participate in IFN suppression as its mutants cannot translocate to the nucleus and disrupt the binding of CREB-binding protein (CBP) with IRF3 through inducing the degradation of CBP (115, 116). On the other hand, the PCPα domain and CTE are suggested to be essential for IFN-β inhibition and suppression of NF-κB activation (117). Recently, nsp1α is reported to inhibit NF-κB signaling by interacting with HOIP, one catalytic subunit of the linear ubiquitin chain assembly complex, and reduce the linear ubiquitination of NF-κB essential modulator (NEMO) (118).

Nsp1β is also a strong IFN antagonist. Nsp1β inhibits the phosphorylation and nuclear translocation of IRF3 and the production of NF-κB-mediated gene induction induced by dsRNA (119).

It also inhibits Sendai virus-mediated porcine IFN-β promoter activation in a porcine monocytic cell line. In addition, nsp1β has been shown to block STAT1/STAT2 nuclear translocation via inducing karyopherin-α1 (KPNA1) degradation for the inhibition of type I IFN-activated downstream signaling (120, 121).

Nsp2: the most variable PRRSV protein

PRRSV nsp2 is the largest PRRSV protein encoded by 21 to 23% contents of the genome. It contains an N-terminal conserved putative cysteine protease domain (PLP2), a hypervariable (HV) region of 500-700 amino acids, and a transmembrane domain near the C-terminal tail (122). The PLP2 domain possesses both papain- and chymotrypsin-like cysteine protease catalytic abilities (123), which allows nsp2 releasing itself from pp1a/pp1ab polyprotein by its trans- and cis-cleavage features (124). Nsp2 is also proposed to serve as a co-factor for nsp4 protease to cleave nsp4/5 junction when processing nsp3-8 fragment (125). The PLP2 domain has been also identified to be a member of mammalian ovarian tumor domain (OTU) family of deubiquitinating enzymes (DUBs) (126-128). Moreover, studies based on immunoelectron microscopy and Western blot assay reveal that nsp2 is present in mature PRRSV particles with multiple forms (129).

Though PRRSV nsp2 features important enzymatic functions, it has been shown to be highly variable and heterogeneous due to the HV region. Spontaneous insertions, deletions, and mutations are common in the HV region among different PRRSV strains. The high-level variability in nsp2 indicates that it has nonessential sequence for virus replication. Consequently, GFP recombinant virus by inserting GFP gene into nsp2 region has been constructed (122). In addition, nsp2 is possibly an indicator for PRRSV genetic variation and can be used for differential diagnosis.

Recently, it was revealed that nsp2 is associated with the modulation of the host immune responses. A deletion of one immunodominant B-cell epitope ES3 enhances the cytolytic activity of PRRSV and promotes viral replication (130). Furthermore, the ΔES3 mutant virus induces lower levels

of IL-1β and TNF-α in macrophages and peripheral blood mononuclear cells (PBMCs) compared with its parental virus. These results indicate that some regions of nsp2 are dispensable for PRRSV replication but might play a role in modulation of the host immune response. In addition, with the DUB function, nsp2 suppresses ISG15 production and conjugation (131, 132). The DUB domain also interferes with the degradation of IκBα via preventing its polyubiquitination, which consequently inhibits NF-κB activation (133). The newly identified proteins nsp2TF and nsp2N that are generated via the -2/-1 ribosomal frameshifting in nsp2 region are also shown to interfere with the host immune response (15). On the other hand, nsp2 is involved in the formation of DMV via inducing host cell membrane rearrangement together with nsp3 and nsp5 (12, 42).

Nsp4: the main protease

Following the auto-proteolytic release of three N-terminal proteases: nsp1α, nsp1β and nsp2, the main protease nsp4 is released with simultaneous generation of nsp3 through self-cleavage. Nsp4 subsequently cleaves the remaining pp1a and pp1ab polyproteins and facilitate the release of nsp5 to 12 (134). Nsp4 belongs to the 3C-like serine protease (3CLSP) group, which combines the substrate specificity of the 3C-like cysteine proteases and the catalytic triad of the chymotrypsin-like proteases. Crystal structures reveal that nsp4 contains a unique C-terminal domain which is essential for its proteolytic activity, and this critical domain is connected to the typical chymotrypsin-like two-β-barrel structures (135).

Nsp4 not only functions as the main protease, but also acts as an antagonist of the host innate immune response. For example, PRRSV nsp4 has been shown to suppress NF-κB-mediated IFN-β production by cleaving the NEMO at the E349-S350 site (136). Moreover, the nsp4 of highly-pathogenic (HP)-PRRSV has recently been revealed to undermine type I IFN response by cleaving MAVS and releasing MAVS from mitochondrial membrane (137). Also, the localization in the nucleus of nsp4 is critical for the modulation of type I IFN system (138).

Nsp5: a transmembrane protein

Arterivirus nsp5, a transmembrane protein, is highly hydrophobic and is thought to be involved in the induction of membrane rearrangement to form the replication and transcription complex together with nsp2 and nsp3 (12, 139). Nsp5 induces autophagic cell death when overexpressed alone (67). Moreover, nsp5 has been implicated in the induction of IFN-γ (140).

Nsp11: the endoribonuclease

PRRSV nsp11 contains a nidovirus uridylate-specific endoribonuclease (NendoU) domain, which is conserved in all nidoviruses and indispensable for arterivirus replication (141). NendoU, similar to the endoribonuclease XendoU in eukaryotes, has been demonstrated to cleave 5' uridine nucleotides of RNA substrates to generate a 2'-3'-cyclic phosphate end product (142, 143). According to the crystal structure analysis (144), nsp11 has three different domains including N-terminal domain, linker domain and C-terminal domain. The C-terminal domain is the endoribonuclease domain. Nsp11 exists as a dimer with the N-terminal domain of one molecule interacting with the C-terminal domain of the other molecule. Recently, nsp11 is reported to have DUB activity, which facilitates the perturbation of NF-κB activation (145) and interacts with the cellular deubiquitinase OTULIN (146) when overexpressed alone. However, the crystal structure analysis (144) does not support this as there is no DUB domain is identified. It is most likely that nsp11 interacts with the cellular deubiquitinase OTULIN and exerts the reported function in NF-κB inhibition. Further work using infectious cDNA clone is needed to verify the finding.

PRRSV nsp11 is also an IFN antagonist by promoting the degradation of MAVS and RIG-I mRNA through its endoribonuclease domain (147-149). Additionally, the endoribonuclease activity of nsp11 inhibits lipopolysaccharide (LPS)-mediated NLRP3 inflammasome in PAM cells through the reduction of pro-IL-1β mRNA and IL-1β protein level in late stage infection (150).

N protein: the nucleocapsid protein

The N protein is a major structural protein with multiple functions. N protein is the only protein component of the viral capsid encapsidating the viral RNA genome via covalent and non-covalent self-interactions (151). Phosphorylation of N proteins are common for nidoviruses but with unknown function and importance (152). Similar to other +ssRNA viruses, PRRSV replicates in the cytoplasm, but N protein can localize at the nucleolus (153). Sequence analysis shows that N protein contains two classic nuclear localization signals (NLS), NLS-1 and NLS-2, among which NLS-2 is essential and sufficient for the localization of N protein in the nucleolus. Currently, there are some hypotheses attempting to explain why the nucleocapsid protein of some +ssRNA viruses enters into the nucleolus: 1. By localizing in the nucleolus, N protein can modulate the function of nucleolus such as rRNA synthesis and regulation of cell cycle to optimize virus replication. 2. It is a host cell defensive strategy to accumulate N protein in the nucleolus to inhibit viral assembly, whereas virus produces more N and incorporates NES in N protein to surmount this strategy (154-156).

In addition, N protein has been reported to disturb dsRNA-mediated phosphorylation and nuclear translocation of IRF3 to inhibit type I IFN induction (157). N protein was also shown to inhibit the expression of IFN-activated ISRE reporter expression via blocking the nuclear translocation of STAT1 (158). On the other hand, N protein stimulates DNA-binding activity of NF-κB to induce the expression of NF-κB-responsive genes, indicating that N protein might participate in PRRSV-induced inflammatory response (159).

Other mechanisms PRRSV utilizes to evade host innate immune response

PRRSV has also been found to inhibit poly(I:C)-mediated phosphorylation of PKR in PAM cells during the early stage of infection, leading to lower phosphorylation of eIF2α, a translation initiator, and consequently evading the PKR's antiviral function. Structural components of PRRSV virions appear to be required for the inhibition as inactivated virus also shows the inhibition (160). High PRRSV burden pigs have upregulation of the suppressor of cytokine signaling (SOCS) 1 protein compared with low

burden pigs, which has the ability to antagonize JAK-STAT signaling pathway (161). Recently, PRRSV was reported to elevate a host microRNA, miR-30c, via activating NF-κB (162). The miR-30c is shown to negatively regulate type I IFN signaling by targeting JAK1. In addition, PRRSV induces the expression of miR-373 to facilitate viral replication and inhibit the production of IFN-β (163). Moreover, nsp7, nsp12, and GP3 have been shown to antagonize IFN-activated signaling (158). The interference with type I IFN induction and downstream signaling by PRRSV is illustrated in Fig. 1.5.

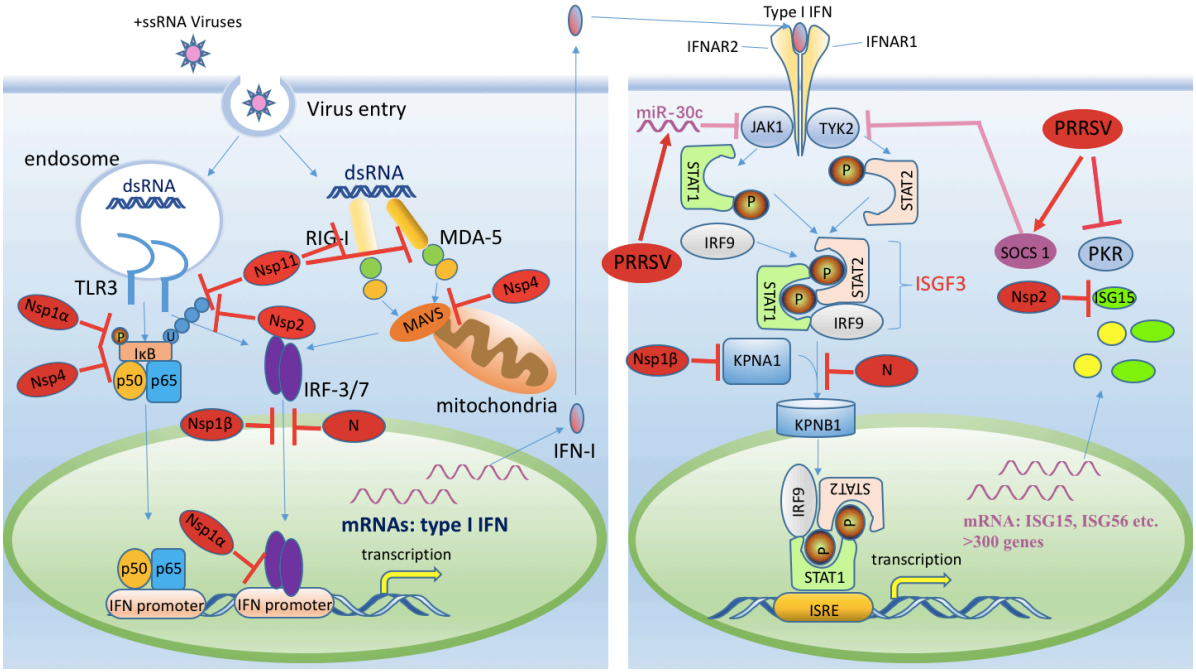

Fig. 1.5 PRRSV Interference with type I IFN induction and signaling. For IFN induction, PRRSV nsp1α inhibits NF-κB signaling and IFN promoter activation. Nsp1β and N protein inhibit the phosphorylation and nuclear translocation of IRF3. Nsp2 and nsp11 interfere with the degradation of IκBα via preventing its polyubiquitination. Nsp4 suppresses NF-κB and MAVS-mediated IFN-β production by cleaving NEMO and MAVS, respectively. Nsp11 also induces RIG-I and MDA-5 RNA degradation. For IFN downstream signaling, PRRSV nsp1β inhibits ISGF3 nuclear translocation via inducing degradation of KPNA1. PRRSV N protein also inhibits ISGF3 nuclear translocation. PRRSV nsp2 reduces ISG15 production and conjugation via its deubiquitination activity. PRRSV induces elevation of miRNA miR-30c to downregulate JAK1 and SOCS1 to inhibit JAKs. PRRSV inhibits PKR during its early infection of pulmonary alveolar macrophages.

PRRSV infection also stimulates the translocation and secretion of the high mobility group box 1 (HMGB1) protein via protein kinase C (PKC) δ activation (164, 165). HMGB1 is a nuclear protein in

normal cells but induces the inflammatory response via TLR2/4 when released out of the cells (166). PRRSV E and ORF5a proteins are responsible for the PKCδ activation.

PRRSV modulates the host adaptive immune response

Different from the innate immunity, the adaptive immunity is highly specific and can provide long-lasting protection to a particular pathogen. Moreover, immunological memory cells are generated after the primary exposure to a foreign antigen and generally mount a recall response of greater magnitude with faster kinetics. There are two types of adaptive immune response: humoral immunity and cell-mediated immunity.

Humoral immunity is mediated by B lymphocytes, which produce antibodies that circulate in the blood and mucosal secretions. Antibodies recognize specific antigens and induce agglutination, opsonization, neutralization, activation of complement, and antibody-dependent cell-mediated cytotoxicity (ADCC) to protect the host from the invading pathogens (167).

Cell-mediated immunity is mediated by T lymphocytes to destroy intracellular pathogens and eliminate the infected cells. T cells are composed of functionally distinct populations, such as helper T cells, cytotoxic T cells (CTLs), and regulatory T cells. CD4+ helper T cells are the mediators of immune response through secreting cytokines to stimulate B cell differentiation, activate macrophages and CTLs, and induce inflammation (168). Effector CTLs deliver the granules containing granzymes and perforins into the target cells, leading to their apoptotic death (169). Regulatory T cells modulate immune responses via suppressing other lymphocytes (170).

Passive transfer of PRRSV neutralizing antibodies (NAbs) protects the pigs against the challenge of homologous virulent PRRSV strain, indicating that NAbs play important roles in protective immune response against PRRSV (171, 172). However, PRRSV-infected pigs display the weak and delayed generation of virus-specific IFN-γ-producing cells and NAbs (173, 174). Moreover, the levels of CD4+

and CD8+ T cells are stable during PRRSV infection (52), which suggests that PRRSV has certain strategies to evade the host adaptive immune system.

Similar to other viruses, PRRSV uses post-translational modifications in envelope proteins to dampen the induction of NAbs (175-177). The ectodomain of GP5 from both PRRSV-1 and PRRSV-2 contains a major epitope stimulating NAbs (178-181). Moreover, the mutant PRRSV lacking of N-glycosylation sites surrounding the neutralization epitope in GP5 and GP3 could elicit higher level NAbs than wild-type virus, indicating that PRRSV glycan shielding can evade the NAb responses. Another possible strategy that PRRSV escapes the humoral immunity is by preventing the exposure of viral antigens on the surface of viral-infected cells, to avoid the clearance by antibody-mediated phagocytosis or cell lysis (182).

In addition, PRRSV has been found to downregulate the level of the swine leukocyte antigen class I (SLA-I) molecules, the swine major histocompatibility complex (MHC), on the surface of macrophages and dendritic cells through nsp1α-, nsp2TF-, and GP3-induced degradation, resulting in weak induction of CTL responses (183-186). PRRSV nsp4 can downregulate the transcription and expression of β2-microglobulin that is required for SLA-I antigen presentation. This observation reveals another mechanism that PRRSV might modulate SLA-I antigen presentation and cell-mediated immune response (187).

PRRS control and treatment

Since the discovery of PRRS, there have been considerable efforts to establish rapid diagnosis, heighten control strategies and develop effective vaccines.

Diagnosis of PRRS

First, the clinical signs of PRRS are variable due to infection by various PRRSV strains, different environment and management, as well as distinct immune and growth status of the herd. Generally,

PRRSV-infected sows manifest high rate in abortions, stillborn, and mummified piglets. PRRSV also causes severe respiratory diseases, fever, and loss of appetite in adults and weaned pigs.

Secondly, laboratory tests allow the accurate identification and confirmation of PRRSV infection, even as strain-specific. After obtaining serum, lung, lymph node, or tonsil samples, virus isolation in cultured cells and immunofluorescence assay can be done to detect live virus; RNA isolation, reverse transcription polymerase chain reaction (RT-PCR) can be used to determine the presence of PRRSV genome and generate template for sequencing to determine the sequence of the PRRSV strain; real-time PCR can also be done for speed and specificity; and serological tests can be used to detect PRRSV antibodies.

Control and prevention

PRRSV is stable when it is held under low temperature or frozen, however, the stability becomes lower with increasing temperature: only survive for 6 days at 20°C, and 20 minutes at 50°C (188). Moreover, PRRSV is very sensitive to chemical disinfection, such as chloroform, formaldehyde, phenols, etc. Acidic and basic environments are also detrimental to PRRSV (189).

In addition to control PRRSV transmission, vaccination is often used to control PRRSV infection of virulent strains (190). Modified-live virus (MLV) and killed virus (KV) vaccines have been licensed for commercial application in many countries worldwide. The MLV vaccine confers delayed but effective humoral and cell-mediated protective immune responses against homologous PRRSV and partial protection against heterologous virus strain. However, this vaccine has a major disadvantage for its potential reversion to virulence and causing disease. On the other hand, the KV vaccine is safe but elicits limited protection against PRRSV infection.

Although substantial efforts have been made, no vaccination regimen or control strategy has been demonstrated to be adequate for long-term PRRS control. The failure to completely control PRRSV infection is due to its genetic diversity, rapid mutation, persistent infection, and poor induction

of protective immune response. Therefore, further studies about the interplay between PRRSV and the host immunity as well as the mechanism of PRRSV evasion are necessary and may pave the way for improving the vaccines and developing new control strategies against PRRS.

Chapter 2: JAK-STAT signaling pathway and PRRSV perturbation

Introduction

Cytokines are a broad and loose group of small cell-signaling proteins that play important roles in cell growth, proliferation, differentiation, apoptosis, angiogenesis, immunity and inflammatory response. They include IFNs, interleukins, chemokines, lymphokines, and TNFs. They are produced by a variety of cells, including macrophages, B and T lymphocytes, mast cells, endothelial cells, epithelial cells, fibroblasts, and various stromal cells. Cytokines that are produced at the site of infection stimulate and coordinate innate and adaptive immune responses against invading pathogens (191-193). They act through their matching receptors on the surface of target cells, followed by cascades of intracellular signaling. One such frequently activated intracellular signaling is the JAK-STAT pathway, which is indispensable and pivotal in many biological processes including immunity and inflammatory response (194, 195). Dysregulation of the JAK-STAT signaling results in immunodeficiency and immune-mediated disorders (195, 196). Mutations in components of the JAK-STAT pathway cause immunodeficient and autoimmune disorders (197, 198).

JAKs and STATs

In mammals, there are four JAKs: JAK1, JAK2, JAK3, and Tyk2, ranging in size from 120 to 140 kDa (199). JAK1, JAK2, and Tyk2 are ubiquitously expressed, whereas JAK3 expression is restricted to cells of the hematopoietic system. The JAK protein is pre-associated with cytokine receptors in the cytoplasmic side, which is an important determinant of their levels and signaling potential (199). Upon cytokine binding, the receptor chains are brought into close proximity, leading to the juxtaposition of two JAK kinase domains and consequent trans-phosphorylation. Once activated, JAKs phosphorylate STAT proteins via Src homology 2 (SH2) domain interaction (200). Even though

responding to different cytokines, JAKs selected by different receptors activate specific STAT members for defined functions (199).

There are seven mammalian STAT proteins: STAT1, STAT2, STAT3, STAT4, STAT5A, STAT5B, and STAT6, which range from 750 to 950 amino acids in polypeptide length and feature several conserved domains (194, 201). STATs are latent transcription factors located in the cytoplasm until activated. Each STAT member responds to a defined set of cytokines (195, 196, 202). The seven STATs go through similar activation processes and exhibit global conservation in function (194). In brief, ligand-mediated receptor multimerization leads to trans-phosphorylation of JAKs, which then create docking sites in the receptor for STATs and phosphorylate the latter. Phosphorylated STATs form the homodimer or heterodimer complexes, followed by translocation into the nucleus by importins and binding to the response element in DNA to activate or repress transcription of a defined set of genes (194).

STAT signaling and functions

Among the seven STATs, STAT1 and STAT2 mainly mediate the IFN-activated signaling (196). STAT1 is involved in signaling by type I, type II, and type III IFNs. In response to type I IFNs (IFN-α, IFN-β, and so on), STAT1 and STAT2 are phosphorylated, followed by heterodimer formation and then interacting with IRF9 to form a heterotrimer known as ISGF3 (107) (Fig. 1.4). The ISGF3 is translocated into the nucleus and binds to ISRE in DNA to activate the expression of ISGs. IFN-γ is the only type II IFN. Upon IFN-γ stimulation, STAT1 is activated to form homodimers, followed by nuclear translocation and activation of gene expression via binding to interferon-gamma-activated-sequence (GAS) in DNA (196). Type III IFNs (IFN-λ1, IFN-λ2, IFN-λ3, and IFN-λ4) also activate STAT1 and STAT2 for ISRE transactivation like type I IFNs and protect primarily mucosal epithelial cells (106, 203).

In addition to the canonical signaling pathway described above, IFNα signaling occurs through alternative complexes containing STAT2 and IRF9 but without STAT1 (204, 205) (Fig. 2.1). Moreover, STAT2 can form a heterodimer with other STATs, like STAT3 and STAT6, followed by binding to diverse sequences, like GAS. Further studies demonstrate the existence of a STAT1-independent IFN signaling pathway, in which STAT2/IRF9 directs a prolonged antiviral activity (206, 207).

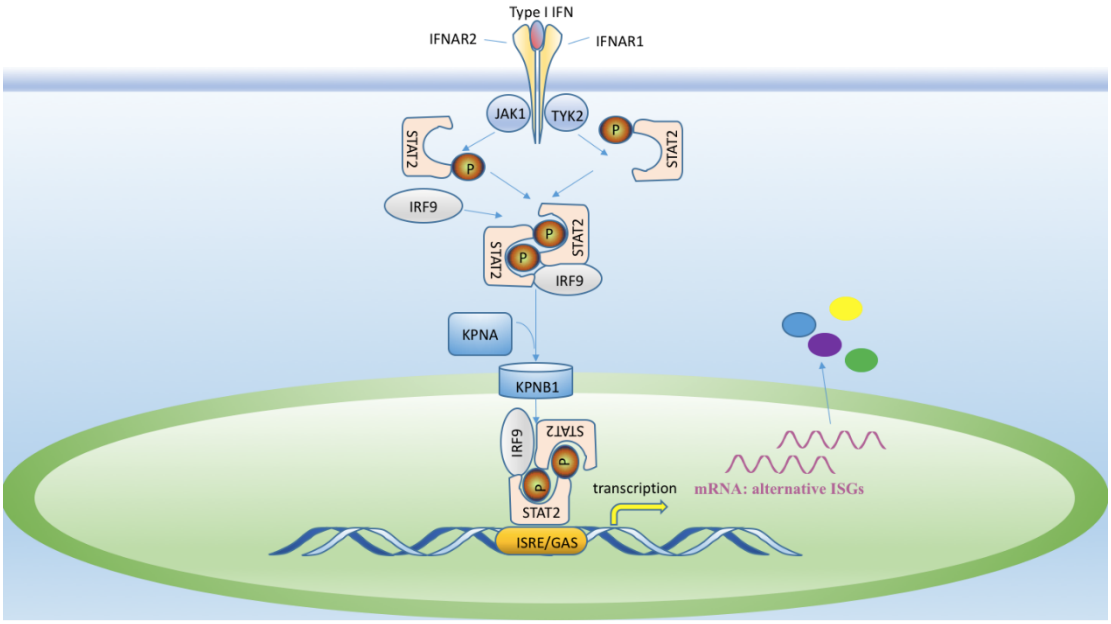

Fig. 2.1 STAT1-independent IFN signaling. Type I IFNs activate alternative JAK-STAT2 signaling without STAT1. The ISGF3-like complex binds to ISRE and interferon-gamma-activated sequence (GAS) to activate alternative sets of ISGs.

STAT3 is activated by many cytokines and had multiple functions including differentiation of T helper 17 (Th17) and generation of CD8+ T cell memory response (195, 208, 209). Numerous cytokines including IL-5, IL-6, IL-9, IL-10, IL-11, IL-12, IL-21, IL-22, IL-27, oncostatin M (OSM), IFN-γ, TNF-α and leukemia inhibitory factor (LIF), trigger STAT3 activation (202, 210). The IL-6 family of cytokines including IL-6, OSM, and LIF bind to the receptor complex containing the common glycoprotein 130 (gp130) and activate STAT3, known as the gp130/JAK-STAT3 signaling (Fig. 2.2). STAT3 is needed for differentiation of follicular T helper and Th1 cells (211), as well as activation and maturation of

dendritic cells (DCs) (212). Mutations in STAT3 cause autosomal dominant hyper-IgE syndrome, a rare multisystem primary immunodeficiency characterized by recurrent bacterial infections in skin and lung and with abnormally high levels of IgE (213, 214). STAT3 is indispensable for promoting host defense against viral infections. For instance, during Herpes simplex virus-1 (HSV-1) infection, STAT3 promotes the activation of CD8+ T cells response (215). It has been shown that the gp130-STAT3 signaling is critical for the innate immune response against coxsackievirus B3 virus (CVB3) infection (216). In addition, STAT3 plays a protective role in regulating virus-induced proinflammatory response, as shown in STAT3 knockout studies (217-219). Highly pathogenic avian influenza (HPAI) H5N1 virus induces strong proinflammatory response in chickens via inhibition of STAT3 phosphorylation (220).

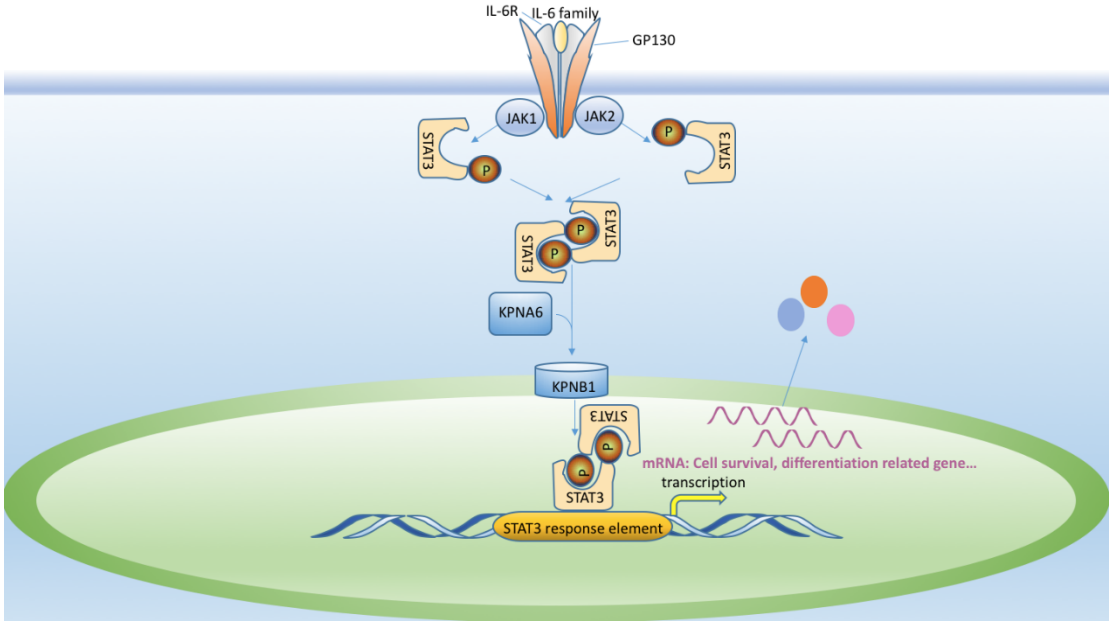

Fig. 2.2 JAK-STAT3 signaling activated by IL-6 family cytokines. IL-6 binds to its receptor IL-6R and gp130, leading to JAK phosphorylation of STAT3, followed by STAT3 homodimer formation. KPNA6 is the adaptor protein to bind to STAT3 and interact with KPNB1 for the nuclear translocation. The STAT3 homodimer binds to STAT3 response element (RE) in DNA to activate transcription of target genes.

STAT4 is activated by IL-12 and is essential for Th1 cell differentiation (221). Even though its distribution is restricted in myeloid cells, testis and thymus, STAT4 is critical for the host immunity. It is also activated by IL-23 to induce expansion of Th17 cells and the associated autoimmunity (221).

Moreover, STAT4 is crucial for the biological effects of macrophage, natural killer cell, mast cell, and dendritic cell as well as IFN-γ production (222).

STAT5 is activated by IL-2, IL-3, IL-5 and granulocyte macrophage colony-stimulating factor (GM-CSF) and is essential for regulatory T cell (Treg) differentiation (196). STAT5 can also be activated by IL-7 and IL-15, contributing to the generation of CD8+ memory cells and B lymphopoiesis (195, 196). STAT5A and STAT5B are two highly related proteins and have indispensable roles, especially to the Treg response, for which STAT5B is dominant (223). Treg takes charge of maintaining homeostasis and controlling the immune response by restraining immunocompetent effector cells (224).

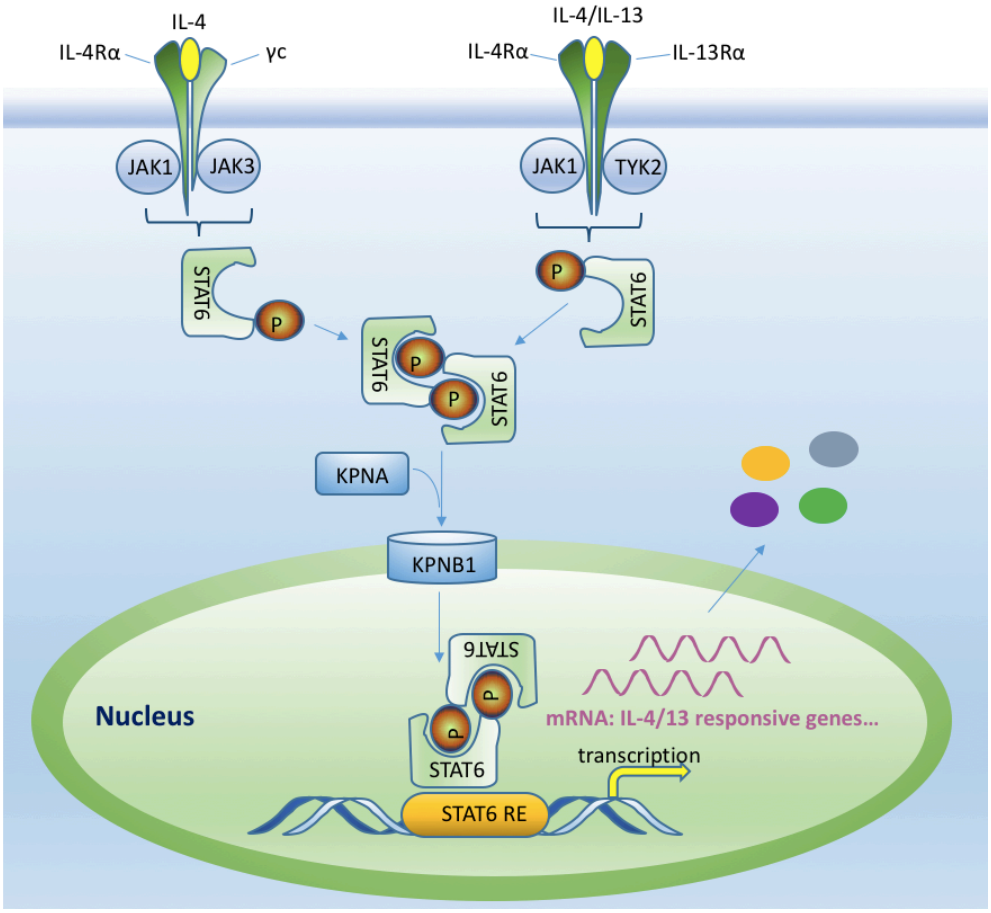

Fig. 2.3 Canonical JAK-STAT6 signaling. IL-4 and IL-13 bind to receptors, leading to JAK phosphorylation of STAT6, followed by homodimer formation and nuclear translocation to activate target genes.

STAT6 is activated by IL-4 and IL-13 and is pivotal for Th2 and Th9 lymphocyte differentiation (195, 225) (Fig. 2.3). STAT6 has been demonstrated to regulate lung inflammatory responses in animal models (225). Moreover, STAT6 contributes to alternative activation of macrophages and lung antiviral responses in a JAK-independent manner (226) (Fig. 2.4). Viral or cytoplasmic nucleic acids trigger STING (stimulator of interferon genes) or MAVS to recruit STAT6 to the endoplasmic reticulum, followed by TBK1 phosphorylation of STAT6 and nuclear translocation. Expression of chemokines, including CCL2, CCL20, and CCL26, are then activated to recruit immune cells to combat viral infection (226).

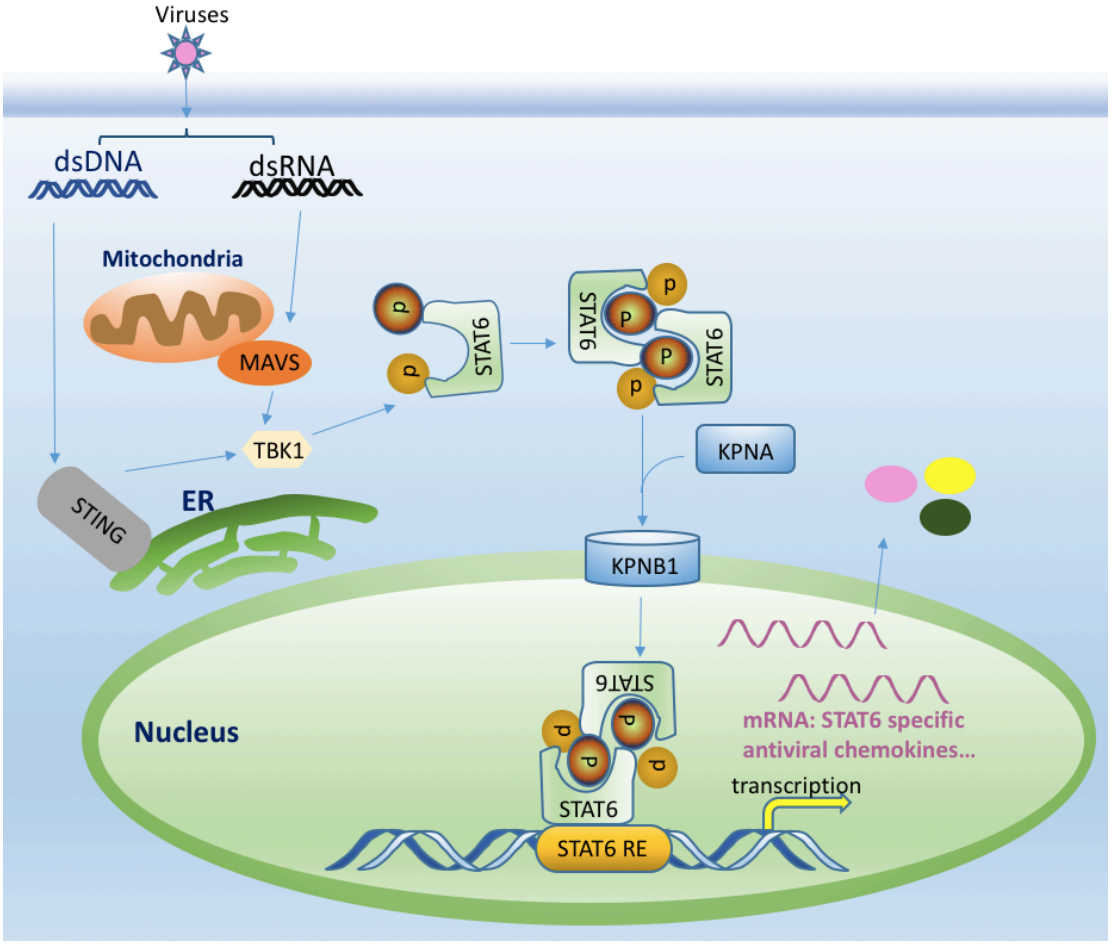

Fig. 2.4 JAK-independent STAT6 signaling. Viral nucleic acids (dsRNA or dsDNA) activate MAVS and STING on mitochondria and ER, respectively, leading to TBK1 phosphorylation of STAT6, followed by homodimer formation and nuclear translocation to activate alternative target genes, including antiviral chemokines.

Viral interference with JAK-STAT signaling

To evade the host antiviral response, viruses have evolved numerous strategies including dysregulating the JAK-STAT pathway. For example, Epstein-Barr virus (EBV) suppresses IFN signaling by inhibiting the expression of the IFN-γ receptor (227). Paramyxovirus V protein induces STAT protein degradation to evade IFN response (228). Dengue virus (DENV) NS5 protein interacts with UBR4 to induce STAT2 degradation (229). Yellow fever virus NS5 binds to STAT2 after IFN stimulation to prevent ISGF3 binding to ISRE (230). Ebola virus VP24 blocks pSTAT1 nuclear translocation by binding KPNA1 (231, 232). Measles virus V protein not only binds to STAT2 to disrupt type I IFN signaling for viral evasion (233), but also inhibits the IL-6 mediated STAT3 signaling (234). The ORF6 product of severe acute respiratory syndrome coronavirus disrupts nuclear import of pSTAT1 by tethering KPNA2 to the endoplasmic reticulum/Golgi membrane (235). HPAI H5N1 influenza virus induces a strong proinflammatory response in chickens by inhibiting STAT3 phosphorylation (220). Zika virus NS5 promotes STAT2 degradation through the ubiquitin-proteasome system in a different mechanism from DENV as UBR4 does not involve (236). Vaccinia virus C6 protein prevents IFN signaling by binding to the TAD domain of STAT2 (237). V protein of mumps virus prevents responses to IL-6 and v-Src by inducing the STAT3 ubiquitination and degradation (238). Rabies virus interferon antagonist P protein inhibits gp130 receptor signaling by interacting with activated STAT3 (239).

PRRSV interference with JAK-STAT signaling

PRRSV inhibits IFN-activated JAK-STAT signaling

PRRSV inhibits the IFN-activated JAK-STAT signal transduction and ISG expression in both MARC-l45 and PAM cells (120, 121, 158). PRRSV proliferation in MARC-145 cells suppresses the JAK-STAT signaling stimulated by IFN-α. The transcripts of ISG15 and ISG56 and protein level of

STAT2 in PRRSV-infected cells were much lower than mock-infected cells upon IFN stimulation. PRRSV blocks the nuclear translocation of the IFN-induced ISGF3 complex via nsp1β (120, 240). Avirulent Ingelvac® PRRS MLV has no effect on the IFN-activated JAK-STAT signaling in PAMs (120).

Further studies demonstrate that nsp1β inhibits the JAK-STAT signaling via inducing the degradation of KPNA1, which is a critical adaptor protein to mediate the nuclear import of ISGF3 (121). Infection of MARC-145 cells by moderate virulent PRRSV strains VR-2332 and VR-2385 also result in KPNA1 reduction, whereas the Ingelvac® PRRS MLV does not. Nsp1β of VR-2385 induces elevation of KPNA1 ubiquitination and shortening of its half-life. Analysis of nsp1β deletion constructs identifies its N-terminal domain to be involved in the ubiquitin-proteasomal degradation of KPNA1 (121). Sequence analysis of nsp1β from VR-2332 and MLV indicates there are only two different nucleotides, leading to two different amino acids at residue 19 and 151. Substitution of the N-terminal nucleotide resulting in alteration of residue 19 from valine to isoleucine abolishes the ability of VR-2385 nsp1β to induce KPNA1 degradation and to inhibit IFN-mediated signaling. In contrast, MLV nsp1β has no effect on KPNA1, however, a mutant MLV nsp1β with residue 19 alternation from isoleucine to valine gains the ability to induce KPNA1 degradation (121). These data demonstrate that nsp1β blocks ISGF3 nuclear translocation to inhibit the JAK-STAT signaling via inducing KPNA1 degradation and that the residue valine-19 in nsp1β correlates with the inhibition.

Besides nsp1β, other PRRSV proteins including nsp7, nsp12, GP3 and N also inhibit the IFN-induced downstream signaling, albeit at a smaller scale (158). The N protein inhibits the IFN-activated signaling by blocking STAT1 nuclear translocation (158). Among PRRSV strains, there are variable effects on the IFN-activated JAK-STAT signaling. In MARC-145 cells, PRRSV strains VR-2385, VR-2332, NVSL97-7895, and Lelystad, but not MN184, block the activity of exogenous IFN-α (158). In primary PAMs, strain VR-2385, VR-2332, MN184, and Lelystad, but not NVSL97-7895, inhibit the

activity of IFN-α. For NVSL97-7895 and MN184, the same virus infection in MARC-145 and PAM cells has variable effects on the IFN-activated signaling. This is not totally unexpected as the NVSL strain differs from other PRRSV strains in its failure to induce IL-10 expression *in vivo* (241). These two strains might have alternative interacting mechanisms with the JAK-STAT signaling in the two types of cells.

A recent study shows that PRRSV upregulates a host microRNA, miR-30c, which is a negative regulator by targeting JAK1 (162). PRRSV reduces JAK1 expression in infected cells and is expected to affect the phosphorylation of both STAT1 and STAT2. However, in our studies, IFN-induced phosphorylation of both STAT1 and STAT2 in PRRSV-infected MARC-145 cells is not affected (120). It may play a role *in vivo* as PRRSV infection in pigs leads to elevation of miR-30c in lungs and PAMs and its level corresponds to the viral load (162). This indicates that PRRSV has multiple strategies to block host IFN-signaling, which is illustrated in Fig. 1.5.

PRRSV effect on other STAT signaling

PRRSV uses multiple strategies to evade the host innate and adaptive immunity. By interfering with the JAK-STAT signaling, PRRSV may perturb the function of cytokines in the regulation of the host immune response. Minimizing the PRRSV's effect on the JAK-STAT signaling is assumed to improve the PRRSV-elicited protective immune response, which should be a desirable feature for an improved vaccine against PRRSV.

As aforementioned, other STATs also have important roles in the host immune response. Besides inhibiting the JAK-STAT1/STAT2, PRRSV might interfere with other STATs.

STAT2 is involved in STAT1-independent signaling by interacting with IRF9 to drive the expression of ISRE-containing genes (205, 206). We assume PRRSV inhibits the STAT1-independent antiviral signaling through disturbing STAT2.

STAT3 has pleiotropic activity and plays important roles in many biological processes. STAT3 is a central regulator of lymphocyte differentiation and function (197). STAT3 is needed for activation and maturation of dendritic cells (DCs) and plasmacytoid DCs are considered to be the major source of IFN-α production during viral infection. STAT3 deficiency affects the generation of memory CD8+ T cells (242, 243) and memory B cells (244, 245). PRRSV infection induces a weak cell-mediated immune response, in which PRRSV-specific T cells transiently appears two weeks after infection without a change in frequencies of CD4+ and CD8+ T-cells (52). PRRSV might antagonize STAT3 for interference with the host development of the protective immune response.

PRRSV's effect on the signaling of STAT4, STAT5 and STAT6 has not been determined yet. STAT4 distribution is restricted to myeloid cells, testis and thymus (221). STAT5 and STAT6 distribution are more ubiquitous. The main target cells for PRRSV infection are certain lineages of monocytes/macrophages in vivo. The PRRSV effect on the JAK-STAT signaling in T cells would be indirect, such as by exosomes from infected cells (246, 247). However, its interference of the JAK-STAT signaling in infected macrophages would have significant consequence as the response of PAMs against viral or bacterial pathogens is critical in determining the outcome of infection in the host. Cytokines like IFN-γ and GM-CSF activate the JAK-STAT signaling to regulate macrophage phenotype and activation (248). Activated macrophages secrete immune regulatory cytokines including IL-1β, IL-6, IL-12, TNF-α and so on (22). STAT6 has been demonstrated to have JAK-independent antiviral signaling (226). PRRSV might inhibit this alternative STAT6 signaling, which may contribute to the PRRSV evasion.

Conclusion

In conclusion, PRRSV perturbs the JAK-STAT signaling pathways by disturbing STATs protein level and their nuclear translocation. PRRSV has been found to inhibit the IFN-activated JAK-STAT signaling by blocking nuclear translocation of ISGF3 (120, 121). PRRSV might also disturb other JAK-

STAT signaling to interfere with the host protective immune response. PRRSV interaction with the JAK-STAT signaling pathways is complex and consequences would be possibly depending on the context of the milieu during infection.

Despite substantial efforts to study and control PRRS, no production or vaccination regimen has demonstrated sustained success (249, 250). This is likely in part due to the PRRSV poor induction of the protective immune response, allowing for PRRSV replication, spread, and persistence in the infected populations. Elucidation of the mechanisms of PRRSV evasion of the JAK-STAT signaling would yield insightful information that may facilitate the development of improved vaccines or therapeutics against PRRSV and other pathogens.

Chapter 3: Nuclear importins and viral manipulation

Introduction

For JAK-STAT signaling, the nuclear translocation of STAT complexes is an essential step to activate the expression of ISGs. Importins are the transport factors to assist the nuclear translocation of the STAT complexes. For example, the importin α5 is responsible for STAT1 nuclear translocation and the importin α7 is responsible for STAT3 nuclear translocation. Karyopherins mediate the nuclear import and export of numerous proteins. So they are also known as importins and exportins. In this chapter, the nuclear importins, their functions and virus manipulation of importins are to be discussed.

Nuclear transport

The nuclear pore complex

The nucleus is tightly controlled to protect the cellular genetic material from other cellular components, maintain the integrity of genetic information and control gene expression. The double membrane nuclear envelope encloses and isolates the entire nucleus from the cytoplasm. Despite the protective isolation is important for the nucleus to organize and control genetic information, its communication with the cytoplasm is also indispensable for the nuclear and cytoplasmic activities, such as exchange proteins, RNAs, ions, and other molecules. To accomplish this, nuclear pore complexes (NPCs) provide aqueous channels for these molecules travelling between the nucleus and the cytoplasm.

NPC is the largest macromolecular structure of approximately 125 megadaltons (MDa) in mammalian cells, composed of more than 30 proteins, named nucleoporins (Nups) (251). NPC has an eightfold symmetrical cylindrical structure with a 65 nm-central pore decorated with eight filaments attached to the cytoplasmic and nuclear rings on the cytoplasmic and nuclear side, respectively. The filaments of the nuclear face connect each other at their distal ends to form a nuclear basket (252).

The transport cycle

Due to the gap in the center of the pore is only 9 nm wide, NPCs only allow the passive shuttling of small hydrophilic molecules. Therefore, transport of macromolecules, including large proteins (>40 kDa) and nucleic acids, requires highly coordinated active process, relying on importins to enter the nucleus and exportins to exit. In canonical nuclear transport system, cargo proteins bearing nuclear localization signals (NLS) are recognized and translocated into the nucleus by the importins, while those proteins containing nuclear export signals (NES) are recognized and transported from the nucleus to the cytoplasm by the exportins (253). The transport receptors act as chaperones to assist the cargos to pass through the central pores of NPCs via the interaction with Nups. A typical feature of Nups is rich in hydrophobic motifs, such as the FG-repeat regions, which is critical for the interactions with the importins and exportins (252, 254). Additionally, the assembly and disassembly of transport receptors and cargo complexes are tightly regulated by Ras-related GTPase Ran through its interconversion between RanGTP and RanGDP states due to different locations. Once the complex composed of importin and cargo encounters RanGTP in the nucleus, the complex is disassembled, leaving the protein cargo in the nucleus and the importin recycled back to the cytoplasm. On the other hand, exportin binding to its cargo protein requires the interaction with RanGTP in the nucleus, resulting in a ternary complex consist of RanGTP, exportin and cargo. After the ternary complex translocates throughout the NPC, hydrolysis of GTP to GDP leads to dissociation of the complex to release the cargo in the cytoplasm and recycle exportin back to the nucleus (253, 255).

Karyopherin α

Karyopherins are the largest group of nuclear transport receptors in eukaryotic cells, including importins and exportins. Karyopherins α (KPNAs) are also known as importins α and karyopherins β (KPNBs) are known as importins β. KPNAs act as the adaptor to recognize the classical NLS (cNLS)

and form a heterotrimeric KPNB1/KPNA/cNLS-cargo complex (Fig. 3.1). KPNB1 has high affinity to associate with Nups and RanGTP to facilitate the import of the cNLS-cargo into the nucleus. Different KPNA proteins show differences in their abilities to interact with specific cargos, indicating that each KPNA subtype has distinctive roles involving specific subsets of target proteins (256).

The structural features of KPNAs

Human cells encode 7 subtypes of KPNAs, from KPNA1 to KPNA7, featuring a highly conserved architecture consisting of three functionally distinct domains. The N-terminal domain is importin β-binding (IBB) domain, which functions to recruit KPNB1 for nuclear transport (257). A series of 10 tandem armadillo (Arm) repeats are located next to the IBB and functions to bind the cNLS-containing cargos. There are two major groups of cNLSs: monopartite NLS, such as SV40-NLS, and bipartite NLS, exemplified by nucleoplasmin (NPM)-NLS. The Arm repeats form major and minor helical surface grooves for binding monopartite and bipartite NLS, respectively (256). The IBB domain contains a short basic region containing an NLS and functions an autoinhibitory effect to regulate KPNA's NLS-cargo binding (258). In the absence of KPNB1, the flexible IBB domain occupies the cNLS-binding groove formed by Arm motifs, to inhibit cNLS-cargo binding to the groove. The autoinhibitory function precludes KPNA from binding cargo proteins until KPNB1 interacts with the IBB domain. The C-terminal region containing a short hydrophilic acidic cluster, together with Arm repeats, are responsible for interacting with the nuclear exportin of KPNA, CAS (cellular apoptosis

susceptibility) protein, leading to KPNA recycling back to the cytoplasm for reuse (259). The nucleocytoplasmic shuttling cycle of importin α is illustrated in Fig. 3.1.

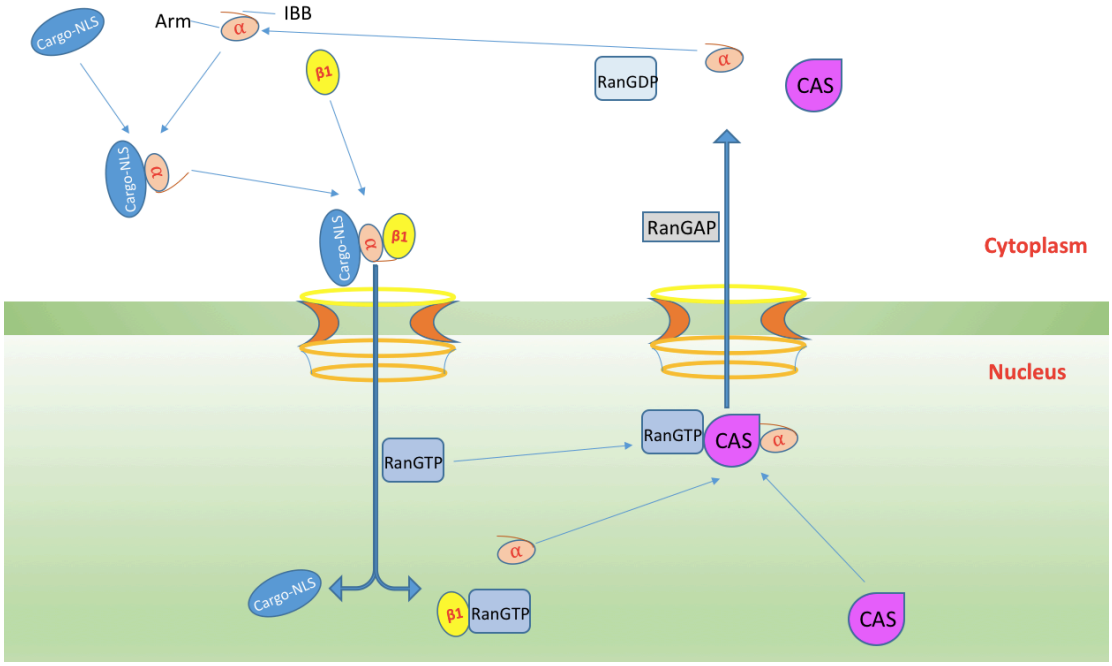

Fig. 3.1 The nucleocytoplasmic shuttling cycle of importin α. Importin α acts as adaptor to bind the cargos containing NLS signals, and form complexes with importin β which has the ability to interact with the nuclear pore complex. After transporting into the nucleus, the trimer dissociates once binding to Ran-GTP to release the cargo protein into the nucleus. The importin α shuttles to the cytoplasm via interacting with its exportin CAS.

The distinctive functions of KPNAs

In spite of the same architecture, KPNAs are classified into three subfamilies based on their sequence homology: clade α1 is composed of KPNA1, KPNA5 and KPNA6; clade α2 contains KPNA2 and KPNA7; clade α3 is made up of KPNA3 and KPNA4 (256). Different KPNAs exhibit different specificity for their cargos, resulting in diverse roles due to particular target proteins.

The three members of clade α1 have a high sequence identity at approximately 80% identical amino acids. When KPNA1 was first discovered, it was named NPI-1 (nucleoprotein interact 1) due to its interaction with influenza virus nucleoprotein (260). Afterwards, KPNA1 was shown to interact with tyrosine-phosphorylated STAT1 relying on its C-terminal region to mediate specific NLS-dependent nuclear import of STAT1 homodimer or STAT1/2 heterodimer (261, 262). KPNA5 and KPNA6 were

discovered according to their high homology to known importins (263, 264). Unlike most importins, which express ubiquitously in human tissues, KPNA5 has restricted expression only in the testis (263). KPNA6 and KPNA1 have been shown to be responsible for the nuclear transport of the activated STAT3 upon cytokine stimulation (265). KPNA6 has also been shown to mediate the nuclear import of keap1 (Kelch-like ECH-associated protein 1), the repressor of Nrf2 (nuclear factor erythroid 2-related factor 2)-mediated adaptive response to oxidative stress (266).

KPNA2 and KPNA7 belonging to clade α2 share only 53% identical amino acids, which is the least conserved among the three subfamilies. KPNA2 was discovered to be the human homologue of yeast SRP1 (serine-rich protein 1) which is a suppressor of RNA polymerase I mutations (267, 268). KPNA2 was also named Rch1 (Rag cohort 1), derived from its interaction with RAG-1, the recombination activating proteins regulating V(D)J recombination (269, 270). KPNA2 has been identified to have the affinity to both monopartite and bipartite NLS sequences (268). KPNA7, another member in clade α2, was identified recently (271). Even though KPNA7 and KPNA2 are closely related, KPNA7 has some divergent properties. In contrast to KPNA2 distributing in the cytoplasm, KPNA7 predominantly localizes in the nucleus. KPNA7 prefers to recognize retinoblastoma (RB) NLS motif rather than SV40-NLS and NPM-NLS. In addition, the IBB domain of KPNA7 is distinct from other KPNAs, with much stronger affinity to KPNB1. On the other hand, KPNA7 was recently reported to mainly express in mouse oocytes and early embryo to facilitate the fertility of mouse (272). KPNA7 has also been found to be highly expressed and promote the malignancy in pancreatic cancer cells (273). These results indicate that KPNA7 mediates the nuclear translocation of specific NLS-cargos and might be involved in the developmental biological process.

The identity between KPNA3 and KPNA4 in clade α3 is extremely high, up to 86% identical amino acids, resulting in their similar functions. They have been demonstrated to mediate the nuclear transportation of the NF-κB p50/p65 heterodimer activated by TNF-α. KPNA4 has also been shown to

directly bind the NLS signals of p50 and p63 and mediate p50 homodimer translocation into the nucleus without stimulation (274). RCC (regulator of chromosome condensation)-1, the chromatin-bound RanGDP/GTP exchange factor, could only be imported by KPNA4, not by other importin members (264).

The manipulation of nuclear transport in viral replication

Viruses must take advantage of host cells for their infection and replication. Many viruses have to transport their genomes into the nucleus, in order to replicate in the nucleus, or integrate their genomic information into the host chromosomes. For those RNA viruses not replicating in the nucleus, certain viral proteins traffic into the nucleus to antagonize host activities and facilitate viral replication.

DNA virus

A DNA virus contains DNA as its genetic material and generally replicates in the nucleus of host cells. There are various strategies for nuclear import of the incoming viral DNA genomes. For instance, Parvovirus is a small non-enveloped virus containing a single-stranded DNA genome associated with capsid protein VP1/VP2. After internalization by endocytosis, parvovirus releases the nucleocapsid allowing VP1 to interact with NPC to deliver the genomic DNA into the nucleus. It has been demonstrated that the N-terminal basic clusters of VP1 are required for the genome import and efficient infection (275, 276).

A large DNA virus, herpes simplex virus type 1 (HSV1), belonging to the *Herpesviridae* family, is enveloped and contains a nucleocapsid of 120 nm. After fusion of the viral envelope with the cellular membrane, the nucleocapsid is released to the cytoplasm, followed by transportation to the NPCs. The interaction between the capsid and NPCs must have specific spatial orientation, with the portal DNA channel of the capsid adjacent to the NPC entrance. Subsequently, the docked nucleocapsid is capable to uncoat and release the DNA genome into the nucleus. The affinity of HSV-1 capsid proteins including

VP1/2, VP13/14, and VP22 to NPCs have been reported to rely on importin β (252, 277, 278). Recently, KPNA2 was found to be required for the nuclear import of several HSV-1 proteins for capsid assembly to assist HSV-1 replication in neurons and fibroblasts (279).

Retrovirus

Unlike other single-stranded positive-sense RNA viruses, retrovirus depends on a DNA intermediate for its replication. Once entered into the host cytoplasm, retrovirus utilizes its reverse transcriptase (RT) to synthesize double-stranded DNA (proviral DNA) from its genomic RNA, generating preintegration complex (PIC). The PIC is composed of proviral DNA, RT, integrase (IN), matrix (MA), the small accessory protein Vpr, and several cellular proteins (280). After transported into the nucleus, PIC integrates the proviral DNA into the host chromosomes for persistent infection. Vpr has been documented to play critical roles in the nuclear import of PIC through its association with NPC protein hCG1 (281). Also, importin 7, which is able to interact with Ran and NPC directly, is crucial for the transportation through binding to the C-terminal region of IN (282).

Negative-sense RNA virus

Influenza virus, belonging to Orthomyxovirus, contains eight segmented negative-sense RNA genomes. Each segmented RNA genome is encapsidated by the viral nucleoprotein (NP) into a ribonucleoprotein (RNP) complex, composed of RNA, NP, and the heterotrimeric RNA-dependent RNA polymerase (RdRp) containing PB1, PB2, and PA (252). Unlike the most RNA viruses, for which the replication is restricted to the cytoplasm of the host cells, influenza viruses transport their RNPs into the nucleus for transcription and replication. After the import of influenza virions to the host cells through clathrin-mediated endocytosis or macropinocytosis, the increasing acidity in late endosomes induces the dissociation of matrix protein M1 from RNPs. The low pH in the late endosomes triggers the

conformational changes of hemagglutinin (HA) to mediate fusion of the viral envelope with the endosomal membrane, followed by the release of RNPs to the cytoplasm (283).

The complex of RNPs recruit cellular transport factors to enter into the nucleus. This process requires NP and PB2, the critical virulence factors involved in viral pathogenicity and host adaptation, to interact with importin α (284). NP has been shown to be recognized by KPNA1 (NPI-1) and KPNA2 (NPI-3) in digitonin-permeabilized cells through its non-classical NLS signal (285, 286). On the other hand, it has been demonstrated that the import of NP and PB2 into the nucleus depends on KPNA4 (importin-α3) for avian influenza viruses, while for mammalian influenza viruses, the specificity switched to KPNA2 (importin-α1) and KPNA6 (importin-α7) which is required for the replication of H1N1 influenza virus in the alveolar epithelium and enhanced virulence in mice (287-289). Moreover, the structural analysis indicated that the bipartite NLS sequence in PB2 could bind with KPNA1 (importin-α5) to allow influenza viruses adapting from avian to mammalian cells (290).

Positive-sense RNA virus

Positive-sense single-stranded RNA (+ssRNA) viruses contain RNA genomes, which function as the messenger RNA to translate into proteins directly by cellular machinery in the host cells. Thus, +ssRNA viruses generally replicate in the cytoplasm rather than in the nucleus of infected cells. However, some viral proteins localize to the nucleus for specific functions, such as interference with host gene expression, hindering host antiviral immune response or other essential activities. Nucleocapsid proteins are the typical ones that enter into the nucleus or nucleolus of the host cells. The nucleocapsid proteins of arteriviruses contain NLS motif and nucleolar retention/localization signal (NoRS/-LS) allowing its interaction with importin α/β to transport into the nucleus and accumulate in the nucleoli (291). It has been reported that the nuclear localization of PRRSV N protein is crucial in viral pathogenesis in vivo even though it might be non-essential for PRRSV infection and replication (292).

On the other hand, hepatitis C virus (HCV) was shown to induce a significant relocation of the nuclear transport factors from the nuclear membrane to ER membrane-derived membranous vesicles (293). In the vesicles, the viral RNA and RdRp of HCV are concentrated and protected from the host defenses and nucleases in the cytoplasm, supporting viral replication with a high efficiency (294). The redistributed host transport factors are supposed to form an NPC-like structures to promote specific cargos to the membranous vesicles in order to promote viral RNA replication (295).

The modulation of karyopherins in viral pathogenesis

Due to their importance in host activities, especially immune response, importins are often targeted by viruses to disturb the host antiviral response. For instance, Ebola virus has been shown to block the interaction between KPNA1 and phosphorylated STAT1 (pSTAT1) through VP24 competitively binding with KPNA1, followed by inhibition of the nuclear translocation of pSTAT1 in order to prevent IFN-activated antiviral signaling pathway (231, 296). Hepatitis B virus was found to block the nuclear transportation of STAT1/2 complex via the polymerase competitively interacting with KPNA1 by its RNase H domain (297). PRRSV was shown to interfere with the IFN signaling by nsp1β inducing the degradation of KPNA1 to inhibit the nuclear translocation of STAT1/2 complex (121). Moreover, HCV could trigger the cleavage of KPNB1 by NS3/4A complex to restrain the nuclear import of IRF3 and NF-κB p65, resulting in the inhibition of antiviral response (298).

Despite substantial efforts have been made to research the interplay between viruses and host nucleocytoplasmic trafficking system, there are still many unknowns. For instance, the cellular proteins and viral factors required for viral genome uncoating and the translocation of the nucleoprotein complexes for many viruses remain unknown. In addition, the subsequent events after the nuclear translocation of the complexes are not well understood. On the other hand, it is not clear that certain viral proteins without identifiable NLS locate in the nucleus. Conducting further research on this front

and addressing these questions will yield informational data to assist our understanding of the virus-host interactions and facilitate the development of unique antiviral strategies.

Chapter 4: Porcine reproductive and respiratory syndrome virus inhibits STAT2 signaling via nsp11-mediated downregulation

Abstract

IFNs play a crucial role in host antiviral response via activating JAK-STAT signaling pathway to induce expression of myriad genes. PRRSV antagonizes the antiviral response by inhibiting IFN synthesis and JAK-STAT signaling. STAT2 is a key player in the IFN-activated JAK-STAT signaling. The objective of this study was to investigate the PRRSV effect on STAT2 signaling. Here, we discovered that PRRSV downregulated STAT2 to inhibit the IFN-activated signaling. PRRSV strains of both *PRRSV-1* and *PRRSV-2* species decreased STAT2 protein level, whereas its transcript had minimal change. PRRSV reduced STAT2 level in a dose-dependent manner and shortened STAT2 half-life significantly from approximately 30 to 10 hours. PRRSV-induced STAT2 degradation could be restored by treatment with the proteasome inhibitor MG132. In addition, PRRSV nsp11 was identified to reduce STAT2. The N-terminal domain (NTD) of nsp11 was responsible for STAT2 degradation and interacted with STAT2 NTD and coil-coil domain (CCD). Mutagenesis analysis showed that three amino acids (57-59, IHK) located in the nsp11 NTD were critical for the interaction of nsp11 with STAT2, resulting in the reduction of STAT2 protein level. Together, these results demonstrate that PRRSV antagonizes STAT2 signaling via nsp11-mediated downregulation. This study provides further insight of PRRSV interference with IFN signaling and the consequent host immune response.

Introduction

IFN is an indispensable component in the innate immunity. Three types of IFNs have been uncovered: type I, II and III (299-301). Upon binding specific receptors, IFNs trigger a signaling

cascade through JAK and STAT, and induce antiviral state by activating expression of a myriad of ISGs, such as ISG15, ISG56, PKR, 2',5'-oligoadenylate synthetase, and Mx GTPases (301, 302).

Both type I and type III IFNs can activate the same canonical JAK-STAT pathway, in which JAKs phosphorylate STAT1 and STAT2, followed by interaction with IRF9 to form a heterotrimer termed ISGF3 (221, 301). The ISGF3 complex translocates into the nucleus to activate the expression of ISGs. On the other hand, there is a STAT1-independent pathway, named non-canonical JAK-STAT signaling. This pathway induces expression of certain ISGs, including APOBEC3G (A3G) having a broad antiviral activity (207). In this non-canonical JAK-STAT pathway, STAT2 and IRF9 form a complex that has ISGF3-like functions to induce prolonged expression of ISGs as well as STAT2/IRF9-specific ISGs, such as A3G, retinoic acid-induced gene G (RIG-G), CCL8 and CX3CL1, in the absence of STAT1 (207). Therefore, STAT2 is indispensable in both canonical and non-canonical IFN-activated signaling pathways.

Due to its essential role in the JAK-STAT pathway, many viruses target STAT2 to antagonize IFN signaling. For example, measles virus V protein binds to STAT2 (233). Yellow fever virus NS5 binds to STAT2 upon IFN stimulation (230). Dengue virus (DENV) NS5 protein recruits the E3 ligase UBR4 to induce STAT2 degradation (229). Similar to DENV, Zika virus (ZIKV) NS5 also promotes STAT2 degradation (236).

Since the first emergence in the late 1980s, PRRS has remained a top challenge to the swine industry (46). PRRSV, the causative agent, is a member of the genus *Porartevirus*, the family *Arteriviridae*, the order *Nidovirales* (1, 50, 303). The conventional two genotypes, Type 1 (European) and Type 2 (North American) PRRSV, have been classified as two species, *PRRSV-1* and *PRRSV-2*, respectively (7). PRRSV is a small enveloped virus containing a positive-sense, single-stranded RNA genome of approximately 15 kb in length. The genome encodes 11 known ORFs (46). The replicase-

associated polyproteins pp1a and pp1ab are encoded by the ORF1a and ORF1b regions, which comprise 4/5 of the viral genome. The polyproteins are processed into more than 14 nonstructural proteins (nsp1-nsp12) by the host and viral proteases. The ORF2, 2a, 3, 4, 5a, 5, 6, and 7 encode structural proteins including minor membrane-associated proteins GP2, E, GP3, GP4, ORF5a, a major envelope glycoprotein (GP5), a membrane protein (M), and a nucleocapsid protein (N), respectively (46, 304). PRRSV has a very restricted tropism for cells of monocyte/macrophage lineage, and pig is the only natural host. *In vivo*, PRRSV preferentially targets porcine PAMs (305). *In vitro*, PRRSV is generally propagated in MARC-145 cell, an epithelial cell-derived cell line from African green monkey kidney (28).

PRRSV infection of pigs induces poor innate (306) and adaptive immune responses (51). It has been shown that PRRSV has several evasion strategies to interfere with the host innate immune response (139, 307). PRRSV appears to suppress the induction of type I IFNs by interfering with the RIG-I signaling pathway (308). PRRSV nsp1α, nsp1β and nsp11 modulate induction of type I IFNs (115, 119, 240). Moreover, PRRSV interferes with the IFN downstream signaling by blocking STAT1/STAT2 nuclear translocation via nsp1β-mediated degradation of KPNA1, which is responsible for ISGF3 nuclear translocation (120, 121, 139). N protein could also inhibit ISGF3 nuclear translocation (158). PRRSV also antagonizes STAT3 signaling via nsp5 (309). PRRSV elevates miR-30c to downregulate JAK1 to inhibit IFN signaling (162). However, the effect of PRRSV infection on STAT2 signaling is unknown.

In this study, we demonstrated that PRRSV downregulated STAT2 to inhibit the IFN-activated signaling. PRRSV strains from both *PRRSV-1* and *PRRSV-2* species reduced STAT2 protein level, whereas its transcript had minimal change. PRRSV infection shortened STAT2 half-life significantly. PRRSV nsp11 was shown to reduce STAT2 protein level. Specifically, nsp11 N-terminal domain (NTD)

interacts with STAT2 NTD and CCD domains. Three amino acids (57-59) in nsp11 are crucial for the interaction with and reduction of STAT2. In conclusion, this study demonstrates that PRRSV antagonizes STAT2 signaling via nsp11-mediated degradation. The data improves our understanding on the mechanism of PRRSV interference with the IFN-activated JAK-STAT signaling.

Materials and methods

Cells, viruses, and chemicals

MARC-145 (28), HEK293 (ATCC CRL-1573) and HeLa (ATCC CCL-2) cells were cultured in Dulbecco modified Eagle medium (DMEM) supplemented with 10% fetal bovine serum (FBS). Primary porcine PAM cells were revived from cryopreserved stock and cultured in RPMI 1640 medium with 10% FBS as previously described (120, 310).

PRRSV strains VR-2385 (29), Ingelvac PRRS MLV (311), Lelystad (312) and A2MC2 (313) were used to inoculate MARC-145 cells at an MOI of 1 or amount indicated in figure legends or results. The median tissue culture infectious dose ($TCID_{50}$) of PRRSV was determined in MARC-145 cells (314).

For virus inactivation, virus inoculum was treated in a UV cross-linker for two 10-min pulses separated by a 1-min interval. Virus inactivation was confirmed by lack of PRRSV-positive cells in inoculated MARC-145 cells at 72 hpi (120).

Cycloheximide (Sigma-Aldrich, St. Louis, MO), a protein translation inhibitor, was added to PRRSV-infected and mock-infected cells at a final concentration of 50 μg/ml to determine the half-life of STAT2. MG132 (Sigma), a proteasome inhibitor, was used to treat cells at a final concentration of 10 μM for 6 h prior to harvesting. Human IFN-α (Genscript) was used to activate the JAK-STAT signaling pathway at a final concentration of 300 U/ml.

Plasmids

The nsp11 of PRRSV VR-2385 was cloned into a pCAGEN-HA vector and pCDNA3-VenusC1 vector (309) with the primers 32nsp11F1 and 85nsp11R1 (Table 1). The nsp11 deletion mutants were cloned into pCAGEN-HA vector using the following primers: 32nsp11F1 and 85nsp11-NTD-R for nsp11-NTD, 32nsp11F1 and 85nsp11-NL-R for nsp11-NTDL, 85nsp11-LC-F and 85nsp11R1 for nsp11-LCTD, and 85nsp11-CTD-F and 85nsp11R1 for nsp11-CTD (Table 1). Nsp11-NTD was also cloned into pCDNA3-VenusC1 vector with the same primers. The nsp11-NTD truncate fragments were cloned into pCDNA3-VenusC1 using the following primers: 32nsp11F1 and 85nsp11-NTD-1R for nsp11-NTD-D1, 85nsp11-NTD-2F and 85nsp11-NTD-R for nsp11-NTD-D2, 85nsp11-NTD-3F and 85nsp11-NTD-3R for nsp11-NTD-D3. STAT2 was cloned into a pCAGEN-Myc vector and pCDNA3-VenusC1 vector with the primers STAT2F1 and STAT2R1. The STAT2 deletion mutants were cloned into pCAGEN-Myc vector using the following primers: STAT2F1 and STAT2R2 for STAT2-D1, STAT2F1 and STAT2R3 for STAT2-D2, STAT2F2 and STAT2R1 for STAT2-D3. The mutants of nsp11-NTD-D2 were cloned into pCDNA3-VenusC1 vector using the following primers: 85nsp11N-D2-m1-F1 and 85nsp11-NTD-R for D2M1, VenusC1F-HindIII, 85nsp11N-D2-m2-F1, 85nsp11N-D2-m2-R1, and 85nsp11-NTD-R for D2M2. The resulting recombinant plasmids were confirmed by restriction enzyme digestion and DNA sequencing.

The construction of the other PRRSV nsp plasmids were described previously (158). The pCDNA3-STAT2 was a gift from Curt M. Horvath (228). The pGL-ISRE used for the IFN-STAT1/2 reporter assay was described previously (158).

RNA isolation and real-time PCR

Total RNA was isolated from MARC-145 cells with TRIzol reagent (ThermoFisher Scientific, Waltham, MA) in accordance with the manufacturer's instructions. Reverse transcription and real-time

PCR (RT-qPCR) (ThermoFisher Scientific) were conducted as described previously (310). Transcripts of ribosomal protein L32 (RPL32), the reference gene, were also detected. The relative transcript levels were shown as fold compared to the control cells after RPL32 normalization. The real-time PCR primers used for STAT2 were R-STAT2-F1 and R-STAT2-R1 (Table 1). The primers used for PRRSV, ISG15, ISG56, and RPL32 were described previously (120). All experiments were repeated at least three times, with each conducted in triplicate.

Western blot (WB) analysis

Cell lysates in Laemmli sample buffer were subjected to SDS-PAGE and WB as described previously (315). The primary antibodies used in this study were against STAT2 (Santa Cruz Biotechnology, Inc., Dallas, TX), STAT1 (Santa Cruz), PRRSV nsp2 protein (14, 316), β-tubulin (Sigma), ubiquitin (Santa Cruz), hemagglutinin (HA) tag (ThermoFisher Scientific), cMyc tag (ThermoFisher Scientific) and GFP (Rockland Immunochemicals, Inc., Gilbertsville, PA). The secondary antibodies used in this study was goat anti-mouse IgG conjugated with horseradish peroxidase (Rockland). The chemiluminescence signal acquisition was conducted by the Quantity One program (v4.6) and a Chemi-Doc XRS imaging system (Bio-Rad Laboratories, Hercules, CA). All experiments were repeated at least three times to warrant the reliability of the results.

Immunoprecipitation (IP)

IP was conducted as previously described (309, 317). The clarified cell lysates were incubated with specific antibodies indicated in Results or Figure Legends, followed by incubation with protein A/G-magnetic beads (Bimake.com, Houston, TX). The IP products were subjected to WB for detection of target proteins. To determine ubiquitinated STAT2, ubiquitin aldehyde (Boston Biochem, Inc., Cambridge, MA), a specific inhibitor of ubiquitin C-terminal hydrolases, was added into the lysis buffer at a final concentration of 2.53 μM.

ISRE Reporter assay

HEK293 cells were transfected with the ISRE reporter plasmid pGL3-ISRE and nsp11 plasmids. The *Renilla* luciferase vector pRL-TK (Promega, Madison, WI), expressing *Renilla* luciferase under the control of a constitutively active promoter, was also transfected for normalization. At 24 hours post transfection (hpt), the cells were treated with 300 U/ml IFN-α and, 24 h later, harvested for luciferase activity assay of firefly and *Renilla* luciferases according to the manufacturer's instructions (Promega). The relative levels of firefly luciferase activity are shown as fold values compared to that of empty vector control after normalization with the *Renilla* activity, as described previously (158, 309).

Immunofluorescence assay (IFA)

IFA was conducted as reported previously (317, 318) with antibodies against HA tag (ThermoFisher Scientific) and cMyc tag (ThermoFisher Scientific). The specific reactions were detected by the conjugated secondary antibodies: goat anti-mouse IgG (H&L) Dylight^{TM} 549 and goat anti-rabbit IgG (H&L) Dylight^{TM} 488 (Rockland Immunologicals). The cover glasses were mounted onto slides using SlowFade Gold antifade reagent containing 4'6'-diamidino-2-phenylindole (DAPI) (ThermoFisher) and observed using Zeiss LSM 510 Meta Confocal Microscope.

Statistical analysis

Differences in indicators between the treatment group and control were assessed by using the Student *t* test. A two-tailed *P* value of 0.05 was considered significant.

Results

PRRSV infection reduces STAT2 protein level

When we studied the effect of PRRSV infection on JAK-STAT signaling, we discovered that PRRSV reduced STAT2 and STAT3 (309) protein levels, while STAT1 remained stable. To confirm the

effect of PRRSV infection on STAT2, we inoculated MARC-145 cells with PRRSV strain VR-2385 and harvested the cells at 36 hours post infection (hpi). Compared to mock-infected cells, PRRSV-infected cells had lower level of STAT2 at 16% but similar level of STAT1 (Fig. 4.1A). PRRSV nsp2 was determined to verify PRRSV infection. As PRRSV targets PAMs during pig infection, we infected primary porcine PAM cells with VR-2385 to confirm the effect of PRRSV infection on STAT2. Due to the enhanced replication of PRRSV in PAM cells, these cells were harvested at 16 hpi (309). Like in MARC-145 cells, PRRSV infection reduced STAT2 level in PAM cells to 16% in comparison with mock-infected control, whereas STAT1 had a minimal change (Fig. 4.1B).

STAT2 plays a critical role in IFN-activated JAK-STAT signaling pathway. We conducted an IFN treatment to confirm that PRRSV infection interfered with type I IFN signaling (120, 121). MARC-145 cells were inoculated with VR-2385 and, at 24 hpi, treated with IFN-α for 24 h. The reverse transcription and quantitative PCR (RT-qPCR) results showed that the transcript levels of ISG15 and ISG56 in IFN-treated cells increased by 55- and 32-fold, respectively, in comparison with mock-treated cells (Fig. 4.1C). As expected, the transcript level of ISG15 and ISG56 in PRRSV-infected cells with IFN treatment were at 9% and 11%, respectively, compared to the mock-infected cells (Fig. 4.1C), which is consistent with the previous observation (120).

We speculated that VR-2385-induced reduction of STAT2 could be relevant to other PRRSV strains. Therefore, other strains from both *PRRSV-1* and *PRRSV-2* species were used to infect MARC-145 cells to verify that the STAT2 reduction is a common effect among different strains. The strains used were Lelystad virus, the prototype of *PRRSV-1,* Ingelvac® PRRS MLV, and IFN-inducing vaccine candidate strain A2MC2 (313, 319), strain of *PRRSV-2*. As expected, A2MC2 elevated protein level of STAT2. In contrast, VR-2385, MLV and Lelystad reduced STAT2 to 12%, 10%, and 33%, respectively, compared to mock infected control. STAT1 level in the infected cells remained unchanged (Fig. 4.1D). PRRSV RNA of these strains were determined by RT-qPCR (Fig. 4.1E). The Lelystad virus had the

lowest RNA level, which is in consistent with the least effect on STAT2 level in the cells infected by this strain.

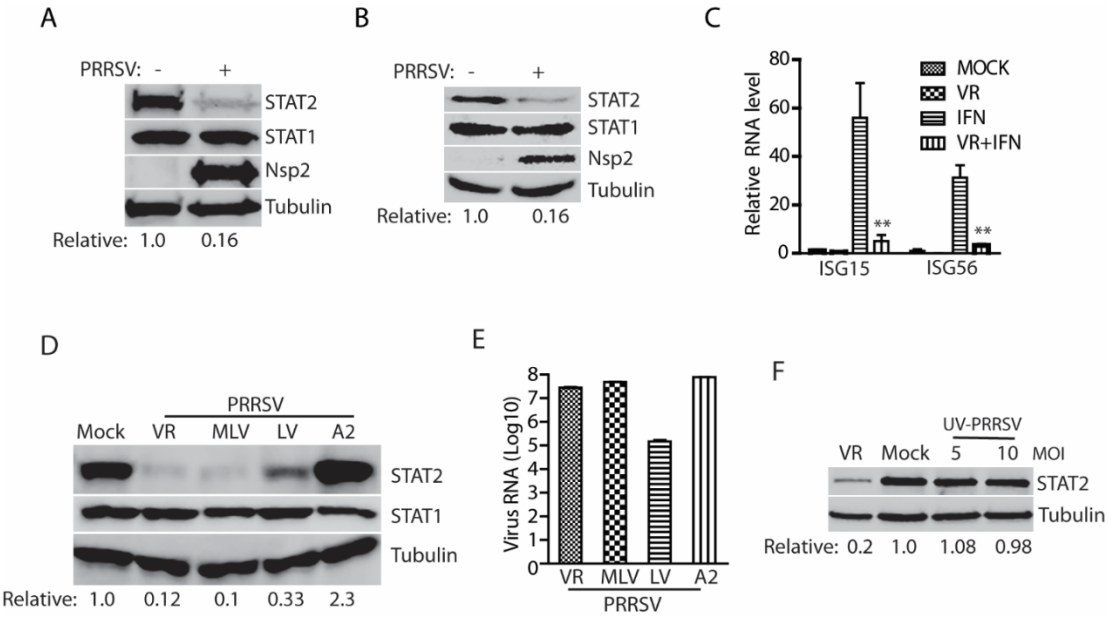

Fig. 4.1 PRRSV infection reduces STAT2 in MARC-145 and PAM cells. A. PRRSV reduces STAT2 protein level but has minimal effect on STAT1. MARC-145 cells were infected with VR-2385 at an MOI of 1 and harvested 36 hours post-infection (hpi) for Western blotting (WB) with antibodies against STAT2, STAT1, PRRSV nsp2, and tubulin. Relative levels of STAT2 are shown below the images after normalization with tubulin in densitometry analysis. B. PRRSV reduces STAT2 in PAM cells but has minimal effect on STAT1. The cells were infected with VR-2385 at an MOI of 1 and harvested for WB at 16 hpi. C. PRRSV inhibits IFNα-activated expression of ISG15 and ISG56 detected by RT-qPCR. MARC-145 cells were infected with VR-2385 at an MOI of 1 and, 24 hpi, treated with IFN-α at a final concentration of 300 U/ml for another 24 hours. VR: VR-2385. D. Reduction of STAT2 by different PRRSV strains with the exception of A2 (A2MC2) in MARC-145 cells. The cells were infected with VR-2385, MLV (Ingelvac PRRS$^{@}$ MLV), LV (Lelystad virus), and A2 at the MOI of 1. The relative levels of STAT2 are shown below the images after normalization with tubulin. E. PRRSV RNA levels of the PRRSV strains detected by RT-qPCR. Viral-infected MARC-145 cells were harvested for RNA isolation and RT-qPCR at 24 hpi. Error bars represent the standard errors of the results of three repeated experiments. F. UV-inactivated PRRSV has minimal effect on STAT2 level. The cells were inoculated with PRRSV VR-2385 at an MOI of 1 or UV-inactivated VR-2385 at the MOI of 5 and 10, followed by WB at 36 hpi.

To interrogate if PRRSV replication was indispensable for STAT2 reduction, we inactivated VR-2385 by UV light and inoculated MARC-145 cells with the UV-inactivated VR-2385 at the multiplicities of infection (MOIs) of 5 and 10. Western blotting (WB) result showed that only live PRRSV virions led to the STAT2 reduction, while the UV-inactivated PRRSV had minimal effect (Fig.

4.1F), suggesting that PRRSV replication is needed to induce STAT2 reduction and that PRRSV structural proteins in the inactivated virions had negligible effect.

PRRS reduces STAT2 protein level in a dose and time-dependent manner

To further study PRRSV-mediated reduction of STAT2, we infected MARC-145 cells with VR-2385 at the MOIs of 0.1, 1, and 10. Along with the increased amount of VR-2385 inoculum, the STAT2 protein level decreased in a dose-dependent manner. Compared to the mock-infected cells, the cells

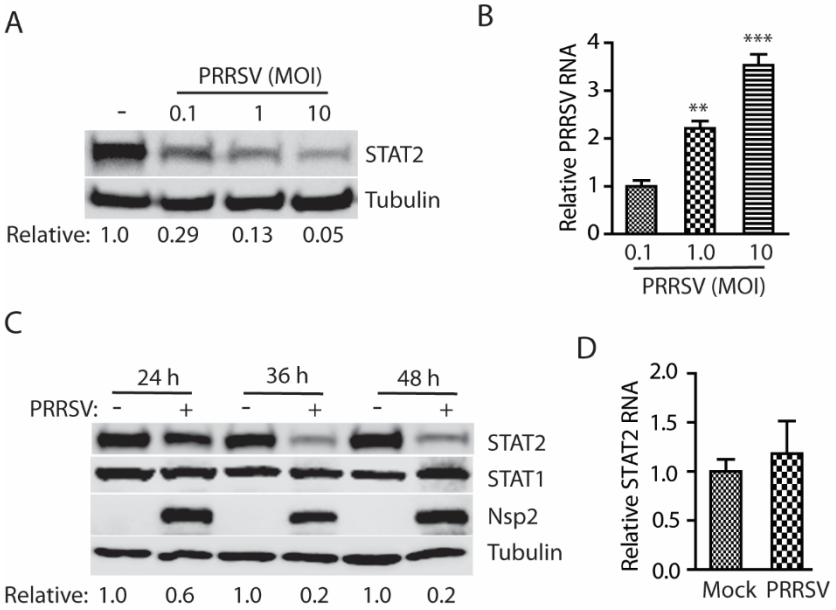

Fig. 4.2 PRRSV reduces STAT2 in a dose and time-dependent manner. A. Dose-dependent reduction of STAT2 by PRRSV. MARC-145 cells were inoculated with incremental MOI of VR-2385 and harvested for WB at 36 hpi. Relative levels of STAT2 are shown below the images after normalization with tubulin. B. PRRSV RNA levels detected by RT-qPCR. Error bars represent the standard errors of the means of three repeated experiments. Significant differences in RNA level from an MOI of 0.1 are denoted by asterisks (**, $P < 0.01$; ***, $P < 0.001$). C. Temporal kinetics of STAT2 levels in PRRSV-infected cells. MARC-145 cells were infected with VR-2385 at an MOI of 1. At different time points, the cells were harvested for WB. Mock-infected cells at corresponding time points were included as controls. Relative levels of STAT2 are shown below the images after normalization with tubulin at corresponding time point. D. PRRSV infection has minimal effect on STAT2 mRNA level. The cells were harvested at 24 hpi for RNA isolation and RT-qPCR. The relative STAT2 mRNA levels are shown in comparison with the mock-infected cells. Error bars represent standard errors of the results of three repeated experiments.

inoculated at the MOIs of 0.1, 1, and 10 had STAT2 levels at 29%, 13%, and 5%, respectively (Fig. 4.2A). PRRSV RNA levels in the infected cells significantly increased, which was consistent with the incremental inoculum (Fig. 4.2B).

Temporal kinetics of STAT2 protein level in the infected cells was analyzed to determine if the change of STAT2 level occurred during a specific period post infection. MARC-145 cells were infected with PRRSV VR-2385 at an MOI of 1 and harvested at 24, 36 and 48 hpi. Compared to the mock-infected cells, the STAT2 levels in the virus-infected cells at 24, 36, and 48 hpi decreased to 60%, 20%, and 20%, respectively, while STAT1 levels remained stable (Fig. 4.2C). This result demonstrated that PRRSV infection reduced STAT2 protein level in a time-dependent manner.

In mammalian cells, the protein reduction could be due to a decrease in transcription and/or translation or accelerated protein degradation. To investigate the reason for PRRSV-induced STAT2

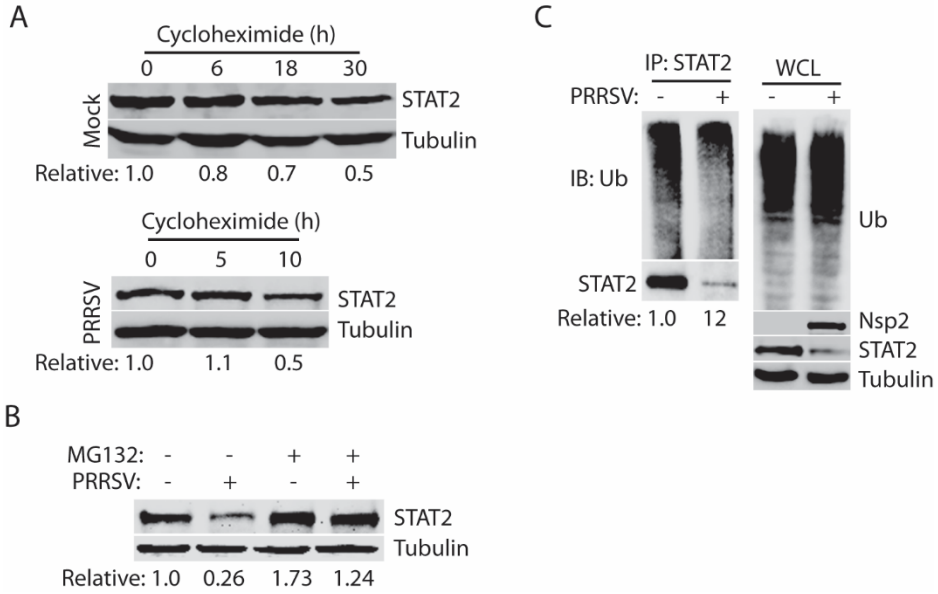

Fig. 4.3 PRRSV infection shortens STAT2 half-life and mediates STAT2 reduction via ubiquitin-proteasome degradation pathway. A. PRRSV extends STAT2 half-life. MARC-145 cells were infected with VR-2385 at an MOI of 1. The cells were treated with cycloheximide at 24 hpi and harvested at the indicated time (h) for WB. The relative levels of STAT2 are shown below the images. B. MG132 treatment restores STAT2 level in PRRSV-infected cells. MARC-145 cells were infected with VR-2385 at an MOI of 1. At 24 hpi, the cells were treated with MG132 for 6 h and then harvested for WB. Non-treated and mock-infected cells were included as controls. C. PRRSV induces elevation of STAT2 polyubiquitination. MARC-145 cells were infected with PRRSV VR-2385 at an MOI of 1 and harvested for IP with STAT2 antibody at 36 hpi, followed by WB with the ubiquitin (Ub) antibody. WB of whole cell lysate (WCL) was conducted. The relative levels of Ub after normalization with STAT2 are shown below the images.

reduction, we performed RT-qPCR to determine the transcript level of STAT2 in PRRSV-infected cells. In comparison with mock-infected cells, PRRSV-infected cells had similar mRNA level of endogenous

STAT2 (Fig. 4.2D). The result demonstrated that PRRSV-induced STAT2 reduction was not due to the decreased level of mRNA transcription.

PRRSV infection shortens STAT2 half-life

Since PRRSV infection did not affect the transcript level of STAT2, we speculated that PRRSV might accelerate the rate of STAT2 degradation. We then wondered whether the half-life of STAT2 would be shortened by PRRSV. PRRSV infected MARC-145 cells for 24 hours were treated with cycloheximide, a translation inhibitor, followed by harvesting and immunoblotting at indicated time points. In the presence of PRRSV, the STAT2 half-life was shortened to 10 hours, compared to that of 30 hours in mock-infected cells (Fig. 4.3A). The results suggest that the shortened STAT2 half-life may account for its lower level in PRRSV-infected cells.

PRRSV mediates STAT2 reduction via the ubiquitin-proteasome degradation pathway

Since PRRSV shortened STAT2 half-life, we further identified the protein degradation pathway for PRRSV infection in reducing STAT2 level. The ubiquitin-proteasome system accounts for the turnover of most short-lived cellular proteins. We used MG132, a proteasome inhibitor to treat MARC-145 cells at 30 hpi. After MG132 treatment for 6 hours, the cells were harvested for immunoblotting. The MG132-treated PRRSV-infected cells displayed a similar level of STAT2 to mock-infected cells (Fig. 4.3B). As described previously, the short treatment with MG132 did not cause detectable cytotoxicity or inhibition of PRRSV replication (317). This result indicates that PRRSV induces STAT2 reduction through the ubiquitin-proteasome degradation pathway.

Since MG132 treatment could restore STAT2 protein level in PRRSV-infected cells, we speculated increased level of STAT2 poly-ubiquitination level in the cells. MARC-145 cells infected with PRRSV were lysed for immunoprecipitation (IP) with an antibody against STAT2. WB with

antibodies against ubiquitin and STAT2 showed the poly-ubiquitination level of STAT2 in PRRSV-infected cells was 12-fold higher than that of mock-infected cells after normalization with STAT2 protein level (Fig. 4.3C). In contrast, WB analysis of whole-cell lysates (WCL) showed similar levels of the total ubiquitination with or without PRRSV infection.

PRRSV nsp11 reduces STAT2 protein level

As Fig. 1F indicated that PRRSV replication was critical for STAT2 reduction, we speculated

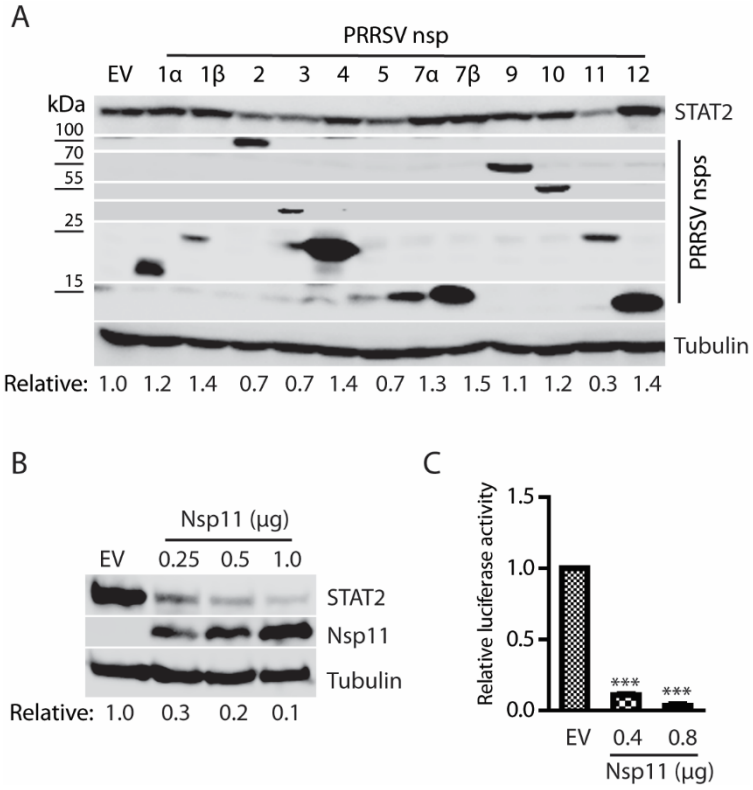

Fig. 4.4 PRRSV nsp11 induces reduction of STAT2. A. Nsp11 reduces STAT2 in HEK293 cells, whereas other PRRSV nsps have minimal effect. The cells were transfected with individual HA-nsp plasmids and STAT2 plasmid. An empty vector (EV) was included as a control. The relative levels of STAT2 protein are shown below the images. Molecular mass markers are added on left side of the nsp images. B. Nsp11 reduces STAT2 in HeLa cells in a dose-dependent manner. HeLa cells were transfected with nsp11 plasmid in incremental amounts. C. Nsp11 inhibits IFN-α activated expression of ISRE reporter in HEK293 cells. The cells were co-transfected with ISRE luciferase reporter, Renilla luciferase plasmid, and HA-nsp11. The relative levels of firefly luciferase activity are shown as fold compared to the EV control after normalization with the Renilla activity. A significant difference in firefly luciferase activity from the EV control is denoted by asterisks (***, $P < 0.001$).

that certain non-structural proteins (nsps) were responsible for PRRSV-induced STAT2 reduction.

HEK293 cells were transfected with plasmids encoding PRRSV VR-2385 nsps to assess their effects on STAT2 degradation. WB results showed that nsp11 resulted in a lower level of STAT2 protein compared to that of empty vector (EV), whereas other PRRSV plasmids did not affect STAT2 degradation (Fig. 4.4A). Therefore, we further analyzed the role of nsp11 in STAT3 degradation.

HeLa cells were transfected with nsp11 plasmid to confirm its effect on STAT2. Densitometry analysis showed that the STAT2 levels in HeLa cells transfected with 0.25, 0.5, and 1.0 g of nsp11 plasmid were reduced to 30%, 20%, and 10%, respectively, compared to that of the empty vector control (Fig. 4.4B). The nsp11 protein level increased along with the incremental DNA in the transfection. This indicated that nsp11 reduced STAT2 protein level in a dose-dependent manner. IFN-stimulated response element (ISRE) promoter luciferase assay confirmed that nsp11 significantly inhibited type I IFN signaling (Fig. 4.4C).

The N-terminal domain of nsp11 is responsible for the reduction of STAT2 via interacting with STAT2

PRRSV nsp11 contains a nidovirus uridylate-specific endoribonuclease (NendoU) domain, which is indispensable for arterivirus replication (141, 144). NendoU has been demonstrated to cleave 5' uridine nucleotides of RNA substrates to generate a 2'-3'-cyclic phosphate end product, similar with XendoU, an endoribonuclease in eukaryotes (142, 143). STAT2 mRNA level in PRRSV-infected cells remained the same level as mock-infected cells (Fig. 4.2D), indicating that the NendoU did not contribute to the nsp11-mediated STAT2 reduction.

The crystal structure analysis of nsp11 shows that nsp11 has three different domains, N-terminal domain (NTD), linker domain, and C-terminal domain (CTD) (144). To map the nsp11 domain corresponding to the STAT2 degradation, we constructed four truncation plasmids of VR-2385 nsp11: NTD from amino acid (aa) 1 to 90, NTD with linker domain (NTDL) from aa 1 to 106, linker domain with C-terminal domain (LCTD) from aa 91 to 223, and CTD from aa 107 to 223 (Fig. 4.5A). HEK293

cells were transfected with the nsp11 truncation plasmids. WB results and densitometry analysis showed that the cells transfected with nsp11-NTD and nsp11-NTDL had lower STAT2 protein levels at 40% and 30%, respectively, compared to that of the cells transfected with the empty vector (Fig. 4.5B). The expression levels of the nsp11 truncation constructs in HEK293 cells were confirmed with HA antibody. The results indicate that the NTD of nsp11 is responsible for the PRRSV-induced degradation of STAT2.

Furthermore, we evaluated whether nsp11-NTD had interaction with STAT2. HEK293 cells were transfected with myc-STAT2 and YFP-nsp11-NTD plasmids. Indeed, IP of STAT2 co-precipitated nsp11-NTD (Fig. 4.5C). The expression of YFP, YFP-nsp11-NTD, and myc-STAT2 was confirmed in whole cell lysate.

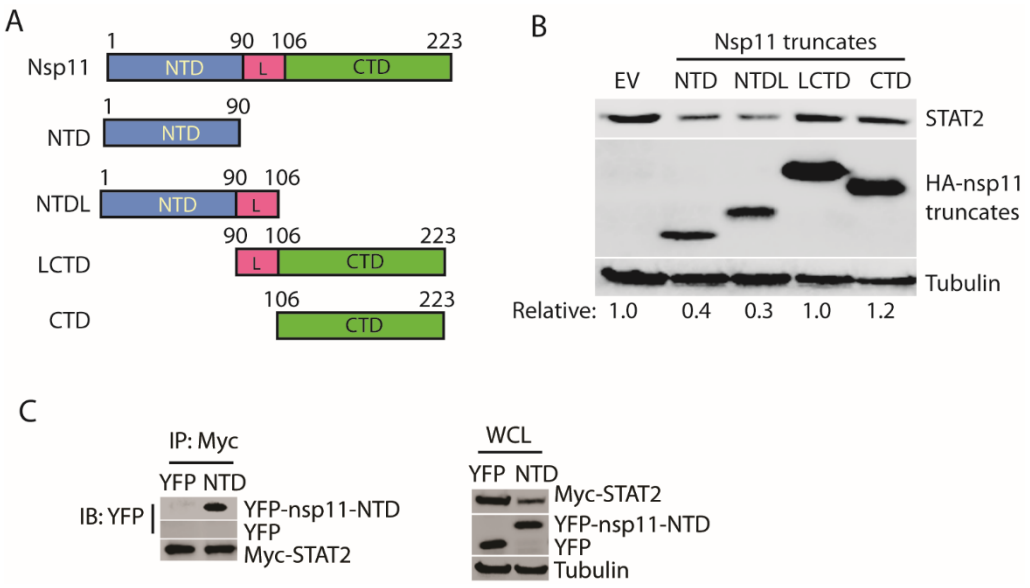

Fig. 4.5 The N-terminal domain of PRRSV nsp11 is required for STAT2 reduction. A. Schematic illustration of truncation plasmids of nsp11: NTD, NTDL, LCTD, and CTD. The numbers above the lines indicate amino acid positions in nsp11. NTD: N-terminal domain; CTD: C-terminal domain; L: linker domain. B. The NTD and NTDL lead to STAT2 reduction, whereas LCTD and CTD have minimal effect. HEK293 cells were co-transfected with the HA-tagged nsp11 truncation plasmids and STAT2 plasmid. EV was included as a control. C. IP of STAT2 co-precipitates nsp11-NTD. IP with cMyc antibody followed by WB with YFP and cMyc antibodies were done. Samples of whole-cell lysate (WCL) were included as controls.

The N-terminal domain of STAT2 interacts with nsp11-NTD

As a transcription factor, STAT2 has a conserved structure containing several domains, such as coil-coil, DNA binding, Src homology 2 (SH2) and transactivation domains (320). To identify interacting domains with nsp11-NTD, we constructed three truncates of STAT2: D1 (aa 1-315), D2 (aa 1-480) and D3 (aa 481-851) using Myc-tagged recombinant plasmids (Fig. 4.6A). HEK293 cells were transfected with YFP-nsp11-NTD and one of the Myc-tagged STAT2 truncates, followed by IP with

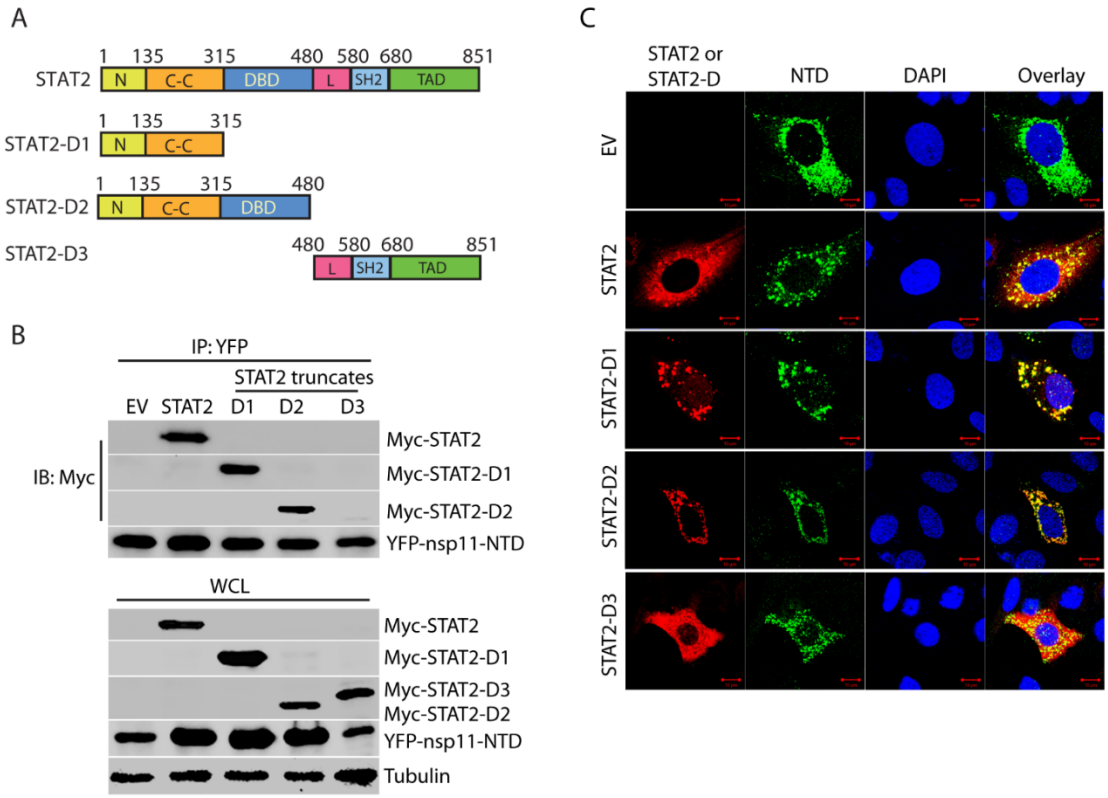

Fig. 4.6 Nsp11 NTD interacts with N-terminal domain of STAT2. A. Schematic illustration of truncation plasmids STAT2: D1, D2 and D3. The numbers above the lines indicate amino acid positions in STAT2. N: N-terminal domain; C-C: coil-coil domain; DBD: DNA binding domain; L: linker domain; SH2: Src homology 2 domain; TAD: transactivation domain. B. IP of nsp11-NTD co-precipitates STAT2, STAT2-D1 and STAT2-D2, but not STAT2-D3. HEK293 cells were transfected with YFP-nsp11-NTD and Myc-STAT2 or STAT2 truncate plasmids. IP with YFP antibody followed by WB with cMyc and YFP antibodies was done. Empty vector (EV) was included as control. WB of whole cell lysate (WCL) were done. C. Nsp11-NTD has co-localization with STAT2, STAT2-D1, and STAT2-D2, but not STAT2-D3 in HeLa cells. The cells were transfected with plasmids of HA-nsp11-NTD and Myc-STAT2 or STAT2 truncate plasmids. IFA with antibodies against HA and cMyc was conducted, followed by confocal microscopy. The red fluorescence indicates STAT2 or STAT2 truncates, while the green fluorescence indicates nsp11-NTD. DPAI staining of DNA is also shown. The bars in lower right corners of the images denote 10 μm.

YFP antibody and WB with antibodies against cMyc and YFP. The IP of nsp11-NTD co-precipitated

STAT2, STAT2-D1 and STAT2-D2, whereas it failed to pulldown STAT2-D3 (Fig. 4.6B). The expression of these plasmids was confirmed in HEK293 cell lysates.

The IP results suggest that nsp11-NTD might have co-localization with STAT2, STAT2-D1 and STAT2-D2, but not STAT2-D3. Therefore, we further transfected HeLa cells with HA-nsp11-NTD and Myc-STAT2 or STAT2 truncate plasmids, followed by IFA with antibodies against HA and cMyc. Confocal microscopy analyses showed that nsp11-NTD had co-localization with STAT2, STAT2-D1, and STAT2-D2, but not STAT2-D3 (Fig. 4.6C). STAT2-D3 had homogenous distribution throughout the cytoplasm, different from the puncate pattern of nsp11-NTD.

Both co-IP and confocal microscopy results indicate that nsp11-NTD interacts with STAT2-D1 and STAT2-D2. These two STAT2 truncates have the same first 315 aa in the N-terminal and coil-coil domains of STAT2, thus identifying this first 315 aa of STAT2 as the nsp11 interaction site.

Three amino acids of nsp11 are crucial for the interaction with STAT2

Structural analysis of the nsp11 showed several stretches of amino acids in nsp11-NTD with potential surface orientation, indicating that these surface-oriented amino acids might correlate with STAT2 degradation. Therefore, we constructed three truncates of nsp11-NTD: D1 (aa 1-51), D2 (aa 52-90), and D3 (aa 35-65) into pCDNA3-VenusC1 vector (Fig. 4.7A). HEK293 cells were transfected with nsp11, nsp11-NTD, and the three nsp11-NTD truncates to determine their effects on STAT2 protein level. WB analyses showed that except for the empty vector and nsp11-NTD-D1, all the others induced STAT2 degradation (Fig. 4.7B). The nsp11-NTD-D2 induced the STAT2 reduction to 17% and nsp11-NTD-D3 to 46%. This indicates that aa 52-65 of nsp11 contain the key site for the induction of STAT2 decrease. The expression of these proteins were confirmed by WB with YFP antibody.

The fragment of aa 52-65 contains one stretch of amino acids, aa 57-62, with potential surface orientation, which are also highly conserved across different PRRSV strains. We then conducted

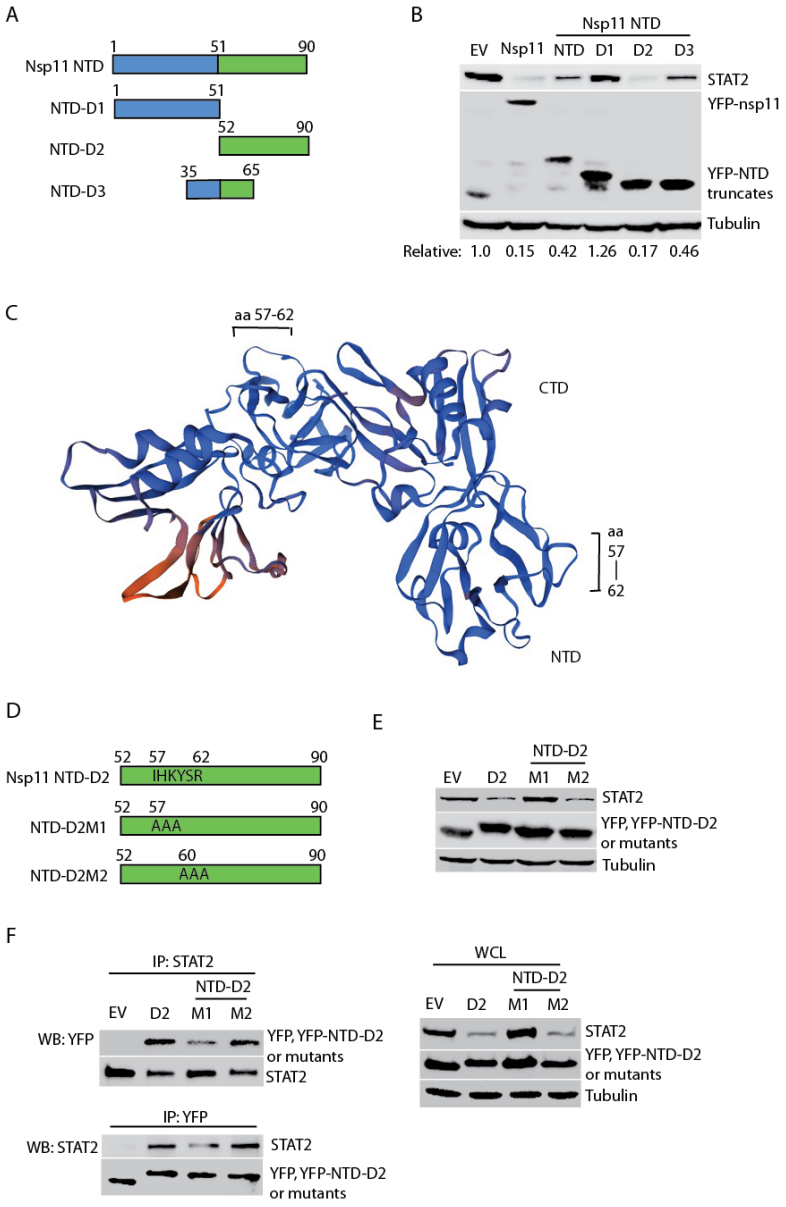

Fig. 4.7 Mapping motifs in Nsp11-NTD that are required for STAT2 reduction. A. Schematic illustration of truncation plasmids nsp11-NTD: D1, D2 and D3. The numbers above the lines indicate amino acid positions in nsp11. B. The NTD-D2 and NTD-D3 lead to STAT2 reduction, whereas NTD-D1 has minimal effect. HEK293 cells were co-transfected with the YFP-tagged nsp11-NTD truncation plasmids and STAT2 plasmid. EV was included as a control. The cells were harvested at 36 hpt for immunoblotting with antibodies against STAT2, YFP, and tubulin. Relative levels of STAT2 are shown below the images after normalization with tubulin. C. A possible model of nsp11 protein constructed by SWISS-MODEL (https://swissmodel.expasy.org/). The loop of aa 57-62 is shown on upper and right side of the nsp11 dimer. D. Schematic illustration of mutant plasmids of nsp11-NTD-D2: D2M1 (I57A, H58A, and K59A) and D2M2 (Y60A, S61A, and R62A). E. The NTD-D2M1 fails to reduce STAT2, whereas NTD-D2M2 induces STAT2 decrease similarly to wild type NTD-D2. F. IP of STAT2 co-precipitates nsp11 NTD-D2 and NTD-D2M2 but much less NTD-D2M1. IP of YFP-tagged nsp11 NTD-D2 and NTD-D2M2 co-precipitates STAT2, whereas much less STAT2 in NTD-D2M1 pulldown. WB of WCL was done.

SWISS-MODEL analysis (https://swissmodel.expasy.org/) to determine if the aa 57-62 (IHKYSR) are located on surface of nsp11 protein. Indeed, aa 57-62 are located on one of the outside loops in the nsp11 NTD (Fig. 4.7C). PRRSV nsp11 is known to form a homodimer with by interaction between NTD and CTD of each monomer (144, 321). Accordingly, two loops of aa 57-62 are shown.

We speculated that aa 57-62 might correlate with STAT2 interaction or degradation. We constructed two mutants of nsp11-NTD-D2: D2M1 (I57A, H58A, and K59A) and D2M2 (Y60A, S61A, and R62A) with each having three amino acids changed to alanine (Fig. 4.7D). HEK293 cells were transfected with these mutants to test their effect on STAT2 protein level. WB results showed that nsp11 NTD-D2M1 could not induce STAT2 reduction, while NTD-D2M2 had the similar effect to wild type NTD-D2 (Fig. 4.7E). These results indicate that the mutations in NTD-D2M1 led to the loss of the capability to induce STAT2 reduction and that aa 57-59 (IHK) were crucial for the nsp11 induction of STAT2 degradation.

We further conducted co-immunoprecipitation to determine whether the mutation in NTD-D2M1 led to the loss of interaction with STAT2. IP of STAT2 co-precipitated nsp11 NTD-D2 and NTD-D2M2 in similar levels but NTD-D2M1 at a reduced level. In contrast, cells transfected with EV and NTD-D2M1 had higher level of STAT2 than those of NTD-D2 and NTD-D2M2, as shown in WB of whole cell lysate (Fig. 4.7F). Conversely, YFP IP of NTD-D2 and NTD-D2M2 co-precipitated STAT2, whereas much less STAT2 could be co-precipitated by IP of NTD-D2M1 and no STAT2 in IP of YFP empty vector. These results demonstrated that the mutations of aa 57-59 in NTD-D2M1 affected nsp11 function in the STAT2 degradation via weakening its interaction with STAT2.

Discussion

Canonical JAK-STAT pathway is activated by many cytokines, including IFNs, interleukins, and granulocyte-macrophage colony-stimulating factor (GM-CSF). In mammalian cells, there are seven

STAT members: STAT1, STAT2, STAT3, STAT4, STAT5A, STAT5B, and STAT6. Among these seven STATs, STAT2 is unique (320). STAT2 is only activated by type I and type III IFNs, while STAT1 can respond to all three types of IFNs, IL-4, and IL-6 (322). Except for STAT2, all other STAT proteins have at least two isoforms with specific functions. Moreover, STAT2 is the largest STAT with the molecular mass of 113 kDa.

In addition to be a key component in the canonical IFN-activated JAK-STAT signaling, STAT2 involves in STAT1-independent IFN signaling (207). In the non-canonical IFN signaling pathway, STAT2/IRF9 complex functions an ISGF3-like response and provides an alternative antiviral activity in the deficiency of STAT1 (207). It was reported that STAT2 binds to the ISRE of ISG15, ISG56, IFI27, MX1, OAS2, and IFIT3 genes in the absence of STAT1. Moreover, the study of STAT2/IRF9 identified a set of ISGF3-independent ISGs, including CCL8 and CX3CL1. In addition, during lymphocytic choriomeningitis virus (LCMV) infection, STAT2/IRF9 directed pro-inflammatory immune response in the absence of STAT1, suggesting that the ISGF3-like complex has a novel role in inflammation (323). Therefore, STAT2 is indispensable in IFN-activated signaling.

In this study, we demonstrated that PRRSV antagonizes STAT2 signaling via nsp11-mediated degradation. The observation was confirmed from multiple aspects. First, PRRSV induced STAT2 degradation in both MARC-145 and PAM cells but had no effect on STAT1 protein level. Several strains from both PRRSV species reduced STAT2, without affecting STAT1, which indicates that the PRRSV-induced STAT2 reduction was specific and might be an inherent property of PRRSV infection. Secondly, the PRRSV-induced STAT2 reduction was dose and time-dependent. Thirdly, MG132 treatment restored STAT2 level in PRRSV-infected cells, which indicates that PRRSV-mediated STAT2 reduction was via the ubiquitin-proteasome pathway. Consistent with this result, STAT2 half-life was

shortened by PRRSV from 30 to 10 hours. PRRSV infection had minimal effect on STAT2 transcript level, but induced significantly higher STAT2 poly-ubiquitination level than mock-infected cells.

UV-inactivated PRRSV had no effect on STAT2 protein level, which indicates that the structural proteins of PRRSV had a negligible role in PRRSV-mediated STAT2 reduction. PRRSV nsp11 was identified to be responsible for STAT2 reduction. Consequently, nsp11 was able to inhibit IFN-α activated expression of ISRE reporter. Nsp11 was found to suppress MAVS and RIG-I expression through its endoribonuclease domain to antagonize type I IFN induction (147, 148). It was reported that nsp11 has DUB activity, which perturbs NF-κB activation (145). Recently, it was reported that nsp11 recruits cellular deubiquitinase OTULIN to inhibit the production of type I IFNs (324).

Since we demonstrated that PRRSV had no effect on STAT2 mRNA level and that nsp11 NTD was responsible for STAT2 reduction, the endoribonuclease activity in the C-terminal domain of nsp11 should have no role in the STAT2 downregulation. Wang et al. (145) reported that nsp11 has pan-DUB activity and that amino acids C112, H144, D173, K180, and Y219 are crucial for the DUB activity. However, we found that STAT2 poly-ubiquitination level in PRRSV-infected cells was higher than mock-infected cells. Overexpression of nsp11 NTD (aa 1-90) also led to higher STAT2 poly-ubiquitination level (data not shown). The discrepancy is possibly because that different PRRSV strains and cells are used in different labs and that nsp11 might exert the DUB activity indirectly. The second speculation is more plausible. Our results is consistent with another report that nsp11 lacks conserved catalytic residues for DUB and cannot pulldown the ubiquitin (321). It was proposed that nsp11 is not directly involved in deubiquitinating activity.

We further determined the mechanism of nsp11-mediated STAT2 reduction. The nsp11 NTD is formed by six β-strands and two α-helices and is connected to the catalytic CTD through a linker domain (144, 321). Mutations of S74A and F76A disrupt nsp11 dimerization. Our data showed that the nsp11-

NTD induced STAT2 degradation. Interestingly, IP of nsp11-NTD co-precipitated STAT2, which suggests that nsp11-NTD induces STAT2 degradation through interacting with STAT2.

We also analyzed the interaction domain in STAT2. Like other STATs, STAT2 has six conserved domains. NTD is required for the tyrosine phosphorylation (325) and the interaction with IFN receptor (326). CCD of STAT2 is the specific domain that IRF9 binds (327). Direct binding of ISGF3 to DNA is mediated by STAT1 and IRF9, not STAT2, so STAT2 DNA-binding domain (DBD) seems to bind the promoter of ISGF3-independent ISGs (328). Moreover, STAT2 DBD contains a cluster of basic amino acids to function as a bipartite NLS when binding with the conserved corresponding region of STAT1 (329). The function of linker domain (LD) remains unknown. The SH2 domain is responsible for STAT2 to bind to phosphorylated IFN receptor and interact with phosphorylated STAT1 to form a heterodimer (330). Transactivation domain (TAD) is indispensable for transcription factors to recruit other co-activators or transcriptional regulators (331). One nuclear export signal (NES) lies in STAT2 TAD to mediate STAT2 exportation from the nucleus back to the cytoplasm (332).

Our IP and confocal microscopy analyses showed that the NTD and CCD of STAT2 interacted with nsp11-NTD. Interestingly, the STAT2 truncates had different distribution pattern from the full-length STAT2 (Fig. 6C). STAT2-D1 and STAT2-D2 showed more punctates in the cytoplasm than the full-length STAT2, whereas STAT2-D3 displayed homogenous cytoplasmic distribution. When co-transfected with nsp11, there were more punctates of STAT2, STAT2-D1 and STAT2-D2 in distribution than they were expressed alone. These results indicate that the interaction of nsp11 and STAT2 results in more punctate distribution pattern.

In addition, we identified the critical amino acids in nsp11 that correlate with the STAT2 reduction. Our results showed that the nsp11 NTD-D2 and NTD-D3 led to STAT2 reduction, whereas NTD-D1 had minimal effect. We conducted mutagenesis of NTD-D2 based on sequence and

computational structure analyses, and generated two mutants. Mutation at aa 57-59 (IHK) in NTD-D2M1 led to the loss of the nsp11 capability in inducing STAT2 degradation. This suggests that aa 57-59 residues are crucial to the nsp11-induced STAT2 reduction. Co-IP results showed that NTD-D2M1 had much weaker interaction with STAT2 than NTD-D2M2 and wild type NTD-D2. The NTD-D2M2 could co-precipitate similar level of STAT2 to NTD-D2. These results indicate that aa 57-59 are indispensable for nsp11 to interact with and downregulate STAT2.

As the first line of defense against viral infections, IFN is indispensable in the host innate immunity. To antagonize IFNs, PRRSV suppresses the production of type I IFNs by inhibiting IRF3 phosphorylation (119), cleaving MAVS (333), and suppressing RIG-I and MAVS expression (147), and blocks IFN-activated downstream signaling by degrading KPNA1 to block STAT1/STAT2 nuclear translocation (121) and inducing STAT3 degradation (309). In this study, we further demonstrated that PRRSV also targets STAT2 to antagonize IFN signaling.

In conclusion, our results demonstrated that PRRSV infection induced STAT2 degradation via the ubiquitin-proteasome pathway. Specifically, PRRSV induces STAT2 degradation by interaction between nsp11-NTD and STAT2 NTD and CCD, and aa 57-59 residues in nsp11 are critical for the interaction with and downregulation of STAT2. This provides further insights of PRRSV interference with IFN signaling, in addition to inhibiting STAT1/2 translocation from the cytoplasm into the nucleus. This study not only identifies additional function of nsp11 having endoribonuclease and DUB activities, but also provides further insight into PRRSV interference with IFN signaling and consequent host immune response.

Table 4.1 List of primers used in Chapter 4

Primer[a]	Sequences (5' to 3')[b]	Target gene/vector

32nsp11F1	CGGAATTCGGGTCGAGCTCTCCGCTCC	Nsp11
32nsp11R1	CCGCTCGAGTTATTCAAGTTGGAAATAGGC	Nsp11
85nsp11-NTD-R	CCGCTCGAGTTAAAATTTTGTGAGGTAGTA	Nsp11-NTD
85nsp11-NL-R	CCGCTCGAGTTAGCCGGTGCTGAAGATCGT	Nsp11-NTDL
85nsp11-LC-F	CGGAATTCGTTAAGGGCGAGGCTCAA	Nsp11-LCTD
85nsp11-CTD-F	CGGAATTCCGAATTGAGGTAGATTGC	Nsp11-CTD
85nsp11-NTD-1R	CCGCTCGAGTTAAACCAGCCGATCTGGCCA	Nsp11-NTD-D1
85nsp11-NTD-2F	CGGAATTCACCAGCCTTCGCCCTATC	Nsp11-NTD-D2
85nsp11-NTD-3F	CGGAATTCTGGCCCGTGGTGACAACT	Nsp11-NTD-D3
85nsp11-NTD-3R	CCGCTCGAGTTAAATGCACGCGCGGCTATA	Nsp11-NTD-D3
STAT2F1	GCGAATTCGCGCAGTGGGAAATGCTGCA	STAT2
STAT2R1	GACTCGAGCTAGAAGTCAGAAGGCATCA	STAT2
STAT2R2	CCGCTCGAGTTAGGCTCTGTGGAGCAGACG	STAT2D1
STAT2R3	CCGCTCGAGTTACTGAAGGTTTGGGCTGAG	STAT2D2
STAT2F2	GCGAATTCAACCAGCAGTTCTTCTCC	STAT2D3
R-STAT2-F1	AACCGTACACGAAGGAGGTG	STAT2
R-STAT2-R1	GATTCGGGGATAGAGGAAGC	STAT2
85nsp11N-D2-m1-F1	GGAATTCACCAGCCTTCGCCCTGCAGCAGCATATAGCCGCGCGTGCAT	Nsp11-NTD-D2M1
85nsp11N-D2-m2-F1	CATAAAGCAGCAGCAGCGTGCATTGGTGCCGGCTATATGGTGG	Nsp11-NTD-D2M2
85nsp11N-D2-m2-R1	CAATGCACGCTGCTGCTGCTTTATGGATAGGGCGAAGGCTGGT	Nsp11-NTD-D2M2
VenusC1F-HindIII	CGAAGCTTCGCCACCATGGTGAGCAAG	pCDNA3-VenucsC1

a. F: forward primer, R: reverse primer. The “32” and “85” before a primer name indicate the primer is based on sequences of PRRSV VR-2332 (GenBank accession# U87392) and VR-2385 (GenBank accession# JX044140), respectively. The “R” before a primer name indicates the primer was designed for real-time PCR.

b. The italicized alphabets indicate restriction enzyme cleavage sites for cloning.

Chapter 5: Porcine reproductive and respiratory syndrome virus antagonizes JAK-STAT3 signaling via nsp5 by inducing STAT3 degradation

Abstract

STAT3 is a pleiotropic signaling mediator of many cytokines including IL-6 and IL-10. STAT3 is known to play critical roles in cell growth, proliferation, differentiation, immunity and inflammatory responses. The objective of this study was to determine the effect of PRRSV infection on the STAT3 signaling since PRRSV induces a weak protective immune response in host animals. Here we report that PRRSV infection of MARC-145 cells and primary porcine pulmonary alveolar macrophages led to significant reduction of STAT3 protein level. Several strains of both PRRSV type 1 and type 2 led to a similar reduction of STAT3 protein level but had minimum effect on its transcripts. The PRRSV-mediated STAT3 reduction was in a dose-dependent manner as STAT3 level decreased along with incremental amount of PRRSV inocula. Further study showed that nsp5 of PRRSV induced the STAT3 degradation by increasing its polyubiquitination level and shortening its half-life from 24 h to approximately 3.5 h. The C-terminal domain of nsp5 was shown to be required for the STAT3 degradation. Moreover, the STAT3 signaling in the cells transfected with nsp5 plasmid was significantly inhibited. These results indicate that PRRSV antagonizes the STAT3 signaling by accelerating STAT3 degradation via the ubiquitin-proteasomal pathway. This study provides insight into the PRRSV interference with the JAK-STAT signaling, leading to perturbation of the host innate and adaptive immune responses.

Introduction

PRRS has been an economically important viral disease in the swine industry since it was first reported in 1987, with an estimated annual loss of $664 million in the United States alone (334). The

causative agent of the devastating disease is PRRSV, a small enveloped RNA virus belonging to the genus *Arterivirus*, family *Arteriviridae*, order *Nidovirales* (7, 335). There are two PRRSV species in the newly proposed taxonomy, *PRRSV-1* and *PRRSV-2*, corresponding to the currently known genotype Type 1 (European) and Type 2 (North American) PRRSV, respectively (7). PRRSV virions contain a single-stranded, positive-sense RNA genome in a size of approximately 15 kb. The PRRSV genome encodes over ten ORFs (46, 312, 335). PRRSV mainly targets PAMs and some lineages of monocytes in pigs (336). PRRSV propagation *in vitro* is generally conducted on MARC-145 cells, which are derived from epithelial cells of a monkey kidney (337).

A typical feature of the immune response to PRRSV infection in pigs is delayed onset and low titer of virus neutralizing antibodies, and weak cell-mediated immune response (52, 338). PRRSV infection is also characterized by prolonged viremia followed by persistent viral replication in regional lymph nodes for as long as 250 days (49). One of the possible reasons for the weak protective immune response is that PRRSV interferes with the innate immunity, such as inhibition of the synthesis and downstream signaling of type I IFNs (120, 121, 306, 339). Cytokines including type I IFNs that are produced at the site of infection, stimulate and coordinate the innate and adaptive immune responses against the invading pathogen (191-193). Many of the cytokines initiate function by binding to specific receptors on cells to activate the JAK-STAT signal pathway (194, 195). STATs are a family of transcription factors that regulate cell growth, differentiation, proliferation, apoptosis, immunity, inflammatory responses, and angiogenesis. There are seven STAT proteins (STAT1, 2, 3, 4, 5A, 5B, and 6) in mammalians. Each STAT member responds to a defined set of cytokines, though some of the cytokines can induce signaling via several STAT proteins (195, 196, 202). STAT proteins are activated by JAK phosphorylation of specific tyrosine residues, followed by homodimer or heterodimer formation and nuclear translocation to activate transcription of a specific set of genes.

Among all the STAT proteins, STAT3 is known as highly pleiotropic in mediating the expression of a variety of genes in response to both cytokines and growth factors, and thus plays a pivotal role in numerous cellular processes including cell survival, proliferation, embryogenesis, and the immune response (195, 208, 209). Numerous cytokines, including IL-5, IL-6, IL-9, IL-10, IL-11, IL-12, IL-21, IL-22, IL-27, OSM, IFN-γ, TNF-α and LIF, trigger STAT3 activation (202, 210). The IL-6 family cytokines including IL-6, OSM, and LIF bind to the gp130 receptor and activate STAT3, known as the gp130/JAK-STAT3 signaling. IL-6, a pleiotropic cytokine, plays important roles in triggering acute phase response of the body to injury or inflammation. OSM, a multifunctional cytokine produced by activated T lymphocytes, monocytes, and dendritic cells, enhances the antiviral effects of IFN-α and plays a role in the induction of the adaptive immune response to pathogens (340, 341). STAT3 is found to be a central regulator of lymphocyte differentiation and function (197). Mutations in STAT3 cause autosomal dominant hyper-IgE syndrome, a rare multisystem primary immunodeficiency characterized by recurrent bacterial infections in skin and lung and with abnormally high levels of IgE (213, 214).

PRRSV blocks the nuclear translocation of STAT1 and STAT2 to inhibit the IFN signaling pathway via the nsp1β (120, 121). However, PRRSV effect on the gp130/JAK-STAT3 signaling remains unknown. In this study, the objective was to determine PRRSV effect on the STAT3 signaling. We discovered that PRRSV inhibits the STAT3 signaling via inducing STAT3 degradation via nsp5. Infection of MARC-145 cells by several PRRSV type 1 and type 2 strains resulted in a reduction of STAT3 protein without affecting its transcript level. The addition of the proteasome inhibitor MG132 to the PRRSV-infected cells restored the STAT3 protein levels. Transient expression of nsp5 led to a reduction of STAT3 protein via degradation through the ubiquitin-proteasome pathway. The C-terminal portion of nsp5 is responsible for the induction of STAT3 degradation. In consequence, nsp5 inhibited the OSM-activated gp130/JAK-STAT3 signaling pathway. This finding provides further insight into PRRSV pathogenesis and its interference with the host immune response.

Materials and methods

Cells, viruses, and chemicals

MARC-145 (337), HEK293 (ATCC® CRL-1573™) and HeLa (ATCC® CCL-2™) cells were maintained in Dulbecco's modified Eagle's medium (DMEM) supplemented with 10% fetal bovine serum (FBS). Primary PAM cells were prepared and cultured in RPMI1640 medium as previously described (310). The cryopreserved PAM cells were revived and pre-cultured for 24 hours before used for virus inoculation.

PRRSV strains VR-2385 (342), VR-2332 (343), Ingelvac PRRS® MLV (311), and Lelystad (312) were used to inoculate MARC-145 cells at a multiplicity of infection (MOI) of 1. The median tissue culture infectious dose ($TCID_{50}$) of PRRSV was determined in MARC-145 cells (344).

MG132 (Sigma-Aldrich, St. Loius, MO), a proteasome inhibitor, was used to treat cells at a final concentration of 10 mM for 6 h prior to harvesting for further analysis. In order to determine the half-life of STAT3, cycloheximide (Sigma) was added to cultured cells at a final concentration of 100 μg/ml to block protein translation. OSM (R&D Systems, Inc., Minneapolis, MN) was used to activate the gp130/JAK-STAT3 signaling pathway at a final concentration of 10 ng/ml. The cells were harvested at the time points indicated in Results or the figure legends for Western blotting. The half-life of STAT3 was determined using nonlinear regression in GraphPad Prism (GraphPad Software, Inc., La Jolla, CA) in the analysis of the densitometry data of the immunoblotting results. 3-Methyladenine (3-MA) (Thermo Fisher Scientific, Waltham, MA), an inhibitor of autophagy by blocking autophagosome formation (345), was used at 5 mM in treatment of cells for 12- 24 h.

Cell viability assay was done with CellTiter-Glo® Luminescent Cell Viability Assay according to the manufacturer's instructions (Promega, Mandison, WI). The cells to be tested were placed into 96-well culture plate and treated as described above.

Plasmids

The nsp5 of PRRSV VR-2385 was cloned into a pCAGEN-HA and pCDNA3-VenusC1 vectors (121) with the primers 32nsp5F1 and 85nsp5R2 (Table 1). The nsp5 deletion mutants were cloned into pCDNA3-VenusC1 vector with the primers: 32nsp5F1 and 85nsp5R7 for nsp5D1, 85nsp5F3 and 85nsp5R2 for nsp5D2, 32nsp5F1 and 85nsp1R5 for nsp5D3, 85nsp5F6 and 85nsp5R2 for nsp5D4 (Table 1). The resulting recombinant plasmids were confirmed by restriction enzyme digestion and DNA sequencing. The construction of pCDNA3-Ubiquitin-Myc plasmid and other PRRSV nsp plasmids was described previously (158, 346).

The pEGFP-C1-STAT1 was a gift from Alan Perantoni (Addgene plasmid # 12301) (347). The pCDNA3-STAT3 was a gift from Jim Darnell (Addgene plasmid # 8706) (348). The pRc/CMV-FLAG-STAT3 was a gift from Jim Darnell (Addgene plasmid # 8707) (349). The 4xM67 pTATA TK-Luc was a gift from Jim Darnell (Addgene plasmid # 8688) (350) and used for STAT3 reporter assay.

Western blot analysis

Protein samples were separated by sodium dodecyl sulfate-polyacrylamide gel electrophoresis (SDS-PAGE) and analyzed by Western blotting as described (313, 315). The primary antibodies used in this study were against STAT3 (Santa Cruz Biotechnology, Inc., Dallas, TX), phospho-STAT3 (Tyr705, clone EP2147Y) (Thermo Fisher Scientific), ubiquitin (Santa Cruz), hemagglutinin (HA) (Thermo Fisher Scientific), FLAG (Sigma), green fluorescence protein (GFP) (Rockland Immunochemicals, Inc., Gilbertsville, PA), glyceraldehyde 3-phosphate dehydrogenase (GAPDH) (Santa Cruz) and β-tubulin (Sigma). The secondary antibodies used in this study were goat anti-rabbit or goat anti-mouse IgG conjugated with horseradish peroxidase (Rockland Immunochemicals). The chemiluminescence signal acquisition and densitometry analysis were conducted using the Quantity One program, version 4.6 in a Chemi-Doc XRS imaging system (Bio-Rad Laboratories, Hercules, CA).

Immunoprecipitation (IP)

IP was conducted as previously described (121). The clarified cell lysate was incubated with the STAT3 antibody (Santa Cruz), followed by incubation with protein G-agarose (KPL, Inc., Gaithersburg, MD). The IP samples were subjected to Western blotting with antibodies against ubiquitin, STAT3, and HA. To determine ubiquitinated STAT3, ubiquitin aldehyde (Boston Biochem, Inc., Cambridge, MA), a specific inhibitor of ubiquitin C-terminal hydrolases, was included in the lysis buffer at a final concentration of 2.53 μM.

RNA isolation and real-time PCR

Total RNA was isolated from HEK293 and MARC-145 cells with TRIzol reagent (Thermo Fisher Scientific) in accordance with the manufacturer's instructions. Reverse transcription and real-time quantitative PCR (RT-qPCR) were conducted as described (310, 351). The real-time PCR primers used for STAT3 were R-STAT3-F1 and R-STAT3-R1 (Table 1). Transcripts of ribosomal protein L32 (RPL32) were also amplified and used to normalize the total input RNA. Primers for PRRSV and RPL32 were described (121). The relative transcript levels were shown as folds in comparison with the mock-treated control after RPL32 normalization.

Reporter assay

HEK293 cells were transfected with the STAT3 reporter plasmid 4xM67 pTATA TK-Luc (350) and nsp5 plasmids. The Renilla luciferase vector pRL-TK (Promega, Madison, WI), which expresses Renilla luciferase under the control of a constitutively active promoter, was also transfected for normalization. At 24h after transfection, OSM was added into the cells at a final concentration of 10 ng/ml. After incubation for another 24 hours, the cells were lysed for luciferase activity assay of firefly and Renilla luciferases by following the manufacturer's instructions (Promega). Lysate of the cells

without OSM treatment was included as a control for assessment of the STAT3 activation level. The relative firefly luciferase activity is shown after normalization with the Renilla level as described (158).

Statistical analysis

Differences in indicators between treatment group and control were assessed using the Student t test. A two-tailed P value of less than 0.05 was considered significant.

Results

OSM inhibits PRRSV replication and PRRSV infection reduces STAT3 without affecting its transcript level

OSM, a member of the IL-6 family, was found to synergistically inhibit the replication of hepatitis C virus in combination with IFN-α (340, 341). We wondered if OSM alone had any antiviral role against PRRSV. MARC-145 cells were pre-treated with OSM for 24 h before inoculated with PRRSV strain VR-2385. Real-time PCR result showed that the OSM treatment significantly reduced PRRSV RNA replication in comparison with mock-treated control, whereas OSM had minimum effect on cell viability (Fig. 5.1A). Based on our early study of the IFN-activated JAK-STAT signaling (120), we reasoned that PRRSV would antagonize the OSM-activated gp130/JAK-STAT3 signaling. We first determined the OSM-activated STAT3 phosphorylation in PRRSV-infected cells. The result showed that the STAT3 phosphorylation level in the PRRSV-infected cells was 15% of the mock-infected cells after OSM stimulation (Fig. 5.1B). The STAT3 protein level in the infected cells was significantly reduced to 0.26 and 0.36-fold in the absence or presence of OSM, respectively, compared to mock-infected cells.

To exclude the possibility that PRRSV reduced STAT3 non-specifically, we examined STAT1 protein level. Compared to mock-infected cells, STAT3 level in the infected cells was reduced to 0.36-fold, whereas STAT1 level was unchanged (Fig. 5.1C). As MARC-145 cells are monkey-derived though they are PRRSV-permissible, we wondered if PRRSV had the same effect on STAT3 in primary PAM cells, which are main target cells in pigs during acute PRRSV infection. PAM cells were infected with VR-2385 and harvested 16 hpi for immunoblotting. Similarly, STAT3 level in the PRRSV-infected PAM cells was reduced to 0.37-fold in comparison to mock-infected control, whereas STAT1 remained steady (Fig. 5.1D). The harvesting of infected PAMs was done at 16 hpi as VR-2385 infection in the

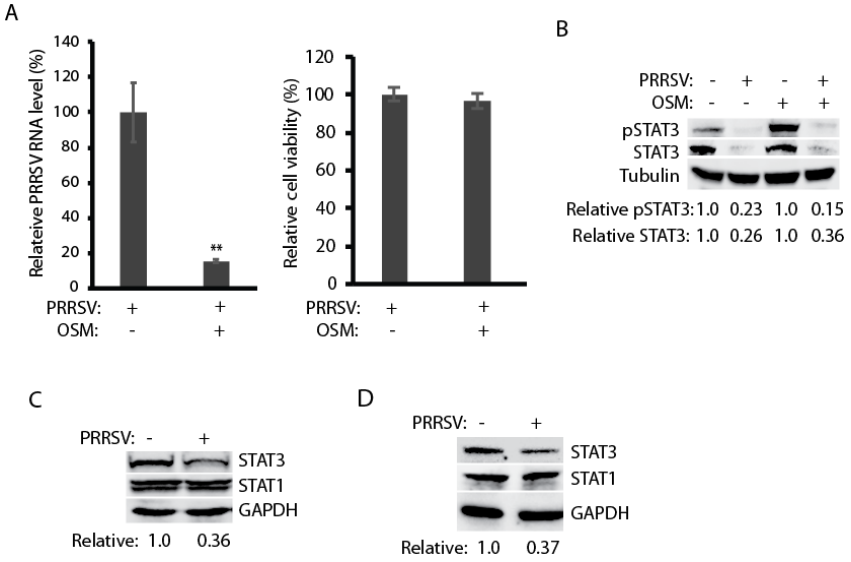

Fig. 5.1 PRRSV infection reduces STAT3 in MARC-145 and PAM cells. A. OSM treatment of MARC-145 cells inhibits PRRSV replication and has minimum effect on cell viability. The cells were pre-treated with OSM for 24 h before inoculated with PRRSV VR-2385 at an MOI of 1. The cells were harvested 24 h post infection (hpi). Relative percentage of PRRSV RNA levels determined by real-time PCR is shown. Significant difference from the untreated cells is denoted by "**" for $P < 0.01$. B. PRRSV reduces STAT3 phosphorylation in MARC-145 cells upon OSM stimulation. The cells were infected with VR-2385 at an MOI of 1, incubated for 48 h, and treated with OSM for 30 min before harvested for Western blotting (WB) with antibody against STAT3, phosphorylated STAT3 (pSTAT3), and tubulin. Relative levels of pSTAT3 and STAT3 are shown below the images after normalization with tubulin in densitometry analysis. C. PRRSV reduces STAT3 protein level in MARC-145 cells but has minimum effect on STAT1. Relative levels of STAT3 are shown below the images after normalization with GAPDH. D. PRRSV reduces STAT3 level in PAM cells but has minimum effect on STAT1 protein. The cells were infected with VR-2385 at an MOI of 1 and harvested for WB at 16 hpi.

cells progresses faster than in the MARC-145 cells.

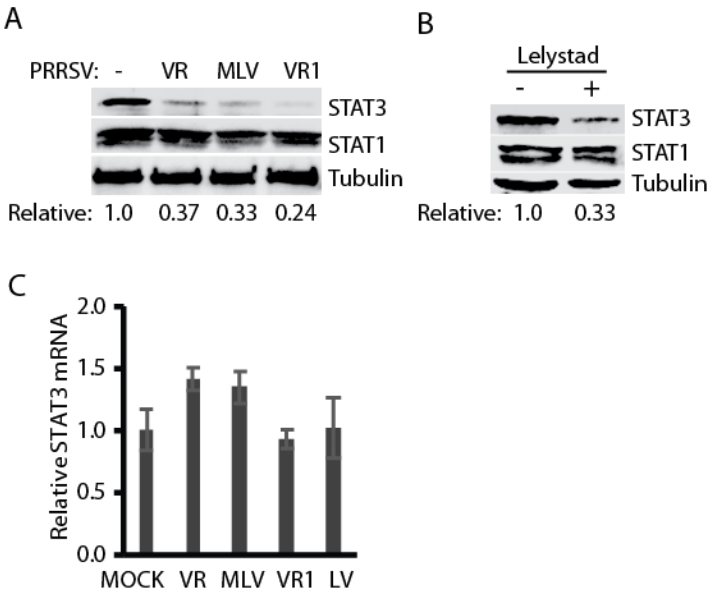

Fig. 5.2 Infection of MARC-145 cells with both PRRSV-1 and PRRSV-2 strains reduces STAT3 protein level, but has minimum effect on STAT3 transcripts. A. Reduction of STAT3 protein level but no effect on STAT1 level in MARC-145 cells infected with PRRSV-1 strains. The cells were infected with PRRSV-1 strains VR-2385 (VR), Ingelvac PRRS® MLV, and VR-2332 (VR1). At 48 hpi, the cells were harvested for WB with antibody against STAT3, STAT1 and tubulin. Relative levels of STAT3 are shown below the images after normalization with tubulin. B. Reduction of STAT3 protein level by PRRSV-2 strain Lelystad. C. STAT3 mRNA levels in PRRSV-infected cells. Relative STAT3 mRNA levels are shown in comparison with mock-infected cells. Error bars represent standard errors of the means of three repeated experiments.

To exclude the possibility that the STAT3 reduction is the consequence from infection of PRRSV strain VR-2385 only, we included strains from both PRRSV type 1 and type 2 in the test. MARC-145 cells were infected with PRRSV type 2 strains VR-2385, Ingelvac PRRS® MLV, and VR-2332 or PRRSV type 1 strain Lelystad. Compared to mock-infected cells, STAT3 protein levels in the cells infected with VR-2385, MLV, VR-2332 and Lelystad were reduced to 0.37, 0.33 0.24, and 0.33-fold, respectively, whereas STAT1 remained steady (Fig. 5.2A and 5.2B). We reasoned that STAT3 reduction could be due to a decrease of transcription and/or translation, or accelerated protein degradation. To determine the mRNA level of STAT3 in the cells with PRRSV infection, we conducted RT-qPCR. The results showed that there was no significant difference in the mRNA levels of endogenous STAT3 between the PRRSV-infected and mock-infected cells (Fig. 5.2C). These results

indicated that the PRRSV-induced reduction of STAT3 protein level was not due to perturbation of its transcripts.

PRRSV reduces STAT3 protein level in a dose and time-dependent manner

To further study the PRRSV-mediated reduction of STAT3, we inoculated MARC-145 cells with

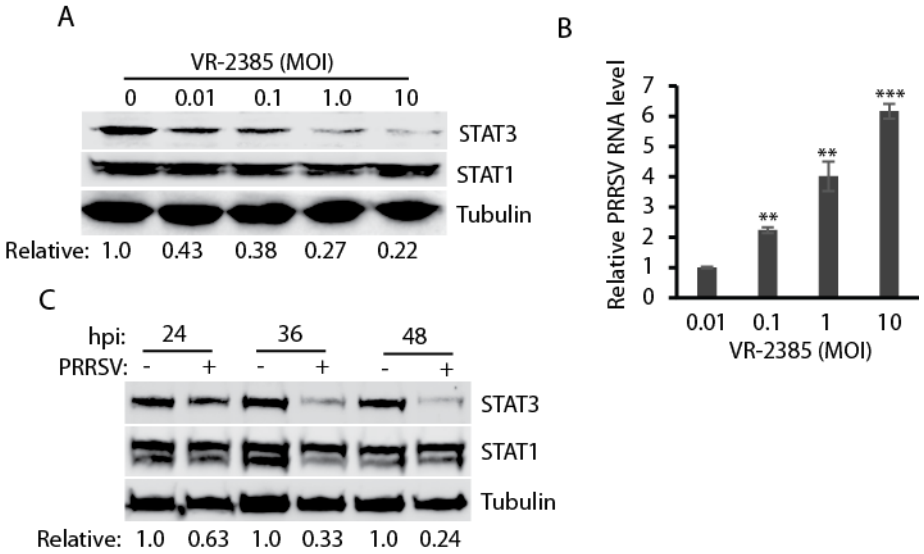

Fig. 5.3 PRRSV reduces STAT3 protein level in a dose and time-dependent manner. A. Dose-dependent reduction of STAT3 by PRRSV strain VR-2385. MARC-145 cells were inoculated with incremental MOI of VR-2385 and harvested for WB with antibodies against STAT3, STAT1, and tubulin at 48 hpi. Relative levels of STAT3 are shown below the images after normalization with tubulin. B. PRRSV RNA levels in the infected cells. The cells were harvested for RNA isolation and RT-qPCR at 24 hpi. Error bars represent standard errors of the results of repeated experiments. Significant differences in RNA level from an MOI of 0.01 are denoted by "**" for $P < 0.01$ and "***" for $P< 0.001$. C. Temporal kinetics of STAT3 levels in PRRSV-infected cells. MARC-145 cells were infected with VR-2385 at an MOI of 1. At different time points, the cells were harvested for WB. Relative levels of STAT3 are shown below the images after normalization with tubulin at each time point.

a different amount of VR-2385. Along with the incremental amount of VR-2385 inoculation, the STAT3 protein level was reduced in a dose-dependent manner, whereas STAT1 level remained relatively stable (Fig. 5.3A). Densitometry analysis showed that the STAT3 level in MARC-145 cells inoculated with an MOI of 0.01, 0.1, 1 and 10 was reduced to 0.43, 0.38, 0.27, and 0.22-fold, respectively, compared with mock-infected control. VR-2385 RNA levels in the infected cells significantly increased along with the incremental inocula (Fig. 5.3B), as expected.

To examine the PRRSV effect on the temporal kinetics of STAT3, we infected MARC-145 cells with VR-2385 and harvested the cells 24, 36, and 48 hpi. Compared to the mock-infected cells at each time point, the STAT3 levels in the virus-infected cells at 24, 36 and 48 hpi were reduced to 0.63, 0.33, and 0.24-fold, respectively (Fig. 5.3C). This result demonstrated that PRRSV infection reduces STAT3 protein level in a time-dependent manner.

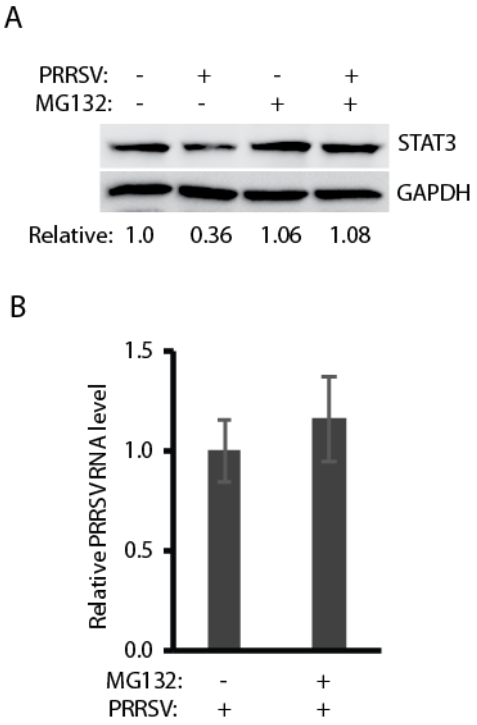

Fig. 5.4 PRRSV mediates STAT3 reduction via ubiquitin-proteasomal degradation pathway. A. MG132 treatment restores STAT3 level in PRRSV-infected cells. MARC-145 cells were infected with VR-2385 at an MOI of 1. At 30 hpi, the cells were treated with MG132 for 6 h and then harvested for Western blotting with antibodies against STAT3 and GAPDH. Non-treated and mock-infected cells were included as controls. Relative levels of STAT3 are shown as folds below the images after normalization with GAPDH. B. PRRSV replication is not affected by the MG132 treatment. Relative PRRSV RNA levels determined by real time PCR are shown in comparison with mock-treated cells.

PRRSV mediates STAT3 reduction via the ubiquitin-proteasomal degradation pathway

The results above showed that PRRSV infection reduced the level of STAT3 protein, but had minimum effect on its transcript level. We reasoned that the STAT3 reduction could be possibly due to accelerated degradation by the ubiquitin-proteasomal pathway. To test this, MG132, a proteasome inhibitor, was added to the cells at 30 h after VR-2385 infection. The cells were harvested 6 h later for STAT3 examination. The MG132 treatment of the infected cells resulted in the restoration of STAT3 to a level similar to the mock-infected cells (Fig. 5.4A). PRRSV RNA levels in the cells with or without MG132 treatment are similar (Fig. 5.4B). This result indicates that PRRSV mediates the STAT3 reduction via ubiquitin-proteasomal degradation pathway.

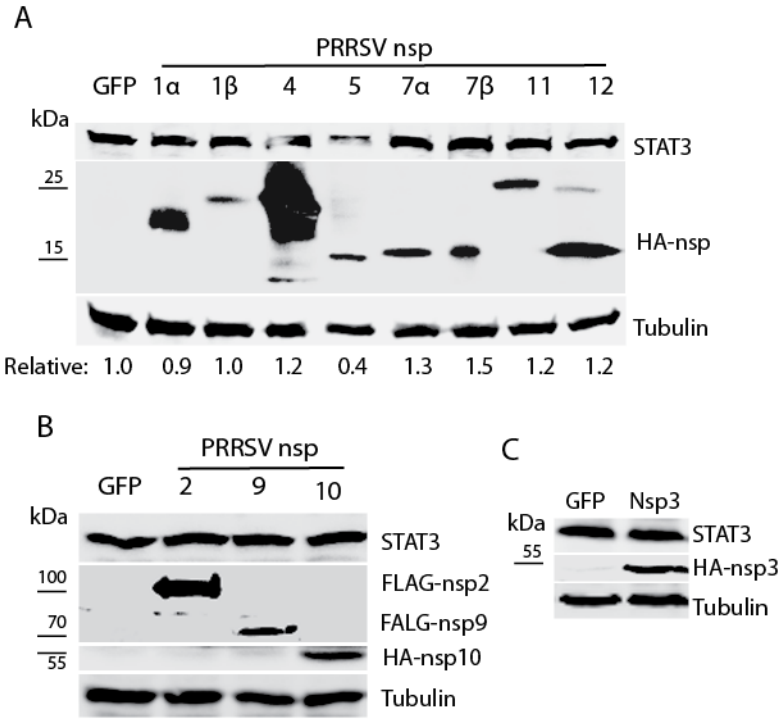

Fig. 5.5 Screening of PRRSV nsps to identify the viral protein that is responsible for reduction of STAT3 level. A. Nsp5 reduces STAT3 in HeLa cells, whereas other PRRSV nsps have minimum effect. The cells were transfected with individual HA-nsp plasmids. A GFP plasmid was included as a control. At 36 hours post transfection (hpt), WB against STAT3, HA and tubulin were done to detect endogenous STAT3 protein level in cells with transient expression of the nsps. Relative levels of STAT3 are shown below the images. B. The nsp2, nsp9, and nsp10 have minimum effect on STAT3 level in HeLa cells. The cells were transfected with FLAG-nsp2, FLAG-nsp9, HA-nsp10 or GFP plasmid. C. The nsp3 has minimum effect on STAT3 level in HeLa cells. The cells were transfected with HA-nsp3 or GFP plasmid.

PRRSV nsp5 reduces STAT3 protein level

Having demonstrated that PRRSV infection reduces the STAT3 protein level, we wondered which protein of PRRSV was responsible for the reduction. HeLa cells were transfected with plasmids encoding PRRSV VR-2385 nsps or structural proteins for assessment of their effect on STAT3 levels. Western blotting results showed that cells transfected with nsp5 plasmid had 0.4-fold STAT3 protein level compared with cells transfected with GFP, whereas cells transfected with the other PRRSV plasmids had no significant reduction (Fig. 5.5A, 5.5B, & 5.5C). The nsp2, nsp3, nsp9, nsp10 are much larger than the other nsps and were analyzed separately in the immunoblotting. The structural proteins had minimum effect on STAT3 and were not pursued further in this study (data not shown). Therefore, nsp5 was selected for further analysis.

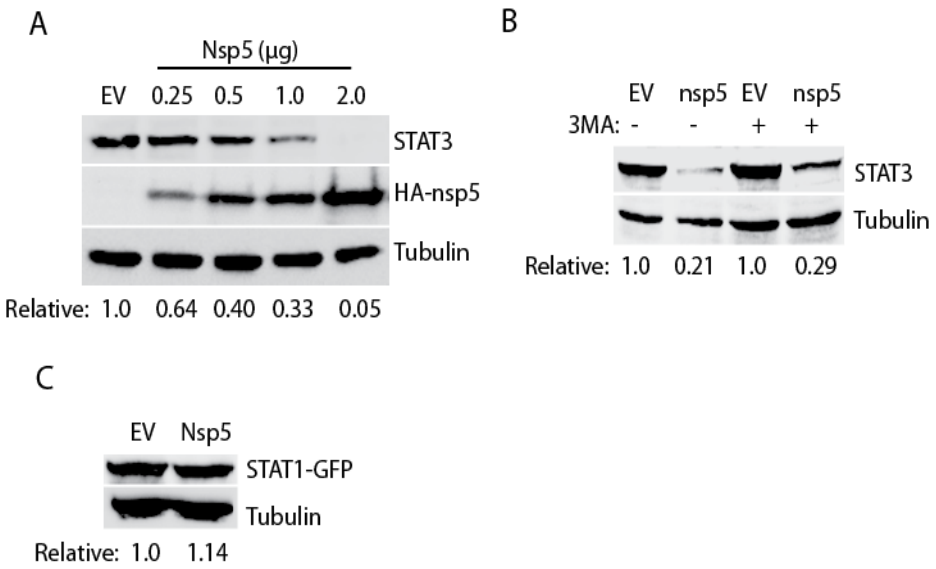

Fig. 5.6 PRRSV nsp5 reduces STAT3 protein level. A. Nsp5 reduces STAT3 protein level in a dose-dependent manner. HEK293 cells were transfected with nsp5 plasmid in incremental amounts. WB with antibodies against STAT3, HA and tubulin was conducted at 48 hpt. Relative levels of STAT3 are shown below the images after normalization with tubulin. B. 3-MA treatment is unable to rescue STAT3 protein level in HEK293 cells co-transfected with 0.5 μg HA-nsp5 and 0.5 μg STAT3 plasmid. Mock-treated cells were included as controls. The cells were treated with 3-MA for 24 h before harvested for WB. Relative levels of STAT3 are shown below the images. C. Nsp5 has no effect on STAT1 expression. HEK293 cells were transfected with 0.5 μg pCAGEN-HA-nsp5 plasmid and 0.5 μg pEGFP-C1-STAT1 plasmid. WB against STAT1 antibody was done at 36 hpt. Relative levels of STAT1-GFP are shown below the images.

Nsp5 plasmid was used to transfect HEK293 cells to confirm the effect on STAT3. Compared with the cells transfected with empty vector, the cells transfected with nsp5 plasmid reduced STAT3 protein level in a dose-dependent manner (Fig. 5.6A). Densitometry analysis showed that the STAT3 levels in HEK293 cells transfected with 0.25, 0.5, 1.0 and 2.0 μg of nsp5 plasmid were reduced to 0.64, 0.40, 0.33 and 0.05-fold, respectively, compared with the empty vector control. Nsp5 protein level increased along with the incremental amount of the plasmid DNA in the transfection.

Nsp5 is known to induce autophagy (352, 353). To exclude the possibility that nsp5 reduces STAT3 via autophagy pathway, we treated the cells with autophagy inhibitor 3-MA (345). Compared with cells transfected with the empty vector, the cells with nsp5 had similar lower STAT3 level in the presence or absence of 3-MA (Fig. 5.6B). Like the whole virus infection, nsp5 alone had no effect on the STAT1 level (Fig. 5.6C).

PRRSV nsp5 leads to elevation of STAT3 ubiquitination and shortening of its half-life

Since MG132 treatment restored STAT3 levels in cells with PRRSV infection, we reasoned that the STAT3 ubiquitination levels in the cells with nsp5 expression would increase. HEK293 cells were co-transfected with STAT3 and nsp5 plasmids. The cells were lysed for IP with an antibody against STAT3. Western blotting with ubiquitin antibody showed that ubiquitinated STAT3 in the cells with nsp5 expression was 12.6-fold greater than that in the cells transfected with the empty vector (Fig. 5.7A), which indicates that there was more polyubiquitination of STAT3 in the cells with nsp5 expression. Blotting with HA antibody failed to determine any nsp5 band in the IP complex lane, which suggests that STAT3 did not interact with nsp5 under our testing conditions. In addition, the input of whole-cell lysate was included in the blotting and results showed that the total ubiquitination level in the cells with nsp5 expression was similar to the cells transfected with empty vector (Fig. 5.7A). These results demonstrated that nsp5 induced elevation of STAT3 ubiquitination in the cells.

We next tested whether the half-life of STAT3 would be shortened. HEK293 cells were co-transfected with STAT3 and nsp5 plasmids and treated with cycloheximide, a translation inhibitor, followed by harvesting and immunoblotting at different time points. In the presence of nsp5, the STAT3 level decreased at a higher rate than that in the cells transfected with the empty vector (Fig. 5.7B). At 5, 10, 24, and 28 h after the cycloheximide treatment, the STAT3 levels in the cells with nsp5 expression were reduced by 59%, 85%, 93%, and 94%, respectively, whereas STAT3 in the cells transfected with the empty vector were reduced by 25%, 20%, 50%, and 71%, separately (Fig. 5.7B). The densitometry analysis was normalized with β-tubulin, which has a long half-life of 50 h (354). The expression of nsp5 induced a shortening of the STAT3 half-life from 24 h to approximately 3.5 h. This result is consistent with the elevation of STAT3 polyubiquitination in the cells with nsp5 expression.

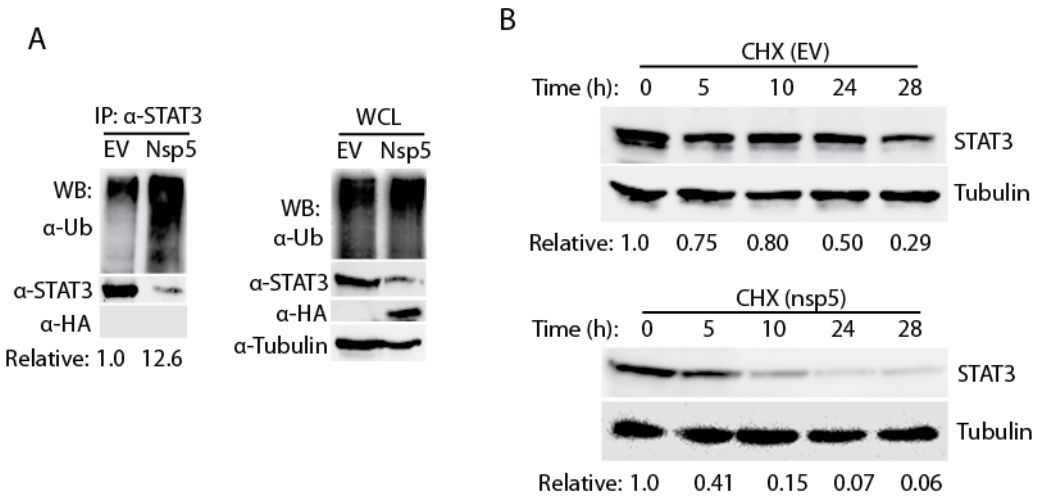

Fig. 5.7 PRRSV nsp5 leads to STAT3 degradation by ubiquitin-proteasomal pathway. A. Presence of nsp5 leads to elevation of STAT3 polyubiquitination level. IP with STAT3 antibody and then WB with antibodies against ubiquitin (Ub), STAT3 and HA were done. Samples of whole cell lysate (WCL) were included as controls. Relative levels of ubiquitinated STAT3 are shown below the images after normalization with STAT3 level. B. Nsp5 shortens STAT3 half-life from around 24 to 3.5 hours. HEK293 cells were transiently co-transfected with 0.5 μg STAT3 and nsp5 plasmids. The cells were treated with cycloheximide (CHX) at 100 μg/ml at 24 hpt and harvested at indicated hours post treatment, followed by WB with antibodies against STAT3 and tubulin. Relative levels of STAT3 are shown below the images after normalization with tubulin.

The C-terminal domain of nsp5 appears to be responsible for the induced degradation of STAT3

To map the domain of nsp5 involved in inducing the degradation of STAT3, deletion constructs of VR-2385 nsp5 were prepared. Based on analysis of nsp5 polypeptide sequence using Lasergene, four fragments of nsp5 were cloned into the pCDNA3-VenusC1 vector (Fig. 5.8A). Overexpression of the nsp5 truncation constructs in HEK293 cells was confirmed by immunoblotting with GFP antibody (Fig. 5.8B).

Immunoblotting results showed that the cells transfected with YFP-nsp5D2 (aa 59 to 170), YFP-nsp5D3 (aa 1 to 122), and YFP-nsp5D4 (aa 86 to 170) had considerably lower STAT3 protein levels than the cells transfected with the empty vector (Fig. 5.8B). Densitometry analysis showed that the cells with YFP-nsp5D1, YFP-nsp5D2, YFP-nsp5D3, and YFP-nsp5D4 had STAT3 levels reduced by 8%, 76%, 58%, and 67%, respectively, compared to the cells transfected with the empty vector. The results indicate that the nsp5D1 (aa 1 to 85) corresponding to the N-terminal domain has minimum effect on STAT3 level, whereas the C-terminal domain (aa 86-170) of nsp5 is responsible for the induced degradation of STAT3.

Sequence analysis suggests that nsp5 polypeptides are highly hydrophobic and may be membrane associated. Analysis with TMHMM, a membrane protein topology prediction method (355), showed that nsp5 has five transmembrane domains spanning residues aa 13-35, 45-67, 79-101, 121-143, and 150-169 (Fig. 5.8C). There are two outside-oriented loops spanning residues aa 36-44 and aa 102-120, and three inside-oriented loops spanning residues aa 1-12, 68-78, and 144-149 in nsp5. The outside-oriented loop spanning aa 102-120 is longer than other loops and located in the C-terminal domain.

Sequence alignment of nsp5 showed that VR-2385 nsp5 has 96.5%, 85.3%, and 69.4% identical amino acid residues with VR-2332, MN184, and Lelystad, respectively. Among the 52 aa variations between nsp5 of VR-2385 and Lelystad, 13 aa distribute in the N-terminal half of nsp5 and the rest 39 aa

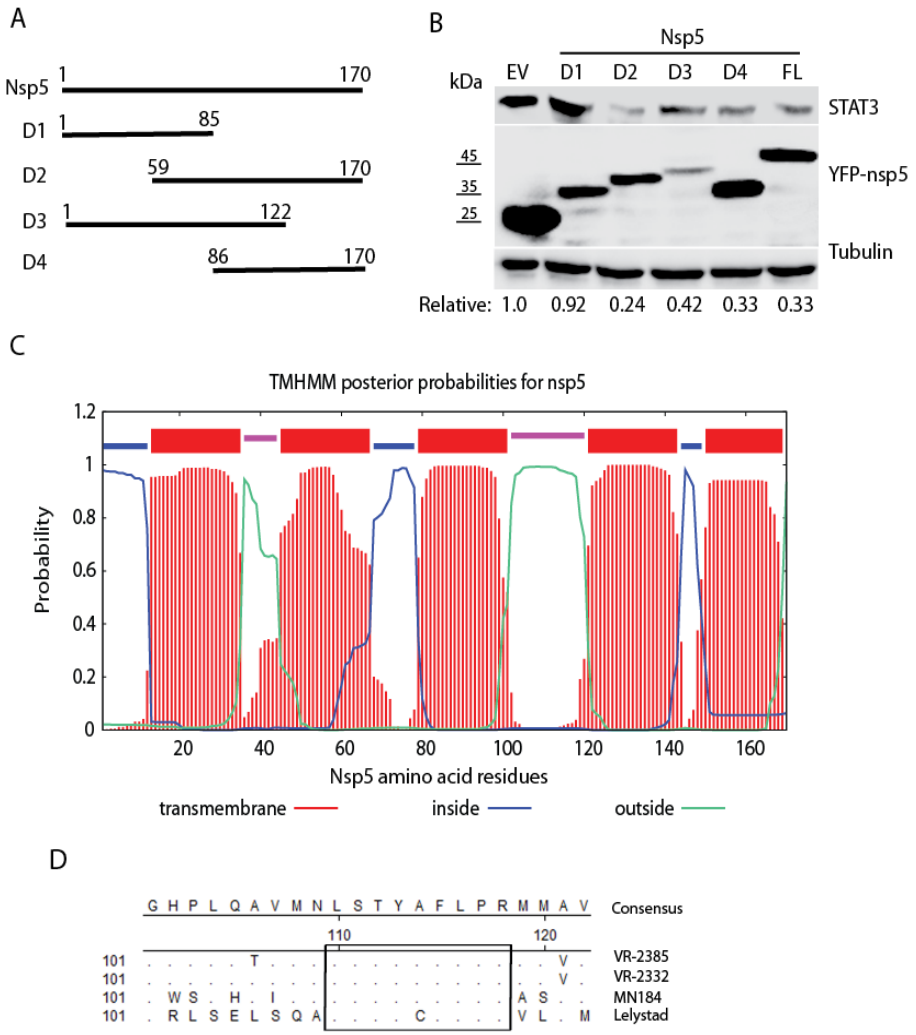

Fig. 5.8 The C-terminal domain of nsp5 is required for STAT3 degradation. A. Schematic illustration of truncation plasmids nsp5D1, nsp5D2, nsp5D3, and nsp5D4. The numbers above the lines indicate amino acid residues of nsp5. B. The nsp5D2, nsp5D3, and nsp5D4 lead to STAT3 degradation, whereas nsp5D1 has minimum effect. HEK293 cells were transfected with 0.5 μg YFP-tagged plasmids and harvested at 36 hpt for immunoblotting with antibodies against STAT3, YFP and tubulin. Relative levels of STAT3 are shown below the images after normalization with tubulin. Molecular weight markers are added on the left of image YFP-nsp5. EV: empty vector. FL: full length. C. Predicted membrane protein topology of nsp5 with TMHMM. The numbers on X-axis denote nsp5 residues. The bars in different colors indicate topology. The loops inside or outside of membrane are indicated by different colors. D. Alignment of amino acid sequence of nsp5 of PRRSV VR-2385, VR-2332, MN184 and Lelystad. The rectangle highlights the highly conserved residues. The numbers below the consensus sequence and on left indicate amino acid residue number of nsp5. The residues that are identical to consensus are not shown.

are in the C-terminal half. There is a highly conserved stretch of residues, aa 110-118, in the outside-oriented loop spanning aa 102-120 (Fig. 5.8D). Among the nine residues in aa 110-118 of nsp5 from the

four PRRSV strains, eight are identical, which needs further study to determine whether they correlate with the nsp5 induction of STAT3 reduction.

Nsp5 inhibits gp130/JAK-STAT3 signaling

As a transcription activator, STAT3 mediates multiple important signaling pathways related to immune responses, cell growth, and cell survival. So we speculated nsp5 would inhibit the STAT3 signaling as it reduced STAT3 protein level. First, we tested whether it inhibits the OSM-mediated STAT3 activation. As expected, the STAT3 phosphorylation in HEK293 cells transfected with nsp5 plasmid was much lower than the cells with empty vector (Fig. 5.9A). The relative phosphorylated STAT3 levels in the cells with 0.25 and 1 μg nsp5 were reduced by 60% and 74%, respectively, in comparison with the control cells with empty vector. The relative STAT3 levels in the cells with 0.25 and 1 μg nsp5 were reduced by 50% and 72%, respectively, in comparison with the control cells. The results indicate that the nsp5 inhibition of STAT3 phosphorylation was due to the reduction of STAT3 protein level.

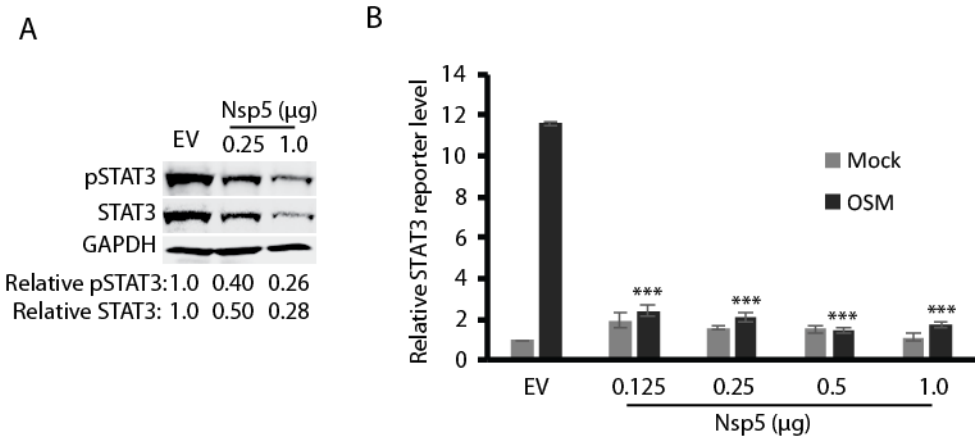

Fig. 5.9 PRRSV nsp5 inhibits STAT3 signaling. A. HEK293 cells transfected with nsp5 has much lower OSM-mediated STAT3 phosphorylation than the control cells with empty vector (EV). The cells were treated with OSM for 30 minutes before harvested for WB. Relative levels of phosphorylated STAT3 (pSTAT3) and total STAT3 are shown below the images. B. Nsp5 inhibits OSM-stimulated STAT3 reporter expression. HEK293 cells were co-transfected with 0.5 μg nsp5 plasmid, 0.5 μg STAT3 reporter and 0.05 μg Renilla plasmids. At 24 h post transfection, the cells were treated with OSM and harvested for luciferase activity assay 24 h later. Relative levels of firefly luciferase activity are shown as folds in comparison with EV control after normalization with Renilla activity. Significant difference in firefly luciferase activity from EV+OSM control is denoted by "***" for $P < 0.001$.

We next tested whether nsp5 inhibits STAT3 reporter expression. HEK293 cells were co-transfected with the incremental amount of nsp5 plasmid DNA along with STAT3 reporter plasmid 4xM67 pTATA TK-Luc and pRL-TK. The cells were then treated with OSM for 24 h before harvested for luciferase assay. OSM induced obvious transactivation of 4xM67 pTATA TK-Luc in the cells transfected with the empty vector (Fig. 5.9B), whereas the luciferase activity values in the cells transfected with nsp5 plasmid from 0.125 to 1.0 μg were significantly ($P < 0.001$) lower. This result demonstrated that nsp5 led to the inhibition of the OSM-mediated gp130/JAK-STAT3 signaling via inducing degradation of the STAT3 protein.

Discussion

Our results in this study demonstrated that PRRSV inhibits the STAT3 signaling pathway by inducing degradation of STAT3. The JAK-STAT pathway is critical in relaying signals from cytokines and growth factors to regulate gene expression in biological processes including apoptosis, angiogenesis, differentiation, cell proliferation, inflammatory response, and immunity (194, 195). In particular, STAT3 is a central regulator of lymphocyte differentiation and function (197). It can regulate $CD4^+$ T cell differentiation and control Th17 cells differentiation by IL-6 and IL-23. STAT3 deficiency affects the generation of memory $CD8^+$ T cells (242, 243) and memory B cells (244, 245). Therefore, STAT3 is indispensable in the host immune system. PRRSV infection induces a weak cell-mediated immune response, in which PRRSV-specific T cells transiently appear two weeks after infection without a change in frequency of $CD4^+$ and $CD8^+$ T-cells (52). The STAT3 antagonizing may be one of the reasons for PRRSV interference with the development of protective immune response.

We discovered that PRRSV inhibits the STAT3 signaling by inducing degradation of STAT3. The PRRSV-mediated degradation of STAT3 is specific as PRRSV has no effect on STAT1 protein level in MARC-145 and PAM cells. The PRRSV-induced reduction of STAT3 also occurs in primary PAMs, the main target cells in infected pigs. This reduction appears to be an intrinsic property of

PRRSV as several strains from both PRRSV type 1 and type 2 including a vaccine strain are able to do so in MARC-145 cells. The STAT3 decrease was found due to degradation via the ubiquitin-mediated proteasome pathway because blocking this degradation pathway with MG132 resulted in the restoration of STAT3 levels in the cells infected with PRRSV.

Macrophages are important immune effector cells and can respond to endogenous stimuli generated by injury or infection (356). PRRSV infection of PAMs leads to inhibition of IFN induction (339), suppression of the JAK-STAT signaling (120), and may result in the poor generation of stimuli to other cells, consequently ineffectual immune response. PRRSV infection in pigs leads to elevation of IL-10 (357, 358) and induces lung lesions with inflammatory cell infiltration (359). IL-10 signaling via mediator STAT3 results in the generation of regulatory macrophages, which have an anti-inflammatory activity to dampen immunopathology. PRRSV antagonizing the STAT3 signaling could interfere with the IL-10 regulatory function and leads to inflammation.

PRRSV nsp5 was found to be responsible for the STAT3 reduction. Nsp5 induces elevation of the STAT3 polyubiquitination and shortens its half-life from 24 h to approximately 3.5 h. Our data suggests that nsp5 enhances STAT3 degradation via the ubiquitin-proteasomal pathway. There seems no direct interaction between nsp5 and STAT3 because IP with an antibody against STAT3 did not pulldown nsp5. Likewise, immunofluorescence assay and confocal microscopy did not determine co-localization of nsp5 and STAT3 in cells co-transfected with both plasmids (data not shown). These results suggest that STAT3 and nsp5 have no direct interaction or, if any, transient. We presume that nsp5 activates an ubiquitin E3 ligase of STAT3 and accelerates proteasome degradation of the transcription activator. The E3 ligase for STAT3 proteasome degradation remains unknown though TMF/ARA 160, a Golgi-resident protein, was found to mediate the degradation of STAT3 (360). However, nsp5 was found to co-localize with the endoplasmic reticulum, not Golgi (data not shown). Nsp5 induces autophagic cell death when it is overexpressed (353). But treatment of the cells with 3-

MA to block autophagy in this study did not rescue the STAT3 level, indicating autophagy was not the reason for the STAT3 reduction.

Nsp5 is a hydrophobic transmembrane protein and can possibly form a membranous structure in the cytoplasm that could be the site for PRRSV replication (46). The C-terminal domain (aa 86 to 170) of nsp5 might be responsible for the STAT3 degradation as the deletion constructs nsp5D2, nsp5D3, and nsp5D4 containing the full or partial C-terminal domain led to the reduction, while nsp5D1 (aa 1 to 85) failed to do so. This C-terminal domain contains a mixture of hydrophobic and hydrophilic residues with a potential surface location motif, as shown by TMHMM analysis. In the outside-oriented loop in the C-terminal domain, there is a stretch of residues that are highly conserved across the two PRRSV species. This suggests that these conserved residues might play a role in the nsp5-induced STAT3 reduction. Further work is needed to address the speculation.

The nsp5-mediated degradation of STAT3 led to blocking the STAT3 signaling. In the OSM-dependent transactivation of the reporter plasmid of the STAT3 binding promoter, the presence of nsp5 resulted in significant reduction of the reporter expression. This result substantiates that PRRSV nsp5 mediates the inhibition of the gp130-dependent signaling via its inducing STAT3 degradation.

Due to its importance in the host innate and adaptive immune responses, STAT3 has been found to be the target of some viral pathogens. Measles virus V protein inhibits the IL-6 mediated STAT3 signaling (234). V protein of mumps virus prevents responses to IL-6 and v-Src by inducing STAT3 ubiquitination and degradation (238). Rabies virus interferon antagonist P protein inhibits the gp130 receptor signaling by interacting with activated STAT3 (239). Inhibition of the STAT3 signaling by these viruses and PRRSV can lead to inhibition of a broad spectrum of cytokines and growth factors to thwart host antiviral responses and allow virus replication and spread in vivo. PRRSV was shown to inhibit the IFN-activated JAK-STAT signaling via blocking STAT1 nuclear translocation (120). The blocking was found due to PRRSV nsp1β-mediated degradation of karyopherin α1 (KPNA1, importin

α5) (121). Here we found PRRSV interferes with the gp130/JAK-STAT3 signaling via nsp5. This sheds further light on PRRSV antagonizing the JAK-STAT signaling to have a conducive environment for its own replication and spread.

In conclusion, our results demonstrated that PRRSV infection induces STAT3 degradation via the ubiquitin-proteasomal pathway. PRRSV nsp5 was found to be responsible for the STAT3 reduction and blocking its signaling. This finding provides insights for PRRSV pathogenesis and its interference with the host immune response.

Table 5.1 List of primers used in Chapter 5

Primer[a]	Sequences (5' to 3')[b]	Target gene
32nsp5F1	CGGAATTCGGAGGCCTCTCCACCGTCC	Nsp5
85nsp5R2	CCGCTCGAGTTACTCGGCAAAGTACCGCAGG	Nsp5
85nsp5R7	GCTCGAGTTAGCTGAAAAAGGCAAGTGAC	Nsp5D1
85nsp5F3	GGAATTCCCATGGTCTGCGCAAGTTC	Nsp5D2
85nsp5R5	GCTCGAGTTACACAACCATCATCCGAGGCAG	Nsp5D3
85nsp5F6	CGGAATTCAGCCTTGGTGCGGTGACCGG	Nsp5D4
R-STAT3-F1	GTGATGCTTCCCTGATTGTG	STAT3
R-STAT3-R1	GCAAGGAGTGGGTCTCTAGG	STAT3

a. F: forward primer, R: reverse primer. The "32" and "85" before a primer name indicates the primer is based on sequences of PRRSV VR-2332 (GenBank accession# U87392) and VR-2385 (GenBank accession# JX044140), respectively. The "R" before a primer name indicates the primer was designed for real-time PCR.

b. The italicized letters indicate restriction enzyme cleavage sites for cloning.

Chapter 6: Karyopherin alpha6 is required for the replication of porcine reproductive and respiratory syndrome virus and zika virus

Abstract

Movement of macromolecules between the cytoplasm and the nucleus occurs through the nuclear pore complex (NPC). Karyopherins comprise a family of soluble transport factors facilitating nucleocytoplasmic translocation of proteins through the NPC. In this study, we discovered that karyopherin alpha6 (KPNA6, also known as importin alpha7) was required for the optimal replication of PRRSV and Zika virus (ZIKV), which are positive-sense, single-stranded RNA viruses replicating in the cytoplasm. The KPNA6 protein level in virus-infected cells was much higher than that of mock-infected controls, whereas KPNA6 transcript remains stable. Viral infection blocked the ubiquitin-proteasomal degradation of KPNA6, which led to an extension of KPNA6 half-life and the elevation of KPNA6 level in comparison with mock-infected cells. PRRSV nsp12 protein induced the KPNA6 stabilization. KPNA6 silencing was detrimental to the replication of PRRSV, and KPNA6 knockout impaired ZIKV replication. Moreover, KPNA6 knockout blocked the nuclear translocation of PRRSV nsp1β but had a minimal effect on two other PRRSV proteins with nuclear localization. Exogenous restitution of KPNA6 expression in the KPNA6 knockout cells results in restoration of the nuclear translocation of PRRSV nsp1β and the replication of ZIKV. These results indicate that KPNA6 is an important cellular factor for the replication of PRRSV and ZIKV.

Introduction

Transport of macromolecules in to and out of the nucleus must go through the nuclear pore complexes (NPCs), macromolecular structures (>60 MDa) consisting of approximately 30 proteins, on the nuclear envelope (361, 362). Molecules smaller than 40 kDa can passively diffuse through the NPCs.

Transport of macromolecules across the NPCs requires a regulated energy-dependent process, which needs either direct interaction with the NPCs or association with different types of transport receptors. The largest group of transport receptors is designated as karyopherins (259, 363-365), which mediate the nuclear import of many cytoplasmic proteins. In the classical nuclear import pathway, cytoplasmic cargoes bearing a nuclear location sequence (NLS) are first recognized by karyopherin α, followed by association with karyopherin β1 (KPNB1) (259). The ternary importing complex karyopherin β/α/NLS-cargo translocates through the NPCs to the nucleus.

There are seven isoforms of karyopherin α (KPNA1-7) (259, 271, 366). Due to their importance in nucleocytoplasmic trafficking, KPNAs play indispensable roles in signal transduction, especially immune response. For instance, KPNA1 is responsible for the nuclear translocation of STAT1 in interferon-stimulated gene expression (367, 368); KPNA1 and KPNA6 transport STAT3 (265) to activate interleukin-6 signaling pathway. Therefore, KPNAs are often targeted by viruses to interfere with the immune response. For example, Ebola virus VP24 interacts with KPNA1 in the region overlapping with phosphorylated STAT1 (pSTAT1), which blocks pSTAT1 nuclear translocation (231, 232). HCV induces the cleavage of KPNB1 by NS3/4A to disrupt the IRF3 and NF-κB translocation to inhibit the IFN-β production (298). Hepatitis B virus (HBV) polymerase interferes with the IFN-α-stimulated signaling by inhibiting the nuclear transportation of STAT1/2 via binding to KPNA1 competitively (297). PRRSV inhibits the interferon-activated JAK-STAT signaling by blocking the nuclear translocation of the STAT1/STAT2 complex via inducing KPNA1 degradation (121).

On the other hand, many viruses, especially those with DNA genome, have been found to exploit the karyopherins for their own benefit. DNA viruses generally deliver their genetic elements into the nucleus for propagation or integration into the host genome for latent infections. Karyopherins play an essential role in this process and thus are pivotal host dependency factors. For example, parvovirus delivers its DNA into the nucleus through karyopherin α and β (276). Replication of human

papillomavirus is inhibited by antibodies against KPNA2 and KPNB1 (369). Moreover, herpesvirus and adenovirus are shown to rely on karyopherins for their nuclear entry (252). In addition, among RNA viruses, human immunodeficiency virus (HIV) (282) and influenza A virus (289) exploit karyopherins to translocate their proteins or genetic elements into the nucleus. KPNA1 and KPNA6 were found to be positive cellular factors for efficient replication of influenza A virus (287, 289, 370, 371).

However, most RNA viruses, especially +ssRNA viruses, replicate in the cytoplasm rather than in the nucleus. Therefore, the nucleocytoplasmic trafficking machinery has not been linked to +ssRNA viruses. Particularly, it remains unknown whether KPNAs contribute to the replication of +ssRNA viruses.

The +ssRNA viruses including the flavivirus, coronavirus, picornavirus, and arterivirus cause severe human or animal diseases. PRRSV is a small enveloped RNA virus belonging to the genus Rodartevirus, the family Arteriviridae (7, 372). This virus causes a contagious disease that is characterized by reproductive failure in sows and respiratory disease of variable severity in pigs of all ages (46). PRRS causes substantial economic losses to the swine industry and remains one of the top challenges since it was first reported in 1987. Zika virus (ZIKV) is a mosquito-borne flavivirus that caused recent outbreaks accompanied by severe manifestations including fetal microcephaly and the Guillain-Barre syndrome (GBS) (373-375). ZIKV belongs to the same Flavivirus genus of the Flaviviridae family as several other global human pathogens including dengue virus, yellow fever virus and West Nile virus (376).

In a previous study, we discovered that PRRSV mediated KPNA1 degradation to antagonize interferon-activated signaling (121). Unexpectedly, we noticed that KPNA6 protein level was higher in PRRSV-infected cells than mock-infected control. The objective of this study is to examine KPNA6 level in the infected cells, the mechanism of KPNA6 elevation, and its functions in the viral replication. Here, we show that KPNA6 is a common host proviral factor for PRRSV and ZIKV. These viral

infections induce KPNA6 elevation via extending its half-life and abrogating its ubiquitin-proteasomal degradation. KPNA6 knockdown in MARC-145 cells via RNAi silencing inhibits the replication of PRRSV. In addition, KPNA6 knockout in Vero cells via CRISPR/Cas9 system suppresses ZIKV replication. The nuclear translocation of PRRSV nsp1β is blocked in KPNA6 knockout cells. Exogenous restitution of KPNA6 expression in the KPNA6 knockout cells leads to the restoration of ZIKV replication and the nuclear translocation of PRRSV nsp1β. These results demonstrate that PRRSV and ZIKV harness KPNA6 for their own proliferation.

Materials and methods

Cells, viruses, and chemicals

HEK293 (ATCC CRL-1573), MARC-145 (ATCC CRL12231) (337), HeLa (ATCC CCL-2), and Vero (ATCC CCL81) cells were maintained in Dulbecco's Modified Eagle Medium (DMEM) supplemented with 10% fetal bovine serum (FBS) at 37°C. Aedes albopictus clone C6/36 (ATCC CRL-1660) were cultured in Minimum Essential Media (MEM) with 10% FBS at 28°C.

Primary PAMs were revived from frozen stock that was previously collected from broncho-alveolar lavage fluid of 4 to 5 weeks old, PRRSV-negative piglets (120), and maintained in RPMI1640 medium supplemented with 10% FBS at 37°C as previously described (120).

PRRSV VR-2385 (377) and VR-2332 (378) strains used in this study were propagated in MARC-145 cells. ZIKV PRVABC59 strain (379) was reproduced in C6/36 cells. Virus titers were determined in cultured cells by 10-fold serial dilutions and shown as the median tissue culture infectious dose (TCID50) (314).

FuGeneHD (Promega, Madison, WI) was used to transfect plasmid DNA into the cells according to the manufacturer's instructions.

Cycloheximide (CHX) (Sigma-Aldrich, St. Louis, MO), an inhibitor of protein synthesis, was used to treat cells at a final concentration of 50 μM to test the half-life of KPNA6 (121, 380). MG132 (Sigma-Aldrich), a proteasome inhibitor, was used at a final concentration of 10 μM to treat cells for 6 h prior to harvesting cells (121, 380).

MARC-145 cells stably expressing KPNA6 shRNA were established by the transfection of cells with pSIREN-RetroQ-ZsGreen-KPNA6-shRNA and pTK-Hyg plasmids. Then the cells were cultured under antibiotic hygromycin at a concentration of 50 μg/ml. The surviving cells were subjected to single cell cloning by the limited dilution. KPNA6 knockout Vero and HeLa cells by the CRISPR/Cas9 system (381, 382) were established by flow cytometry sorting of GFP-positive cells, that were transfected with the CRISPR plasmid PX461-sgKPNA6 containing a guide RNA (gRNA) and a CRISPR-associated endonuclease (Cas9). The empty vector containing Cas9 but no target gRNA was also used to establish stable Vero cells as controls. Restitution of KPNA6 expression in KPNA6 knockout Vero cells was established by the transfection of KPNA6-/- Vero cells with pCAGEN-KPNA6 and pTK-Hyg plasmids, followed by selection under the pressure of hygromycin.

Plasmids

KPNA6 (GenBank accession number NM_012316) was cloned into pCAGEN (Addgene plasmid 11160) (383) with a Myc-tag at the N-terminus as previously reported (121). Plasmids of PRRSV nsps from strain VR-2385 (GenBank accession number JX044140) were described (121, 380). KPNA6 shRNA were designed and cloned into plasmid pSIREN-RetroQ-ZsGreen according to the instructions of the manufacturer (Takara Bio USA, Inc., Mountain View, CA). Plasmid pTK-Hyg (GenBank accession number U40398) was purchased from Takara Bio USA. To establish KPNA6-knockout Vero cells by CRISPR/Cas9 system, a gRNA was designed and cloned into the vector pSpCas9n(BB)-2A-GFP (PX461) (a gift from Feng Zhang (Addgene plasmid # 48140)) (381). All primers used for the

plasmid construction are listed (Table 1). All plasmids constructed in-house were subjected to DNA sequencing to verify the inserts.

Western blot analysis

Whole cell lysate in Laemmli sample buffer was subjected to SDS-PAGE and Western blotting as previously described (315, 384). Antibodies against KPNA6 (Santa Cruz Biotechnology, Inc., Dalla, TX), KPNA1 (Santa Cruz), KPNA2 (Prosci Inc, Poway, CA), PRRSV nsp2 protein (14, 316), glyceraldehyde 3-phosphate dehydrogenase (GAPDH) (Santa Cruz), flavivirus E protein (385), hemagglutinin (HA) tag (ThermoFisher Scientific, Waltham, MA), cMyc tag (ThermoFisher Scientific), ubiquitin (Santa Cruz), β-tubulin (Sigma-Aldrich), and FLAG tag (Sigma-Aldrich) were used in the blotting. Pig anti-PRRSV serum (386) was used to detect nsp2 of PRRSV strain VR-2332 as the monoclonal antibody against nsp2 (14, 316) did not work with this strain. The secondary antibodies used in this study were horseradish peroxidase-conjugated rabbit anti-goat IgG (Rockland Immunochemicals, Inc., Gilbertsville, PA), goat anti-mouse IgG (Rockland), and goat anti-swine IgG (SeraCare Life Sciences, Gaithersburg, MD). The specific reactions were detected with chemiluminescence substrate, and the signal was recorded digitally using a ChemiDoc XRS imaging system using the Quantity One Program, Version 4.6 (Bio-Rad Laboratories, Hercules, CA). All experiments were repeated at least three times to ensure reproducibility.

Reverse transcription and real-time PCR (RT-qPCR)

Total RNA was isolated from cells with the TRIzol reagent (ThermoFisher Scientific) in accordance with the manufacturer's instructions. Reverse transcription and real-time PCR with SYBR Green detection (ThermoFisher Scientific) were performed as described (310, 380). Transcript of RPL32 (ribosomal protein L32) from the same samples was detected as an internal control (313). Real-time

PCR primers for KPNA6 and PRRSV are listed (Table 1). Primers for ZIKV are described previously (387). All experiments were repeated at least three times, with each experiment performed in triplicate.

Immunofluorescence assay (IFA)

IFA was carried out as reported (318) with antibodies against HA tag (ThermoFisher Scientific), cMyc tag (ThermoFisher Scientific), KPNA6 (Santa Cruz Biotechnology, PRRSV nsp2 protein (14, 316), and flavivirus E protein (385). The specific reactions were detected by the conjugated secondary antibodies: goat anti-mouse IgG (H&L) Dylight™ 549, goat anti-mouse IgG (H&L) Dylight™ 488 and goat anti-rabbit IgG (H&L) Dylight™ 488 (Rockland Immunologicals). The cover glasses were mounted onto slides using SlowFade Gold antifade reagent containing 4'6'-diamidino-2-phenylindole (DAPI) (ThermoFisher) and observed using fluorescence microscopy.

Cell viability assay

To test the cytotoxicity of MG132, MARC-145 cells infected with PRRSV for 24 h were treated with MG132. DMSO-treated and non-infected cells were included as controls. After 6 h, cell viability was detected with CellTiter-Glo (Promega, Madison, WI) according to the manufacturer's instruction. To compare the cell viability of KPNA6 knockdown and knockout cells with control cells, the same number of cells were plated in different wells. After 24 h, cell viability was determined with CellTiter-Glo. All experiments were repeated at least three times, with each experiment performed in triplicate.

Immunoprecipitation (IP)

IP was conducted as described (380). The cell lysate was clarified and incubated with the specific antibody indicated in Results, followed by incubation with protein G-agarose (SeraCare Life Sciences). The IP complexes were subjected to Western blotting. To determine polyubiquitination of KPNA6, we added ubiquitin aldehyde (Boston Biochem, Inc., Cambridge, MA), a specific inhibitor of

ubiquitin hydrolases, to the lysis buffer at a final concentration of 2.53 μM. The IP complexes were subjected to immunoblot analysis with the antibodies against ubiquitin and KPNA6.

Statistical analysis

Differences in indicators between treatment samples, such as KPNA6 mRNA level between the group in the presence of PRRSV infection and the mock-infected control, were assessed by Student t-test. A two-tailed P-value of less than 0.05 was considered significant.

Results

PRRSV induces the increase of KPNA6 protein level

In our study of the PRRSV virus-host interaction, we discovered that PRRSV infection of MARC-145 cells led to a higher expression level of KPNA6, while the KPNA2 level remained unchanged (Fig. 6.1A). To confirm the KPNA6 elevation, we infected MARC-145 cells with two PRRSV strains: VR-2385 and VR-2332, at an MOI of 1 and harvested the cells at 24 h post infection (hpi). We showed that the virus-infected cells exhibited a 2-fold increase in KPNA6 protein level compared to mock-infected cells (Fig. 6.1B). MARC-145 cells are derived from the kidney of an African Green monkey, which is not the natural host of PRRSV (28). Pigs are the only host animals for PRRSV infection, and the main target cells for PRRSV infection are pulmonary alveolar macrophages (PAMs) (46). Thus, we examined KPNA6 level in PAMs after PRRSV infection. The result showed that PRRSV VR-2385 infection also induced KPNA6 elevation (Fig. 6.1C).

To determine if the virus-induced KPNA6 elevation is a dose-dependent response, we infected MARC-145 cells with PRRSV VR-2385 at the MOI of 0.1, 1, and 10 and assessed KPNA6 level with Western blotting. The result showed that KPNA6 protein levels increased in the PRRSV-infected cells in a dose-dependent manner (Fig. 6.1D). Compared with the mock-infected cells, PRRSV infection increased KPNA6 levels by 1.7, 2.2, and 3.9-fold in the cells inoculated with PRRSV at the MOI of 0.1,

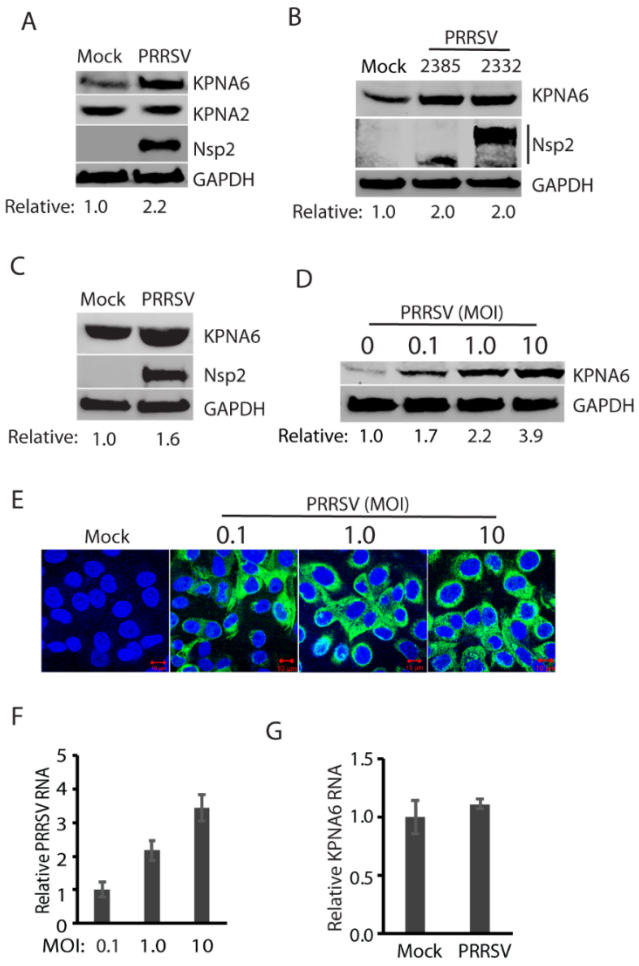

Fig. 6.1 PRRSV infection induces elevation of KPNA6 protein level but has minimal effect on KPNA6 transcript level. A. KPNA6 protein in PRRSV-infected MARC-145 cells is higher than mock-infected control, whereas there is minimal change in KPNA2 level. The cells were infected with PRRSV strain VR-2385 at a multiplicity of infection (MOI) of 1 and were harvested at 24 hours post infection (hpi). Western blotting (WB) with antibodies against KPNA6, KPNA2, PRRSV nsp2, and GAPDH was done. Relative levels of KPNA6 after normalization with GAPDH are shown below the images. B. Elevation of KPNA6 level in MARC-145 cells infected with different PRRSV strains. The cells were infected with VR-2385 and VR-2332 at an MOI of 1, incubated for 24 h before harvested for WB with antibodies against KPNA6, GAPDH and pig anti-PRRSV serum. C. KPNA6 level increased in primary PAM cells infected with PRRSV strain VR-2385 at an MOI of 1. D. The dose-dependent increase of KPNA6 protein level by PRRSV. MARC-145 cells were infected with the incremental MOI of PRRSV VR-2385 and harvested at 24 hpi. Relative levels of KPNA6 are shown below the images. E. IFA of PRRSV-infected cells. The panel of overlay IFA images shows PRRSV-nsp2 in green and nuclear DNA staining with DAPI in blue. The bars in the low right of the images denote 10 µm. F. The relative PRRSV RNA level in the MARC-145 cells infected with the incremental MOI. The cells were harvested at 24 hpi for RNA isolation and RT-qPCR. Error bars represent the standard errors of three repeated experiments. G. The transcript level of KPNA6 remains stable in PRRSV-infected cells 24 hpi detected by RT-qPCR.

1, and 10, respectively, at 24 hours post infection (hpi). IFA results showed that almost all of the cells inoculated at the MOI of 1 and 10 were infected, while majority of the cells inoculated at the MOI of 0.1

were positive (Fig. 6.1E). The increase of PRRSV RNA level in the infected cells was positively correlated to the amount increase of the virus inoculum (Fig. 6.1F).

Multiple factors, such as enhanced mRNA transcription or translation, or less protein degradation, can contribute to elevated KPNA6 expression in virus-infected cells. First, we detected KPNA6 transcript level in PRRSV-infected cells. The RT-qPCR analysis suggested KPNA6 mRNA levels were similar between PRRSV-infected and control cells (Fig. 6.1G). This result indicates that the elevation of KPNA6 protein level was not due to alteration at the transcriptional level.

The KPNA6 half-life is extended, while its poly-ubiquitination level is reduced in the PRRSV-infected cells

Since the KPNA6 increase in the PRRSV-infected cells was not due to the change of its transcriptional level and PRRSV infection stabilized KPNA6, we wondered if the virus infection might extend the KPNA6 half-life. To address this question, we infected MARC-145 cells with PRRSV and treated the cells with cycloheximide, a protein translation inhibitor, at 24 hpi. The KPNA6 half-life in the PRRSV-infected cells was 32 hours, compared to 12 hours in the mock-infected cells (Fig. 6.2A). The results suggest that extended KPNA6 half-life may account for its higher levels in viral infections.

Since KPNA6 half-life was extended by viral infections, we speculated there might be a delay in the degradation of KPNA6. As the ubiquitin-proteasome system is involved in the turnover of most cellular proteins, we hypothesized that treatment of cells with proteasome inhibitors, like MG132, would block KPNA6 degradation. As expected, MG132-treated MARC-145 cells exhibited a higher level of KPNA6 than mock-treated cells (Fig. 6.2B). PRRSV infection did not result in an additive effect to MG132 treatment in the elevation of KPNA6, or vice versa. Due to its short treatment time (6 hours), MG132 did not cause apparent cytotoxicity (Fig. 6.2C) and had a minimal effect on PRRSV replication (Fig. 6.2D). These results indicated that the proteasome blocking stabilized KPNA6 to a level similar to that of PRRSV infection.

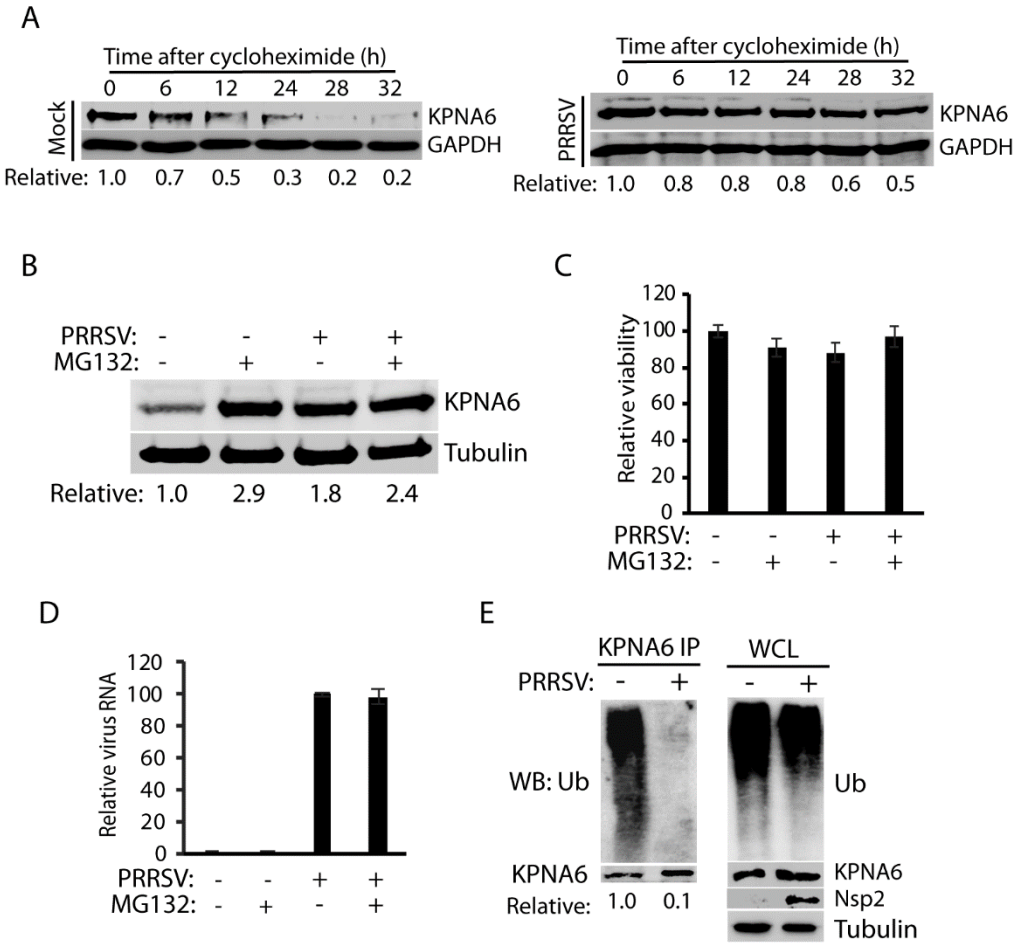

Fig. 6.2 PRRSV extends KPNA6 half-life and reduces KPNA6 poly-ubiquitination. A. PRRSV infection extends KPNA6 half-life. MARC-145 cells were infected with VR-2385 at an MOI of 1. The cells were treated with cycloheximide at 24 hpi and harvested at the indicated time (h) for WB. Mock-infected cells at corresponding time points were included as controls. The relative levels of KPNA6 are shown below the images. B. MG132 treatment blocks KPNA6 turnover in MARC-145 cells. The cells were infected with VR-2385 at an MOI of 1. At 18 hpi, the cells were treated with MG132 and, 6 h later, harvested for WB with antibodies against KPNA6 and tubulin. The MG132-negative wells were treated with the solvent, DMSO. Mock-infected cells were included as controls. The relative levels of KPNA6 are shown below the images after normalization with tubulin. C. The cell viability assay of MARC-145 cells treated with MG132 or DMSO and/or infected with PRRSV. D. PRRSV viral RNA level in the cells treated with MG132 or DMSO. E. PRRSV infection reduces KPNA6 poly-ubiquitination. MARC-145 cells were infected with PRRSV VR-2385 at an MOI of 1 and harvested for IP with KPNA6 antibody at 24 hpi, followed by WB with the ubiquitin (Ub) antibody. WB of whole cell lysate (WCL) with the antibodies against ubiquitin, KPNA6, PRRSV nsp2, and tubulin was conducted. The relative level of Ub after normalization with KPNA6 is shown below the images.

Based on these results, KPNA6 appeared to be degraded via the ubiquitin-proteasomal pathway. KPNA6 poly-ubiquitination level was expected to be down-regulated in PRRSV-infected cells. To confirm this, we conducted an immunoprecipitation (IP) assay of KPNA6 from MARC-145 cells in the presence or absence of PRRSV infection, followed by immunoblotting with a ubiquitin antibody. The

result showed that the KPNA6 ubiquitination level in the PRRSV-infected cells was ten-fold lower than that of mock-infected control, whereas there was minimal difference in the total ubiquitination level of whole cell lysates from both infected and control cells (Fig. 6.2E). Collectively, the extension of KPNA6 half-life through reduction of its ubiquitination may lead to the virus-mediated KPNA6 upregulation.

PRRSV nsp12 protein upregulates KPNA6 protein level in cells

We speculated that some PRRSV proteins were responsible for the KPNA6 elevation in the virus-infected cells. To determine the viral proteins, we transfected HEK293 cells with plasmids encoding the PRRSV non-structural proteins (nsps) and assessed their effects on the KPNA6 level. WB results showed that PRRSV nsp1β, nsp7α, nsp7β, and nsp12 led to a higher KPNA6 level, compared with the empty vector, whereas the other PRRSV proteins had less effect (Fig. 6.3A). As nsp12 induced the highest elevation of KPNA6, we selected it to further confirm its effect by using a stable HEK293 cell line expressing nsp12 that was established earlier in the laboratory. WB result showed there was a 2.1-fold increase in KPNA6 protein level in the nsp12-stable cells compared with the control HEK293 cells (Fig. 6.3B). In addition, IP assay showed that PRRSV nsp12 also reduced KPNA6 ubiquitination (Fig. 6.3C). This suggested that the nsp12 might interfere with the KPNA6 turnover in cells. Yet, no physical interaction between KPNA6 and nsp12 was detected in the IP (Fig. 6.3C), implicating that mechanisms other than direct protein binding might mediate the effect.

KPNA6 silencing impairs PRRSV replication

To determine whether KPNA6, stabilized in the virus-infected cells, could play a positive role in viral replication, we generated a KPNA6 shRNA construct for knockdown of KPNA6 expression in MARC-145 cells via RNAi silencing. A random shRNA was included as a negative control. Cells were transfected with the shRNA plasmids and stable cell lines were generated under the selection pressure of

the antibiotics G418. WB results showed KPNA6 was reduced to 0.3-fold in the cells with stable expression of KPNA6 shRNA, while KPNA1 level had minimal change (Fig. 6.4A). The KPNA6 knockdown had no detectable effect on the cell viability (Fig. 6.4B). To investigate the effect of the KPNA6 knockdown on PRRSV replication, we infected the KPNA6-silenced cells with VR-2385. Viral titration assay showed that the KPNA6-silenced cells produced significantly lower virus yield (750-fold decrease) compared with control cells (Fig. 6.4C).

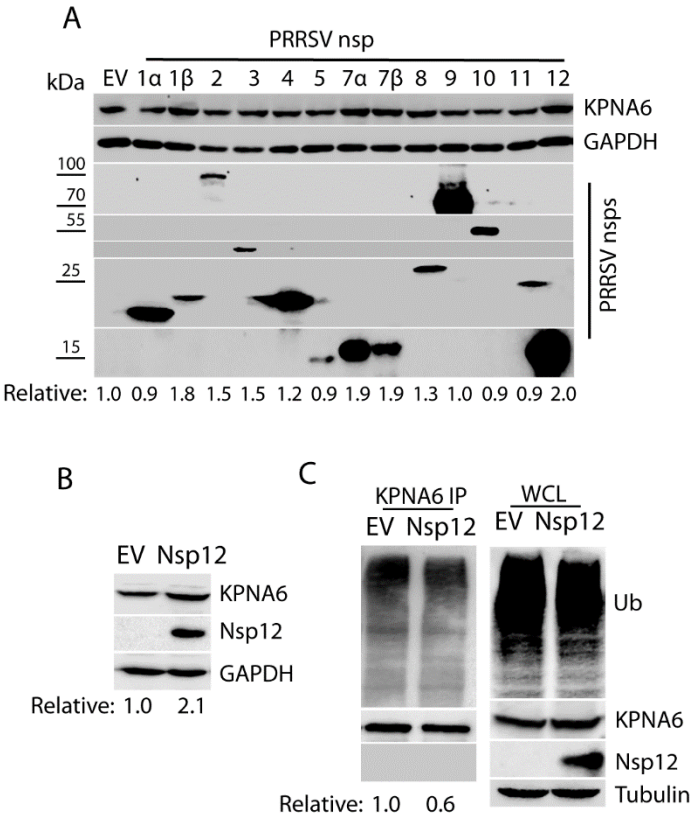

Fig. 6.3 PRRSV nsp12 induces KPNA6 elevation. A. Screening of PRRSV nsps to identify the viral protein that is responsible for the elevation of KPNA6. Empty vector (EV) was included as a control. After 36 hours post transfection (hpt), HEK293 cells were harvested for WB. The lower panel of images show the bands of PRRSV nsps. The relative levels of KPNA6 protein are shown below the images. Molecular mass markers are denoted on left of the images. B. Higher KPNA6 level in the nsp12-stable HEK293 cells than the control. The relative level of KPNA6 is shown below the images. C. Lower KPNA6 poly-ubiquitination in the HEK293 cells transfected with the nsp12 plasmid. The MG132 treatment was done before the cell harvesting. The KPNA6 IP followed by WB with an antibody against ubiquitin (Ub) was done. The relative level of Ub is shown below the images. WB of WCL with the antibodies against Ub, KPNA6, PRRSV nsp12, and tubulin was conducted.

PRRSV nsp1β relies on KPNA6 to translocate into the nucleus

Although PRRSV replicates in the cytoplasm, some viral proteins including nsp1α, nsp1β, and nucleocapsid protein (N) translocate into the nucleus during infection. Nsp1β has been identified to restrain host mRNA in the nucleus to inhibit host protein synthesis (388). Nsp1α may inhibit IFN promoter activation in the nucleus (114). N protein localizes in the nucleus to affect host nuclear processes (156).

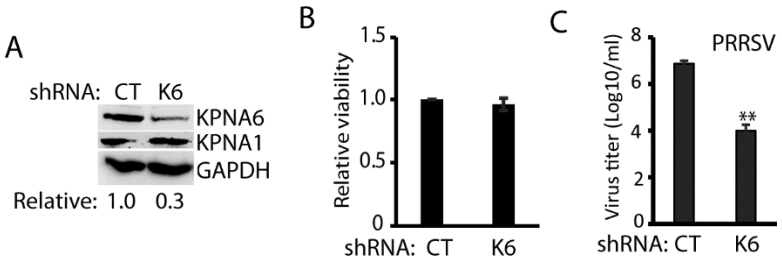

Fig. 6.4 KPNA6 silencing leads to a lower replication of PRRSV. A. KPNA6 protein level in the MARC-145 cells stably transfected with KPNA6-shRNA. CT: control shRNA, K6: shRNA against KPNA6. The WB of KPNA6, KPNA1, and GAPDH was done. B. The relative viability of the shRNA-transfected MARC-145 cells. C. Lower PRRSV yield in the cells with KPNA6 silencing than in the control MARC-145 cells (**, $P < 0.01$). The MARC-145 cells were infected with PRRSV VR-2385 at an MOI of 0.1. The virus was harvested 48 hpi for titration.

To determine if KPNA6 is responsible for the translocation of these viral proteins with nuclear localization, we established KPNA6-/- and control HeLa cells and confirmed the deletion of KPNA6 in the KPNA6-/- cells (Fig. 6.5A). The KPNA6 knockout had no detectable effect on the cell viability (Fig. 6.5B). We then transfected the KPNA6-/- and control HeLa cells with plasmids expressing PRRSV nsp1α, nsp1β, and N for IFA to determine their subcellular locations. Confocal microscopy results showed that KPNA6 knockout blocked the nuclear translocation of PRRSV nsp1β, while there was

minimal change in subcellular location of the other two proteins tested (Fig. 6.5C). This indicates that KPNA6 facilitates nsp1β nuclear translocation and may contribute to optimal virus replication.

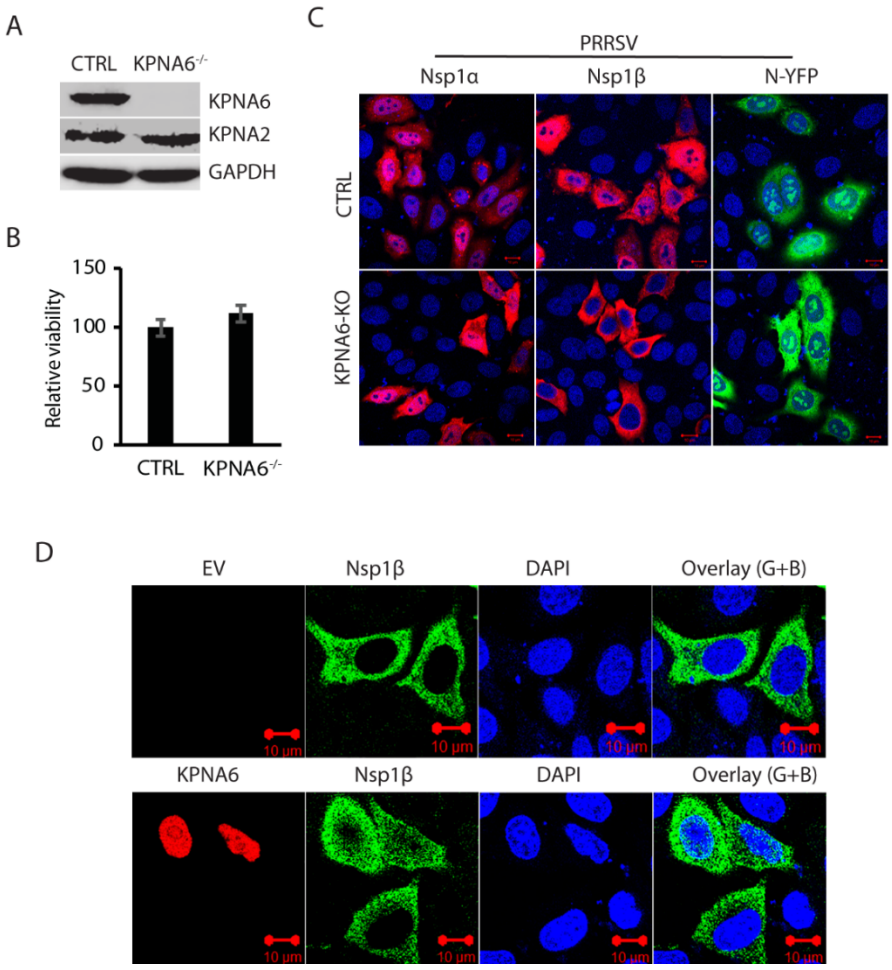

Fig. 6.5 KPNA6-knockout blocks nuclear translocation of PRRSV nsp1β, and exogenous KPNA6 expression restores its nuclear translocation. A. WB of KPNA6 protein in the KPNA6 knockout HeLa cells. CTRL: control cells stably transfected with empty vector with Cas9. KPNA6$^{-/-}$: KPNA6-knockout HeLa cells. WB of KPNA6, KPNA2, and GAPDH was done. B. Relative cell viability of the KPNA6$^{-/-}$ and CTRL HeLa cells. C. Confocal microscopy of the KPNA6$^{-/-}$ and CTRL HeLa cells with transient expression of the PRRSV proteins. The cells were transfected with plasmids encoding HA-nsp1α, HA-nsp1β, and N-YFP proteins. IFA with antibody against HA was done. The overlay IFA images show HA-nsp1α and HA-nsp1β in red fluorescence, N-YFP in green fluorescence, and nuclear DNA staining with DAPI in blue. The bars in the low right of the images denote 10 μm. D. Transient exogenous expression of KPNA6 in KPNA6$^{-/-}$ HeLa cells restores the nuclear translocation of PRRSV nsp1β. The cells were transfected with Myc-KPNA6 and HA-nsp1β plasmids. Empty vector (EV) was included as a control. IFA with antibodies against Myc and HA was done. Overlay of green and blue channels (Overlay (G+B)) are shown. Nuclear DNA was stained with DAPI in blue. The bars in the low right of the images denote 10 μm.

To exclude the possibility of off-target effect by sgRNA, we overexpressed KPNA6 and nsp1β plasmids into KPNA6-knockout HeLa cells to determine if exogenous restitution of KPNA6 would restore the nuclear localization of nsp1β. The results of confocal microscopy showed that restitution of KPNA6 restores the nuclear translocation of nsp1β completely (Fig. 6.5D). This result confirms that KPNA6 is required for nsp1β nuclear translocation.

ZIKV infection induces KPNA6 elevation and requires KPNA6 for optimal replication

PRRSV, a member of +ssRNA virus, replicates in the cytoplasm of infected cells. Nevertheless, KPNA6, a karyopherin, is responsible for the nucleocytoplasmic transportation of cellular proteins. To further test whether KPNA6 elevation is specific for PRRSV infection, we used another +ssRNA virus ZIKV and examined KPNA6 protein level. ZIKV also induced elevation of KPNA6 protein level compared to mock-infected cells (Fig. 6.6A). Effective ZIKV infection was confirmed by IFA detection of E protein using antibody against the flavivirus envelope protein (E) (Fig. 6.6A). Thus, KPNA6 induction seems to be a common feature of the two +ssRNA viruses tested.

To further confirm the role of KPNA6 in ZIKV replication, we established KPNA6-knockout Vero cells via CRISPR/Cas9 system. The empty vector containing Cas9 but no target gRNA was also used to establish stable Vero cells as controls. WB result showed significant reduction of KPNA6 in the stable KPNA6-/- Vero cells (Fig. 6.6B). The KPNA6 knockout had no detectable effect on the cell viability (Fig. 6.6C). To test the effect of the KPNA6 knockout on virus replication, we infected the KPNA6-/- Vero and control Vero cells with ZIKV PRVABC59 strain. The KPNA6-/- Vero produced significantly lower ZIKV replication than control cells (Fig. 6.6D). These results demonstrate that KPNA6 is needed for ZIKV replication.

Furthermore, we transfected KPNA6-/- Vero cells with KPNA6 plasmid and established stable cells for exogenous restitution of KPNA6 expression to exclude the off-target effect of CRISPR/Cas9 system on ZIKV replication. WB result showed the successful restitution of KPNA6 in the KPNA6-/-

Vero cells (Fig. 6.6E). To determine if the exogenous KPNA6 restitution could restore ZIKV replication in the KPNA6-/- Vero cells, we infected the cells with ZIKV PRVABC59 strain and harvested the cells at 24 hpi. The parental KPNA6-/- Vero and control cells were included as controls. The result of RT-qPCR showed that expression of exogenous KPNA6 in the KPNA6-/- Vero cells could restore ZIKV replication (Fig. 6.6F). This result substantiates that KPNA6 is required for ZIKV replication.

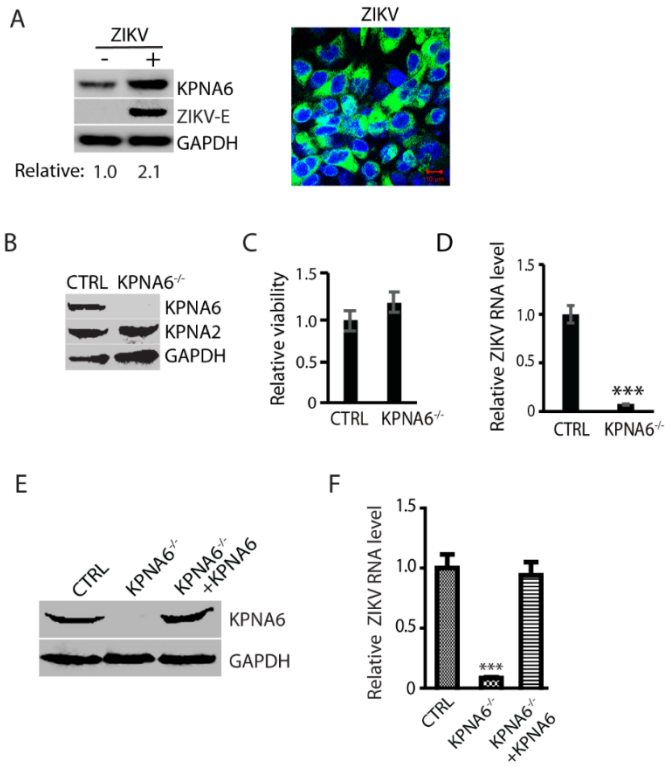

Fig. 6.6 ZIKV infection also increases KPNA6 protein level and requires KPNA6 for efficient replication. A. KPNA6 increase in ZIKV-infected Vero cells. The cells were infected with ZIKV PRVABC59 strain at an MOI of 10 and harvested at 24 hpi. WB with antibodies against KPNA6, ZIKV E protein, and GAPDH was conducted. Relative level of KPNA6 is shown below the images. IFA with antibody against E protein was conducted. The image on right shows overlay of E in green and nuclear DNA staining with DAPI in blue. The bar in the low right of the image denotes 10 μm. B. KPNA6 protein level in the KPNA6 knockout Vero cells. CTRL: control cells stably transfected with the empty vector, KPNA6$^{-/-}$: KPNA6-knockout Vero cells via CRISPR/Cas9 system. WB of KPNA6, KPNA2, and GAPDH was done. C. Relative cell viability of the CTRL and KPNA6$^{-/-}$ Vero cells. D. ZIKV replication in the KPNA6$^{-/-}$ Vero cells is significantly lower than that in the CTRL cells detected by RT-qPCR (***, $P < 0.001$). The CTRL and KPNA6$^{-/-}$ Vero cells were infected with ZIKV PRVABC59 strain at an MOI of 0.1. RNA was isolated at 24 hpi and RT-qPCR was conducted to detect ZIKV RNA level. E. Stable expression of KPNA6 in KPNA6$^{-/-}$ Vero cells restores KPNA6 protein level. F. Stable exogenous KPNA6 expression in KPNA6$^{-/-}$ Vero cells restores ZIKV replication level. The Vero cells were infected with ZIKV PRVABC59 strain at an MOI of 0.1. RNA was isolated at 24 hpi and RT-qPCR was conducted.

Discussion

Karyopherins are critical transport factors in canonical nucleocytoplasmic trafficking system, which is essential for the signal transduction of the host immune response. Accordingly, karyopherins have been found to be targeted by many viruses for an evasion of the host antiviral response, including Ebola virus (231, 232), HCV (298), Hepatitis B virus (HBV) (297), Poliovirus (389) and PRRSV (121). On the other hand, those viruses including DNA viruses (276), HIV (282) and influenza A virus (289) that replicate in the nucleus exploit karyopherins to translocate their proteins or genetic elements into the nucleus.

In this study, we discovered that KPNA6 is required by two cytoplasmic +ssRNA viruses, PRRSV and ZIKV, to facilitate their replication. The viruses protected KPNA6 from the ubiquitin-proteasome degradation. In addition, the KPNA6 knockdown or knockout impairs the viral replication. KPNA6 is involved in the nuclear translocation of PRRSV nsp1β. Notably, restitution of KPNA6 expression in the KPNA6 knockout cells restores the nuclear translocation of PRRSV nsp1β and ZIKV replication. These data indicate that KPNA6 is a positive cellular factor for both PRRSV and ZIKV.

Our data showed that both PRRSV and ZIKV led to the elevation of KPNA6 protein level. The KPNA6 transcript level had minimal change in the PRRSV-infected cells. The KPNA6 elevation was dose-dependent on the PRRSV inoculum amount. The half-life of KPNA6 was extended from 12 h in the mock-infected cells to 32 h in the PRRSV-infected cells, which is consistent with the time kinetics of KPNA6 in the infected cells. The results suggest that the virus infection stabilizes the KPNA6 protein by protecting it from the ubiquitin-proteasome degradation. Consistent with this postulation, the MG132 treatment increased the KPNA6 level. The KPNA6 poly-ubiquitination level in the virus-infected cells was significantly lower than mock-infected cells. The MG132 treatment lasted 6 hours in this experiment and did not affect the PRRSV replication. However, ubiquitin/proteasome system plays a

critical role in flavivirus replication, and MG132, added before or soon after virus inoculation, was shown to strongly repress flavivirus RNA translation and replication (390).

Among the PRRSV nsps tested, nsp1β, nsp7α, nsp7β, and nsp12 were found to induce the KPNA6 elevation when individually overexpressed. It is not known whether they work synergistically in PRRSV-infected cells to exert the effect on KPNA6 elevation. However, none of them is known to have a direct effect on the ubiquitin-proteasome pathway. Nsp1β antagonizes the host interferon induction and downstream JAK-STAT signaling (139). Nsp1β induces the degradation of KPNA1 to block STAT1 nuclear translocation. Interestingly, nsp1β can induce the elevation of KPNA6, a member of the same subfamily as KPNA1. The nsp1β dependence on KPNA6 for its nuclear translocation may account for the reason for the KPNA6 stabilization. Nsp7 is highly conserved and further cleaved into nsp7α and nsp7β, which are known to induce a strong humoral immune response in PRRSV-infected pigs (391). Nsp12 is reported to interact with many cellular proteins with high probability in a proteomic study (392). Among the cellular proteins, chaperone HSP70 is verified to interact with nsp12 and inhibition of HSP70 negatively affects PRRSV replication. Nsp12 induces Serine 727 phosphorylation of STAT1 to activate expression of inflammatory cytokines while having no effect on tyrosine 701 phosphorylation that is activated by interferons (393). The induction of S727 phosphorylation depends on the p38 mitogen-activated protein kinase (MAPK) pathway. Our results confirmed that nsp12 induced the KPNA6 elevation in nsp12-stable HEK293 cells. Nsp12 might indirectly exert the effect, as no direct interaction between nsp12 and KPNA6 was detected in the co-IP. Further study is needed to delineate detail mechanisms on the viral interference with the KPNA6 turnover.

KPNA6 silencing or knockout dramatically inhibits PRRSV and ZIKV replication, demonstrating that KPNA6 is required for the viral replication. Expression of exogenous KPNA6 in the KPNA6 knockout cells restores ZIKV replication, which substantiates the requirement of KPNA6 in the optimal viral proliferation. As we did not do restitution of exogenous KPNA6 in KPNA6-silenced

MARC-145 cells, we cannot exclusively exclude the possibility that the reduced PRRSV replication in KPNA6 knockdown cells could be in part due to off-target effects. Nevertheless, the restoration of ZIKV replication in KPNA6-knockout cells with expression of exogenous KPNA6 clearly demonstrates that KPNA6 is required for the viral replication. PRRSV infection leads to heavy economic losses to the swine industry. ZIKV is a significant global public health problem. However, prevention and therapeutic strategies against these viral pathogens are either limited or unavailable. Our finding may facilitate the development of antiviral strategies by modulating KPNA6 or blocking the interaction of KPNA6 with the viral proteins.

Even though +ssRNA viruses replicate in the cytoplasm, some viral proteins localize to the nucleus. Therefore, we speculated that KPNA6 might take charge of nuclear transport of some of the viral proteins. Indeed, PRRSV nsp1β was found to depend on KPNA6 for the nuclear translocation. This result was substantiated by the restoration of nsp1β nuclear translocation in KPNA6 knockout HeLa cells with expression of exogenous KPNA6. Our data suggest that nsp1β nuclear localization is important for PRRSV replication. Yet, we did not determine the nsp1β subcellular location in PRRSV-infected MARC-145 cells with KPNA6 silencing due to lacking nsp1β antibody. However, our result does not exclude other potential mechanisms of KPNA6 to enhance the viral replication as for ZIKV, the nuclear translocation of ZIKV C and NS5 proteins were not affected by KPNA6 knockout (data not shown). Further studies to examine the mechanisms of KPNA6 on the replication of these +ssRNA viruses are warranted.

In addition, elevation of KPNA6 protein level was also found in cells infected by other +ssRNA viruses, hepatitis C virus (HCV) and porcine epidemic diarrhea virus (PEDV) (data not shown). HCV, a member of the Hepacivirus genus of the Flaviviridae family (394), can cause liver disease upon infection, which could lead to cirrhosis and hepatocellular carcinoma; porcine epidemic diarrhea virus (PEDV), a member of the genus Alphacoronavirus of the family Coronaviridae (395), causes an acute

and highly contagious enteric disease in nursery piglets with the high mortality rate, which has led to tremendous economic losses in swine industry (396). Our data suggest that that KPNA6 might be a potential broad pro-viral protein for +ssRNA viruses.

In conclusion, KPNA6 plays an important role in the replication of PRRSV and ZIKV. The virus infection protects KPNA6 from degradation via inhibition of KPNA6 poly-ubiquitination. RNAi-mediated KPNA6 silencing or CRISPR/Cas9-knockout of KPNA6 leads to a significant reduction of PRRSV and ZIKV replication. KPNA6 is required for the nuclear translocation of PRRSV nsp1β. Notably, expression of exogenous KPNA6 in the KPNA6 knockout cells restores nsp1β nuclear translocation and ZIKV replication. These results suggest that KPNA6 is required for PRRSV and ZIKV, which modulate the KPNA6 turnover to facilitate the virus replication. This finding provides new insights on virus-cell interactions and may facilitate the development of antiviral therapeutics by blocking the viral manipulation of the cellular transport factor.

Table 6.1 List of primers in Chapter 6

Primer[a]	Sequences (5' to 3')[b]	Target gene/use
KPNA6F1	CC*GAATTC*GAGACCATGGCGAGCCCAGGG	KPNA6 cloning
KPNA6R1	GC*CTCGAG*TTATAGCTGGAAGCCCTCC	KPNA6 cloning
R-KPNA6-F1	GGAAGCCTATGGCTTGGATA	KPNA6 real-time
R-KPNA6-R1	CTGTTGCGTTTCATCGACTT	KPNA6 real-time
P7RF1	ATCGCTCACCAAAACCAGTCC	PRRSV real-time
P7RR1	CTTCAGTCGCTAGAGGGAAATGG	PRRSV real-time
KPNA6_S1F	*GATC*CAGCCTATGGCTTGGATAAATTCAAG AGATTTATCCAAGCCATAGGCTTTTTTTACG CGTG	KPNA6 shRNA
KPNA6_S1R	*AATTC*ACGCGTAAAAAAAGCCTATGGCTTG GATAAATCTCTTGAATTTATCCAAGCCATA GGCTG	KPNA6 shRNA
KPNA6-gRNA-p2tF	*CACC*GAAGAGTGGTGGATCGGTTCG	KPNA6 sgRNA
KPNA6-gRNA-p2tR	*AAAC*CGAACCGATCCACCACTCTTC	KPNA6 sgRNA
KPNA6-gRNA-p2bF	*CACC*GTGTTGATAACTTCATCTAT	KPNA6 sgRNA

KPNA6-gRNA-p2bR	*AAAC*ATAGATGAAGTTATCAACAC	KPNA6 sgRNA

a. F: forward primer, R: reverse primer.

b. The italicized letters indicate restriction enzyme cleavage sites for cloning.

Chapter 7: Conclusions and perspectives

Since first reported in 1987, PRRS has been remaining one of the top challenges for swine industry across the world. The PRRSV infection is featured by prolonged viremia, persistent infection, and induction of weak protective immune response, which results in high PRRSV prevalence and big challenges for PRRS control. One of the possible reasons for the weak protective immune response is that PRRSV interferes with the innate immunity and cytokine signaling, including the JAK-STAT pathways. PRRSV inhibits IFN-activated JAK-STAT signaling by blocking the nuclear translocation of STAT1 and STAT2. In this dissertation research, PRRSV was found to antagonize JAK-STAT2 and JAK-STAT3 signaling and manipulate KPNA6 for viral replication. The mechanisms of these interferences of cellular signaling have been characterized.

In addition to the canonical IFN signaling, STAT2 is involved in non-canonical STAT1-independent IFN signaling. In this alternative pathway, STAT2 interacts with IRF9 and other STAT proteins, but not STAT1, to form ISGF3-like complex, followed by driving a prolonged antiviral response. The PRRSV inhibition of this signaling is described in Chapter 4. PRRSV infection of MARC-145 cells and primary PAMs leads to significant reduction of STAT2 protein, whereas it has minimal effect on STAT1 protein level. Several strains of both genera of PRRSV induce a similar reduction of STAT2 protein level but have no effect on its transcript level. The STAT2 reduction is via ubiquitin-proteasome pathway as treatment of the PRRSV-infected cells with MG132, a proteasomal inhibitor, restores the STAT2 protein level. Notably, PRRSV nsp11 is responsible for STAT2 reduction through interaction. The aa 57-59 residues in nsp11 are critical for the interaction with and downregulation of STAT2. These results demonstrate that nsp11 might promote or provide a platform for the interaction between STAT2 and its ubiquitin E3 ligase. Further study will interrogate the E3 ligase of STAT2 targeted by PRRSV nsp11. This study not only provides insight for PRRSV

perturbation of STAT1-independent IFN signaling, but also reveals another function of nsp11 in addition to its endoribonuclease activity.

Among all the STAT proteins, STAT3 is known as highly pleiotropic in mediating the expression of a variety of genes in response to both cytokines and growth factors, and thus plays a pivotal role in numerous cellular processes including cell survival, proliferation, embryogenesis, and immune responses (202, 397). In this study, OSM, a member of the IL-6 family activating the JAK-STAT3 signaling, has been found to inhibit PRRSV replication. To overcome the inhibition, PRRSV uses a strategy to reduce STAT3 protein level, which is described in Chapter 5. PRRSV induces STAT3 reduction by increasing its polyubiquitination level and shortening its half-life. The hydrophobic transmembrane protein nsp5 is responsible for the STAT3 reduction. As a result, nsp5 inhibits the OSM-activated STAT3 signaling. No direct interaction between nsp5 and STAT3 is found, which suggests that nsp5 might activate an E3 ligase of STAT3. Further study is needed to reveal the mechanism of the STAT3 degradation. Inhibition of the STAT3 signaling by PRRSV can lead to inhibition of a broad spectrum of cytokines and growth factors to thwart host antiviral responses and allow virus replication and spread *in vivo*.

For JAK-STAT signaling, nuclear importins play indispensable roles in transporting the activated STAT complexes into the nucleus to activate the transcription and expression of downstream genes. KPNA1 and KPNA6 have been found to be mainly responsible for the translocation of STAT1/2 and STAT3, respectively. PRRSV interrupts the nuclear import of STAT1/2 complex to prevent IFN signaling through nsp1β inducing KPNA1 degradation. However, we unexpectedly discovered that PRRSV could elevate KPNA6 protein level, elaborated in Chapter 6. PRRSV protects KPNA6 from degradation by blocking its poly-ubiquitination via nsp12. KPNA6 silencing suppresses PRRSV replication through blocking the nuclear translocation of nsp1β, which is a strong IFN antagonist. On the other hand, another +ssRNA virus ZIKV also induces KPNA6 elevation and KPNA6 knockout is

detrimental to ZIKV replication. These results indicate that KPNA6 is critical for the replication of PRRSV and ZIKV. However, the mechanism of KPNA6 required for ZIKV replication remains unknown.

In this dissertation study, the mechanisms of PRRSV interference with STAT2 and STAT3 signaling and manipulation of KPNA6 for viral replication have been elucidated. PRRSV nsp11, nsp5 and nsp12 are responsible for STAT2 degradation, STAT3 reduction, and KPNA6 elevation, respectively. The critical amino acids of nsp11 for STAT2 reduction have been identified. Yet, the crucial amino acids of nsp5 and nsp12 for the observed effects in this study remain unknown. The identification of these key amino acid residues may be future research direction. Once these residues are identified, PRRSV infectious cDNA clone can be mutated in these residues for further functional study of these proteins in the context of whole virus infection and vaccine development to minimize the interference with the host cellular signaling and improve protective immune response. Moreover, any other PRRSV proteins interfering with host immune signaling may be considered for inclusion in the mutant infectious clone construction. Under this circumstance, one PRRSV strain with minimized capacity to antagonize host immune system might be recovered and will greatly facilitate the development of an improved vaccine against PRRS. A caveat is that mutation of multiple critical residues might be detrimental to the PRRSV viability and virus recovery might fail or, if successful, the recovered virus might have low titer due to poor replication. One possible alternative is generation of multiple clones with each carrying a limited number of mutations to avoid the detrimental effects and mix the recovered virus for vaccine application.

On the other hand, this study reveals the role of KPNA6 in PRRSV and ZIKV replication. In addition, HCV and porcine epidemic diarrhea virus (PEDV) also induce KPNA6 elevation, and poliovirus replication is impaired by KPNA6 knockout. These results indicate that these +ssRNA viruses manipulate KPNA6 for the viral replication. Further study is warranted to elucidate the

mechanisms of the KPNA6 contribution to the viral replication. Several aspects can be investigated: KPNA6 subcellular location, KPNA6 functional domain, viral proteins interacting with KPNA6, and roles of other KPNAs in the viral replication of these +ssRNA viruses. These studies will provide much more insights into +ssRNA virus–host interactions, and facilitate the development of unique antiviral therapeutics against these important human and animal pathogens.

Bibliography

1. **Rossow KD.** 1998. Porcine reproductive and respiratory syndrome. Vet Pathol **35:**1-20.
2. **Holtkamp DJ, Kliebenstein JB, Neumann EJ, Zimmerman JJ, Rotto HF, Yoder TK, Wang C, Yeske PE, Mowrer CL, Haley CA.** 2013. Assessment of the economic impact of porcine reproductive and respiratory syndrome virus on United States pork producers. Journal of Swine Health and Production **21:**72-84.
3. **Nieuwenhuis N, Duinhof TF, van Nes A.** 2012. Economic analysis of outbreaks of porcine reproductive and respiratory syndrome virus in nine sow herds. Vet Rec **170:**225.
4. **Wensvoort G, Terpstra C, Pol JM.** 1991. ['Lelystad agent'--the cause of abortus blauw (mystery swine disease)]. Tijdschr Diergeneeskd **116:**675-676.
5. **Collins JE, Benfield DA, Christianson WT, Harris L, Hennings JC, Shaw DP, Goyal SM, McCullough S, Morrison RB, Joo HS, et al.** 1992. Isolation of swine infertility and respiratory syndrome virus (isolate ATCC VR-2332) in North America and experimental reproduction of the disease in gnotobiotic pigs. J Vet Diagn Invest **4:**117-126.
6. **Kvisgaard LK, Larsen LE, Hjulsager CK, Botner A, Rathkjen PH, Heegaard PMH, Bisgaard NP, Nielsen J, Hansen MS.** 2017. Genetic and biological characterization of a Porcine Reproductive and Respiratory Syndrome Virus 2 (PRRSV-2) causing significant clinical disease in the field. Vet Microbiol **211:**74-83.
7. **Kuhn JH, Lauck M, Bailey AL, Shchetinin AM, Vishnevskaya TV, Bao Y, Ng TF, LeBreton M, Schneider BS, Gillis A, Tamoufe U, Diffo Jle D, Takuo JM, Kondov NO, Coffey LL, Wolfe ND, Delwart E, Clawson AN, Postnikova E, Bollinger L, Lackemeyer MG, Radoshitzky SR, Palacios G, Wada J, Shevtsova ZV, Jahrling PB, Lapin BA, Deriabin PG, Dunowska M, Alkhovsky SV, Rogers J, Friedrich TC, O'Connor DH, Goldberg TL.** 2016. Reorganization and expansion of the nidoviral family Arteriviridae. Arch Virol **161:**755-768.
8. **Nelsen CJ, Murtaugh MP, Faaberg KS.** 1999. Porcine reproductive and respiratory syndrome virus comparison: divergent evolution on two continents. J Virol **73:**270-280.
9. **Dea S, Sawyer N, Alain R, Athanassious R.** 1995. Ultrastructural characteristics and morphogenesis of porcine reproductive and respiratory syndrome virus propagated in the highly permissive MARC-145 cell clone. Adv Exp Med Biol **380:**95-98.
10. **Dokland T.** 2010. The structural biology of PRRSV. Virus Res **154:**86-97.
11. **Music N, Gagnon CA.** 2010. The role of porcine reproductive and respiratory syndrome (PRRS) virus structural and non-structural proteins in virus pathogenesis. Anim Health Res Rev **11:**135-163.
12. **Fang Y, Snijder EJ.** 2010. The PRRSV replicase: exploring the multifunctionality of an intriguing set of nonstructural proteins. Virus Res **154:**61-76.
13. **Fang Y, Treffers EE, Li Y, Tas A, Sun Z, van der Meer Y, de Ru AH, van Veelen PA, Atkins JF, Snijder EJ, Firth AE.** 2012. Efficient -2 frameshifting by mammalian ribosomes to synthesize an additional arterivirus protein. Proc Natl Acad Sci U S A **109:**E2920-2928.
14. **Li Y, Treffers EE, Napthine S, Tas A, Zhu L, Sun Z, Bell S, Mark BL, van Veelen PA, van Hemert MJ, Firth AE, Brierley I, Snijder EJ, Fang Y.** 2014. Transactivation of programmed ribosomal frameshifting by a viral protein. Proc Natl Acad Sci U S A **111:**E2172-2181.

15. **Li Y, Shang P, Shyu D, Carrillo C, Naraghi-Arani P, Jaing CJ, Renukaradhya GJ, Firth AE, Snijder EJ, Fang Y.** 2018. Nonstructural proteins nsp2TF and nsp2N of porcine reproductive and respiratory syndrome virus (PRRSV) play important roles in suppressing host innate immune responses. Virology **517:**164-176.
16. **Mardassi H, Massie B, Dea S.** 1996. Intracellular synthesis, processing, and transport of proteins encoded by ORFs 5 to 7 of porcine reproductive and respiratory syndrome virus. Virology **221:**98-112.
17. **Meulenberg JJ, Petersen-den Besten A, De Kluyver EP, Moormann RJ, Schaaper WM, Wensvoort G.** 1995. Characterization of proteins encoded by ORFs 2 to 7 of Lelystad virus. Virology **206:**155-163.
18. **Wu WH, Fang Y, Farwell R, Steffen-Bien M, Rowland RR, Christopher-Hennings J, Nelson EA.** 2001. A 10-kDa structural protein of porcine reproductive and respiratory syndrome virus encoded by ORF2b. Virology **287:**183-191.
19. **Wissink EH, Kroese MV, van Wijk HA, Rijsewijk FA, Meulenberg JJ, Rottier PJ.** 2005. Envelope protein requirements for the assembly of infectious virions of porcine reproductive and respiratory syndrome virus. J Virol **79:**12495-12506.
20. **Johnson CR, Griggs TF, Gnanandarajah J, Murtaugh MP.** 2011. Novel structural protein in porcine reproductive and respiratory syndrome virus encoded by an alternative ORF5 present in all arteriviruses. J Gen Virol **92:**1107-1116.
21. **Duan X, Nauwynck HJ, Pensaert MB.** 1997. Virus quantification and identification of cellular targets in the lungs and lymphoid tissues of pigs at different time intervals after inoculation with porcine reproductive and respiratory syndrome virus (PRRSV). Vet Microbiol **56:**9-19.
22. **Franken L, Schiwon M, Kurts C.** 2016. Macrophages: sentinels and regulators of the immune system. Cell Microbiol **18:**475-487.
23. **Flores-Mendoza L, Silva-Campa E, Resendiz M, Osorio FA, Hernandez J.** 2008. Porcine reproductive and respiratory syndrome virus infects mature porcine dendritic cells and up-regulates interleukin-10 production. Clin Vaccine Immunol **15:**720-725.
24. **Chang HC, Peng YT, Chang HL, Chaung HC, Chung WB.** 2008. Phenotypic and functional modulation of bone marrow-derived dendritic cells by porcine reproductive and respiratory syndrome virus. Vet Microbiol **129:**281-293.
25. **Loving CL, Brockmeier SL, Sacco RE.** 2007. Differential type I interferon activation and susceptibility of dendritic cell populations to porcine arterivirus. Immunology **120:**217-229.
26. **Van Breedam W, Delputte PL, Van Gorp H, Misinzo G, Vanderheijden N, Duan X, Nauwynck HJ.** 2010. Porcine reproductive and respiratory syndrome virus entry into the porcine macrophage. J Gen Virol **91:**1659-1667.
27. **Lamontagne L, Page C, Larochelle R, Magar R.** 2003. Porcine reproductive and respiratory syndrome virus persistence in blood, spleen, lymph nodes, and tonsils of experimentally infected pigs depends on the level of CD8high T cells. Viral Immunol **16:**395-406.
28. **Kim HS, Kwang J, Yoon IJ, Joo HS, Frey ML.** 1993. Enhanced replication of porcine reproductive and respiratory syndrome (PRRS) virus in a homogeneous subpopulation of MA-104 cell line. Arch Virol **133:**477-483.
29. **Meng XJ, Paul PS, Halbur PG.** 1994. Molecular cloning and nucleotide sequencing of the 3'-terminal genomic RNA of the porcine reproductive and respiratory syndrome virus. J Gen Virol **75 (Pt 7):**1795-1801.
30. **Calvert JG, Slade DE, Shields SL, Jolie R, Mannan RM, Ankenbauer RG, Welch SK.** 2007. CD163 expression confers susceptibility to porcine reproductive and respiratory syndrome viruses. J Virol **81:**7371-7379.

31. **Kreutz LC.** 1998. Cellular membrane factors are the major determinants of porcine reproductive and respiratory syndrome virus tropism. Virus Res **53:**121-128.
32. **Jusa ER, Inaba Y, Kouno M, Hirose O.** 1997. Effect of heparin on infection of cells by porcine reproductive and respiratory syndrome virus. Am J Vet Res **58:**488-491.
33. **Delputte PL, Vanderheijden N, Nauwynck HJ, Pensaert MB.** 2002. Involvement of the matrix protein in attachment of porcine reproductive and respiratory syndrome virus to a heparinlike receptor on porcine alveolar macrophages. J Virol **76:**4312-4320.
34. **Delputte PL, Costers S, Nauwynck HJ.** 2005. Analysis of porcine reproductive and respiratory syndrome virus attachment and internalization: distinctive roles for heparan sulphate and sialoadhesin. J Gen Virol **86:**1441-1445.
35. **Duan X, Nauwynck HJ, Favoreel H, Pensaert MB.** 1998. Porcine reproductive and respiratory syndrome virus infection of alveolar macrophages can be blocked by monoclonal antibodies against cell surface antigens. Adv Exp Med Biol **440:**81-88.
36. **Duan X, Nauwynck HJ, Favoreel HW, Pensaert MB.** 1998. Identification of a putative receptor for porcine reproductive and respiratory syndrome virus on porcine alveolar macrophages. J Virol **72:**4520-4523.
37. **Vanderheijden N, Delputte PL, Favoreel HW, Vandekerckhove J, Van Damme J, van Woensel PA, Nauwynck HJ.** 2003. Involvement of sialoadhesin in entry of porcine reproductive and respiratory syndrome virus into porcine alveolar macrophages. J Virol **77:**8207-8215.
38. **Munday J, Floyd H, Crocker PR.** 1999. Sialic acid binding receptors (siglecs) expressed by macrophages. J Leukoc Biol **66:**705-711.
39. **Van Breedam W, Van Gorp H, Zhang JQ, Crocker PR, Delputte PL, Nauwynck HJ.** 2010. The M/GP(5) glycoprotein complex of porcine reproductive and respiratory syndrome virus binds the sialoadhesin receptor in a sialic acid-dependent manner. PLoS Pathog **6:**e1000730.
40. **Nauwynck HJ, Duan X, Favoreel HW, Van Oostveldt P, Pensaert MB.** 1999. Entry of porcine reproductive and respiratory syndrome virus into porcine alveolar macrophages via receptor-mediated endocytosis. J Gen Virol **80 (Pt 2):**297-305.
41. **Van Gorp H, Van Breedam W, Delputte PL, Nauwynck HJ.** 2008. Sialoadhesin and CD163 join forces during entry of the porcine reproductive and respiratory syndrome virus. J Gen Virol **89:**2943-2953.
42. **Snijder EJ, van Tol H, Roos N, Pedersen KW.** 2001. Non-structural proteins 2 and 3 interact to modify host cell membranes during the formation of the arterivirus replication complex. J Gen Virol **82:**985-994.
43. **Knoops K, Barcena M, Limpens RW, Koster AJ, Mommaas AM, Snijder EJ.** 2012. Ultrastructural characterization of arterivirus replication structures: reshaping the endoplasmic reticulum to accommodate viral RNA synthesis. J Virol **86:**2474-2487.
44. **Snijder EJ, Meulenberg JJ.** 1998. The molecular biology of arteriviruses. J Gen Virol **79 (Pt 5):**961-979.
45. **Pasternak AO, Gultyaev AP, Spaan WJ, Snijder EJ.** 2000. Genetic manipulation of arterivirus alternative mRNA leader-body junction sites reveals tight regulation of structural protein expression. J Virol **74:**11642-11653.
46. **Lunney JK, Fang Y, Ladinig A, Chen N, Li Y, Rowland B, Renukaradhya GJ.** 2016. Porcine Reproductive and Respiratory Syndrome Virus (PRRSV): Pathogenesis and Interaction with the Immune System. Annu Rev Anim Biosci **4:**129-154.
47. **Albina E.** 1997. Epidemiology of porcine reproductive and respiratory syndrome (PRRS): an overview. Vet Microbiol **55:**309-316.

48. **Rossow KD, Laube KL, Goyal SM, Collins JE.** 1996. Fetal microscopic lesions in porcine reproductive and respiratory syndrome virus-induced abortion. Vet Pathol **33:**95-99.
49. **Wills RW, Doster AR, Galeota JA, Sur JH, Osorio FA.** 2003. Duration of infection and proportion of pigs persistently infected with porcine reproductive and respiratory syndrome virus. J Clin Microbiol **41:**58-62.
50. **Bilodeau R, Archambault D, Vezina SA, Sauvageau R, Fournier M, Dea S.** 1994. Persistence of porcine reproductive and respiratory syndrome virus infection in a swine operation. Can J Vet Res **58:**291-298.
51. **Labarque GG, Nauwynck HJ, Van Reeth K, Pensaert MB.** 2000. Effect of cellular changes and onset of humoral immunity on the replication of porcine reproductive and respiratory syndrome virus in the lungs of pigs. J Gen Virol **81:**1327-1334.
52. **Xiao Z, Batista L, Dee S, Halbur P, Murtaugh MP.** 2004. The level of virus-specific T-cell and macrophage recruitment in porcine reproductive and respiratory syndrome virus infection in pigs is independent of virus load. J Virol **78:**5923-5933.
53. **Bursch W, Ellinger A, Gerner C, Frohwein U, Schulte-Hermann R.** 2000. Programmed cell death (PCD). Apoptosis, autophagic PCD, or others? Ann N Y Acad Sci **926:**1-12.
54. **Elmore S.** 2007. Apoptosis: a review of programmed cell death. Toxicol Pathol **35:**495-516.
55. **Glick D, Barth S, Macleod KF.** 2010. Autophagy: cellular and molecular mechanisms. J Pathol **221:**3-12.
56. **Gutierrez MG, Master SS, Singh SB, Taylor GA, Colombo MI, Deretic V.** 2004. Autophagy is a defense mechanism inhibiting BCG and Mycobacterium tuberculosis survival in infected macrophages. Cell **119:**753-766.
57. **Pujhari S, Baig TT, Zakhartchouk AN.** 2014. Potential role of porcine reproductive and respiratory syndrome virus structural protein GP2 in apoptosis inhibition. Biomed Res Int **2014:**160505.
58. **Pujhari S, Kryworuchko M, Zakhartchouk AN.** 2014. Role of phosphatidylinositol-3-kinase (PI3K) and the mammalian target of rapamycin (mTOR) signalling pathways in porcine reproductive and respiratory syndrome virus (PRRSV) replication. Virus Res **194:**138-144.
59. **Zhou A, Li S, Khan FA, Zhang S.** 2016. Autophagy postpones apoptotic cell death in PRRSV infection through Bad-Beclin1 interaction. Virulence **7:**98-109.
60. **Miller LC, Fox JM.** 2004. Apoptosis and porcine reproductive and respiratory syndrome virus. Vet Immunol Immunopathol **102:**131-142.
61. **Lee SM, Kleiboeker SB.** 2007. Porcine reproductive and respiratory syndrome virus induces apoptosis through a mitochondria-mediated pathway. Virology **365:**419-434.
62. **Choi C, Chae C.** 2002. Expression of tumour necrosis factor-alpha is associated with apoptosis in lungs of pigs experimentally infected with porcine reproductive and respiratory syndrome virus. Res Vet Sci **72:**45-49.
63. **Suarez P, Diaz-Guerra M, Prieto C, Esteban M, Castro JM, Nieto A, Ortin J.** 1996. Open reading frame 5 of porcine reproductive and respiratory syndrome virus as a cause of virus-induced apoptosis. J Virol **70:**2876-2882.
64. **Gagnon CA, Lachapelle G, Langelier Y, Massie B, Dea S.** 2003. Adenoviral-expressed GP5 of porcine respiratory and reproductive syndrome virus differs in its cellular maturation from the authentic viral protein but maintains known biological functions. Arch Virol **148:**951-972.
65. **Pujhari S, Zakhartchouk AN.** 2016. Porcine reproductive and respiratory syndrome virus envelope (E) protein interacts with mitochondrial proteins and induces apoptosis. Arch Virol **161:**1821-1830.

66. **Yuan S, Zhang N, Xu L, Zhou L, Ge X, Guo X, Yang H.** 2016. Induction of Apoptosis by the Nonstructural Protein 4 and 10 of Porcine Reproductive and Respiratory Syndrome Virus. PLoS One **11:**e0156518.
67. **Yang LW, R; Ma, Z; Wang, Y; Zhang Y.** 2015. Inducing Autophagic Cell Death by Nsp5 of Porcine Reproductive and Respiratory Syndrome Virus. Austin Virology and Retro Virology **2:**4.
68. **Chaplin DD.** 2010. Overview of the immune response. J Allergy Clin Immunol **125:**S3-23.
69. **Iwasaki A, Medzhitov R.** 2004. Toll-like receptor control of the adaptive immune responses. Nat Immunol **5:**987-995.
70. **Janeway CA, Jr., Medzhitov R.** 2002. Innate immune recognition. Annu Rev Immunol **20:**197-216.
71. **Kawai T, Akira S.** 2006. Innate immune recognition of viral infection. Nat Immunol **7:**131-137.
72. **Akira S, Takeda K, Kaisho T.** 2001. Toll-like receptors: critical proteins linking innate and acquired immunity. Nat Immunol **2:**675-680.
73. **Rock FL, Hardiman G, Timans JC, Kastelein RA, Bazan JF.** 1998. A family of human receptors structurally related to Drosophila Toll. Proc Natl Acad Sci U S A **95:**588-593.
74. **Takeuchi O, Kawai T, Sanjo H, Copeland NG, Gilbert DJ, Jenkins NA, Takeda K, Akira S.** 1999. TLR6: A novel member of an expanding toll-like receptor family. Gene **231:**59-65.
75. **Hemmi H, Takeuchi O, Kawai T, Kaisho T, Sato S, Sanjo H, Matsumoto M, Hoshino K, Wagner H, Takeda K, Akira S.** 2000. A Toll-like receptor recognizes bacterial DNA. Nature **408:**740-745.
76. **Du X, Poltorak A, Wei Y, Beutler B.** 2000. Three novel mammalian toll-like receptors: gene structure, expression, and evolution. Eur Cytokine Netw **11:**362-371.
77. **Chuang T, Ulevitch RJ.** 2001. Identification of hTLR10: a novel human Toll-like receptor preferentially expressed in immune cells. Biochim Biophys Acta **1518:**157-161.
78. **Bell JK, Askins J, Hall PR, Davies DR, Segal DM.** 2006. The dsRNA binding site of human Toll-like receptor 3. Proc Natl Acad Sci U S A **103:**8792-8797.
79. **Heil F, Hemmi H, Hochrein H, Ampenberger F, Kirschning C, Akira S, Lipford G, Wagner H, Bauer S.** 2004. Species-specific recognition of single-stranded RNA via toll-like receptor 7 and 8. Science **303:**1526-1529.
80. **Akira S, Takeda K.** 2004. Toll-like receptor signalling. Nat Rev Immunol **4:**499-511.
81. **Lawrence T.** 2009. The nuclear factor NF-kappaB pathway in inflammation. Cold Spring Harb Perspect Biol **1:**a001651.
82. **Honda K, Taniguchi T.** 2006. Toll-like receptor signaling and IRF transcription factors. IUBMB Life **58:**290-295.
83. **Honda K, Takaoka A, Taniguchi T.** 2006. Type I interferon [corrected] gene induction by the interferon regulatory factor family of transcription factors. Immunity **25:**349-360.
84. **Yoneyama M, Kikuchi M, Natsukawa T, Shinobu N, Imaizumi T, Miyagishi M, Taira K, Akira S, Fujita T.** 2004. The RNA helicase RIG-I has an essential function in double-stranded RNA-induced innate antiviral responses. Nat Immunol **5:**730-737.
85. **Yoneyama M, Kikuchi M, Matsumoto K, Imaizumi T, Miyagishi M, Taira K, Foy E, Loo YM, Gale M, Jr., Akira S, Yonehara S, Kato A, Fujita T.** 2005. Shared and unique functions of the DExD/H-box helicases RIG-I, MDA5, and LGP2 in antiviral innate immunity. J Immunol **175:**2851-2858.
86. **Reikine S, Nguyen JB, Modis Y.** 2014. Pattern Recognition and Signaling Mechanisms of RIG-I and MDA5. Front Immunol **5:**342.
87. **Kato H, Takeuchi O, Sato S, Yoneyama M, Yamamoto M, Matsui K, Uematsu S, Jung A, Kawai T, Ishii KJ, Yamaguchi O, Otsu K, Tsujimura T, Koh CS, Reis e Sousa C, Matsuura**

Y, Fujita T, Akira S. 2006. Differential roles of MDA5 and RIG-I helicases in the recognition of RNA viruses. Nature **441:**101-105.

88. **Rothenfusser S, Goutagny N, DiPerna G, Gong M, Monks BG, Schoenemeyer A, Yamamoto M, Akira S, Fitzgerald KA.** 2005. The RNA helicase Lgp2 inhibits TLR-independent sensing of viral replication by retinoic acid-inducible gene-I. J Immunol **175:**5260-5268.
89. **Jiang X, Kinch LN, Brautigam CA, Chen X, Du F, Grishin NV, Chen ZJ.** 2012. Ubiquitin-induced oligomerization of the RNA sensors RIG-I and MDA5 activates antiviral innate immune response. Immunity **36:**959-973.
90. **Kawai T, Takahashi K, Sato S, Coban C, Kumar H, Kato H, Ishii KJ, Takeuchi O, Akira S.** 2005. IPS-1, an adaptor triggering RIG-I- and Mda5-mediated type I interferon induction. Nat Immunol **6:**981-988.
91. **Saha SK, Pietras EM, He JQ, Kang JR, Liu SY, Oganesyan G, Shahangian A, Zarnegar B, Shiba TL, Wang Y, Cheng G.** 2006. Regulation of antiviral responses by a direct and specific interaction between TRAF3 and Cardif. EMBO J **25:**3257-3263.
92. **Sasai M, Shingai M, Funami K, Yoneyama M, Fujita T, Matsumoto M, Seya T.** 2006. NAK-associated protein 1 participates in both the TLR3 and the cytoplasmic pathways in type I IFN induction. J Immunol **177:**8676-8683.
93. **Schroder M, Baran M, Bowie AG.** 2008. Viral targeting of DEAD box protein 3 reveals its role in TBK1/IKKepsilon-mediated IRF activation. EMBO J **27:**2147-2157.
94. **Lad SP, Yang G, Scott DA, Chao TH, Correia Jda S, de la Torre JC, Li E.** 2008. Identification of MAVS splicing variants that interfere with RIGI/MAVS pathway signaling. Mol Immunol **45:**2277-2287.
95. **Chen G, Shaw MH, Kim YG, Nunez G.** 2009. NOD-like receptors: role in innate immunity and inflammatory disease. Annu Rev Pathol **4:**365-398.
96. **Ting JP, Lovering RC, Alnemri ES, Bertin J, Boss JM, Davis BK, Flavell RA, Girardin SE, Godzik A, Harton JA, Hoffman HM, Hugot JP, Inohara N, Mackenzie A, Maltais LJ, Nunez G, Ogura Y, Otten LA, Philpott D, Reed JC, Reith W, Schreiber S, Steimle V, Ward PA.** 2008. The NLR gene family: a standard nomenclature. Immunity **28:**285-287.
97. **Tattoli I, Carneiro LA, Jehanno M, Magalhaes JG, Shu Y, Philpott DJ, Arnoult D, Girardin SE.** 2008. NLRX1 is a mitochondrial NOD-like receptor that amplifies NF-kappaB and JNK pathways by inducing reactive oxygen species production. EMBO Rep **9:**293-300.
98. **Kanneganti TD, Body-Malapel M, Amer A, Park JH, Whitfield J, Franchi L, Taraporewala ZF, Miller D, Patton JT, Inohara N, Nunez G.** 2006. Critical role for Cryopyrin/Nalp3 in activation of caspase-1 in response to viral infection and double-stranded RNA. J Biol Chem **281:**36560-36568.
99. **Sutterwala FS, Ogura Y, Szczepanik M, Lara-Tejero M, Lichtenberger GS, Grant EP, Bertin J, Coyle AJ, Galan JE, Askenase PW, Flavell RA.** 2006. Critical role for NALP3/CIAS1/Cryopyrin in innate and adaptive immunity through its regulation of caspase-1. Immunity **24:**317-327.
100. **Muruve DA, Petrilli V, Zaiss AK, White LR, Clark SA, Ross PJ, Parks RJ, Tschopp J.** 2008. The inflammasome recognizes cytosolic microbial and host DNA and triggers an innate immune response. Nature **452:**103-107.
101. **Srinivasula SM, Poyet JL, Razmara M, Datta P, Zhang Z, Alnemri ES.** 2002. The PYRIN-CARD protein ASC is an activating adaptor for caspase-1. J Biol Chem **277:**21119-21122.
102. **Martinon F, Burns K, Tschopp J.** 2002. The inflammasome: a molecular platform triggering activation of inflammatory caspases and processing of proIL-beta. Mol Cell **10:**417-426.
103. **Vilcek J.** 2003. Novel interferons. Nat Immunol **4:**8-9.

104. **O'Brien TR, Prokunina-Olsson L, Donnelly RP.** 2014. IFN-lambda4: the paradoxical new member of the interferon lambda family. J Interferon Cytokine Res **34:**829-838.
105. **Ank N, West H, Bartholdy C, Eriksson K, Thomsen AR, Paludan SR.** 2006. Lambda interferon (IFN-lambda), a type III IFN, is induced by viruses and IFNs and displays potent antiviral activity against select virus infections in vivo. J Virol **80:**4501-4509.
106. **Zhou Z, Hamming OJ, Ank N, Paludan SR, Nielsen AL, Hartmann R.** 2007. Type III interferon (IFN) induces a type I IFN-like response in a restricted subset of cells through signaling pathways involving both the Jak-STAT pathway and the mitogen-activated protein kinases. J Virol **81:**7749-7758.
107. **Darnell JE, Jr., Kerr IM, Stark GR.** 1994. Jak-STAT pathways and transcriptional activation in response to IFNs and other extracellular signaling proteins. Science **264:**1415-1421.
108. **Ziebuhr J, Snijder EJ, Gorbalenya AE.** 2000. Virus-encoded proteinases and proteolytic processing in the Nidovirales. J Gen Virol **81:**853-879.
109. **Kroese MV, Zevenhoven-Dobbe JC, Bos-de Ruijter JN, Peeters BP, Meulenberg JJ, Cornelissen LA, Snijder EJ.** 2008. The nsp1alpha and nsp1 papain-like autoproteinases are essential for porcine reproductive and respiratory syndrome virus RNA synthesis. J Gen Virol **89:**494-499.
110. **Nedialkova DD, Gorbalenya AE, Snijder EJ.** 2010. Arterivirus Nsp1 modulates the accumulation of minus-strand templates to control the relative abundance of viral mRNAs. PLoS Pathog **6:**e1000772.
111. **Tijms MA, Nedialkova DD, Zevenhoven-Dobbe JC, Gorbalenya AE, Snijder EJ.** 2007. Arterivirus subgenomic mRNA synthesis and virion biogenesis depend on the multifunctional nsp1 autoprotease. J Virol **81:**10496-10505.
112. **Sun Y, Xue F, Guo Y, Ma M, Hao N, Zhang XC, Lou Z, Li X, Rao Z.** 2009. Crystal structure of porcine reproductive and respiratory syndrome virus leader protease Nsp1alpha. J Virol **83:**10931-10940.
113. **Tijms MA, van Dinten LC, Gorbalenya AE, Snijder EJ.** 2001. A zinc finger-containing papain-like protease couples subgenomic mRNA synthesis to genome translation in a positive-stranded RNA virus. Proc Natl Acad Sci U S A **98:**1889-1894.
114. **Shi X, Zhang X, Wang F, Wang L, Qiao S, Guo J, Luo C, Wan B, Deng R, Zhang G.** 2013. The zinc-finger domain was essential for porcine reproductive and respiratory syndrome virus nonstructural protein-1alpha to inhibit the production of interferon-beta. J Interferon Cytokine Res **33:**328-334.
115. **Kim O, Sun Y, Lai FW, Song C, Yoo D.** 2010. Modulation of type I interferon induction by porcine reproductive and respiratory syndrome virus and degradation of CREB-binding protein by non-structural protein 1 in MARC-145 and HeLa cells. Virology **402:**315-326.
116. **Han M, Du Y, Song C, Yoo D.** 2013. Degradation of CREB-binding protein and modulation of type I interferon induction by the zinc finger motif of the porcine reproductive and respiratory syndrome virus nsp1alpha subunit. Virus Res **172:**54-65.
117. **Song C, Krell P, Yoo D.** 2010. Nonstructural protein 1alpha subunit-based inhibition of NF-kappaB activation and suppression of interferon-beta production by porcine reproductive and respiratory syndrome virus. Virology **407:**268-280.
118. **Jing H, Fang L, Ding Z, Wang D, Hao W, Gao L, Ke W, Chen H, Xiao S.** 2017. Porcine Reproductive and Respiratory Syndrome Virus nsp1alpha Inhibits NF-kappaB Activation by Targeting the Linear Ubiquitin Chain Assembly Complex. J Virol **91**.
119. **Beura LK, Sarkar SN, Kwon B, Subramaniam S, Jones C, Pattnaik AK, Osorio FA.** 2010. Porcine reproductive and respiratory syndrome virus nonstructural protein 1beta modulates host innate immune response by antagonizing IRF3 activation. J Virol **84:**1574-1584.

120. **Patel D, Nan Y, Shen M, Ritthipichai K, Zhu X, Zhang YJ.** 2010. Porcine reproductive and respiratory syndrome virus inhibits type I interferon signaling by blocking STAT1/STAT2 nuclear translocation. J Virol **84:**11045-11055.
121. **Wang R, Nan Y, Yu Y, Zhang YJ.** 2013. Porcine reproductive and respiratory syndrome virus Nsp1beta inhibits interferon-activated JAK/STAT signal transduction by inducing karyopherin-alpha1 degradation. J Virol **87:**5219-5228.
122. **Han J, Liu G, Wang Y, Faaberg KS.** 2007. Identification of nonessential regions of the nsp2 replicase protein of porcine reproductive and respiratory syndrome virus strain VR-2332 for replication in cell culture. J Virol **81:**9878-9890.
123. **Snijder EJ, Wassenaar AL, Spaan WJ, Gorbalenya AE.** 1995. The arterivirus Nsp2 protease. An unusual cysteine protease with primary structure similarities to both papain-like and chymotrypsin-like proteases. J Biol Chem **270:**16671-16676.
124. **Han J, Rutherford MS, Faaberg KS.** 2009. The porcine reproductive and respiratory syndrome virus nsp2 cysteine protease domain possesses both trans- and cis-cleavage activities. J Virol **83:**9449-9463.
125. **Wassenaar AL, Spaan WJ, Gorbalenya AE, Snijder EJ.** 1997. Alternative proteolytic processing of the arterivirus replicase ORF1a polyprotein: evidence that NSP2 acts as a cofactor for the NSP4 serine protease. J Virol **71:**9313-9322.
126. **Makarova KS, Aravind L, Koonin EV.** 2000. A novel superfamily of predicted cysteine proteases from eukaryotes, viruses and Chlamydia pneumoniae. Trends Biochem Sci **25:**50-52.
127. **Frias-Staheli N, Giannakopoulos NV, Kikkert M, Taylor SL, Bridgen A, Paragas J, Richt JA, Rowland RR, Schmaljohn CS, Lenschow DJ, Snijder EJ, Garcia-Sastre A, Virgin HWt.** 2007. Ovarian tumor domain-containing viral proteases evade ubiquitin- and ISG15-dependent innate immune responses. Cell Host Microbe **2:**404-416.
128. **Akutsu M, Ye Y, Virdee S, Chin JW, Komander D.** 2011. Molecular basis for ubiquitin and ISG15 cross-reactivity in viral ovarian tumor domains. Proc Natl Acad Sci U S A **108:**2228-2233.
129. **Kappes MA, Miller CL, Faaberg KS.** 2013. Highly divergent strains of porcine reproductive and respiratory syndrome virus incorporate multiple isoforms of nonstructural protein 2 into virions. J Virol **87:**13456-13465.
130. **Chen Z, Zhou X, Lunney JK, Lawson S, Sun Z, Brown E, Christopher-Hennings J, Knudsen D, Nelson E, Fang Y.** 2010. Immunodominant epitopes in nsp2 of porcine reproductive and respiratory syndrome virus are dispensable for replication, but play an important role in modulation of the host immune response. J Gen Virol **91:**1047-1057.
131. **Clementz MA, Chen Z, Banach BS, Wang Y, Sun L, Ratia K, Baez-Santos YM, Wang J, Takayama J, Ghosh AK, Li K, Mesecar AD, Baker SC.** 2010. Deubiquitinating and interferon antagonism activities of coronavirus papain-like proteases. J Virol **84:**4619-4629.
132. **Sun Z, Li Y, Ransburgh R, Snijder EJ, Fang Y.** 2012. Nonstructural protein 2 of porcine reproductive and respiratory syndrome virus inhibits the antiviral function of interferon-stimulated gene 15. J Virol **86:**3839-3850.
133. **Sun Z, Chen Z, Lawson SR, Fang Y.** 2010. The cysteine protease domain of porcine reproductive and respiratory syndrome virus nonstructural protein 2 possesses deubiquitinating and interferon antagonism functions. J Virol **84:**7832-7846.
134. **Snijder EJ, Wassenaar AL, van Dinten LC, Spaan WJ, Gorbalenya AE.** 1996. The arterivirus nsp4 protease is the prototype of a novel group of chymotrypsin-like enzymes, the 3C-like serine proteases. J Biol Chem **271:**4864-4871.

135. **van Aken D, Snijder EJ, Gorbalenya AE.** 2006. Mutagenesis analysis of the nsp4 main proteinase reveals determinants of arterivirus replicase polyprotein autoprocessing. J Virol **80:**3428-3437.
136. **Huang C, Zhang Q, Guo XK, Yu ZB, Xu AT, Tang J, Feng WH.** 2014. Porcine reproductive and respiratory syndrome virus nonstructural protein 4 antagonizes beta interferon expression by targeting the NF-kappaB essential modulator. J Virol **88:**10934-10945.
137. **Huang C, Du Y, Yu Z, Zhang Q, Liu Y, Tang J, Shi J, Feng WH.** 2016. Highly Pathogenic Porcine Reproductive and Respiratory Syndrome Virus Nsp4 Cleaves VISA to Impair Antiviral Responses Mediated by RIG-I-like Receptors. Sci Rep **6:**28497.
138. **Chen Z, Li M, He Q, Du J, Zhou L, Ge X, Guo X, Yang H.** 2014. The amino acid at residue 155 in nonstructural protein 4 of porcine reproductive and respiratory syndrome virus contributes to its inhibitory effect for interferon-beta transcription in vitro. Virus Res **189:**226-234.
139. **Yang L, Zhang YJ.** 2017. Antagonizing cytokine-mediated JAK-STAT signaling by porcine reproductive and respiratory syndrome virus. Vet Microbiol **209:**57-65.
140. **Rascon-Castelo E, Burgara-Estrella A, Mateu E, Hernandez J.** 2015. Immunological features of the non-structural proteins of porcine reproductive and respiratory syndrome virus. Viruses **7:**873-886.
141. **Posthuma CC, Nedialkova DD, Zevenhoven-Dobbe JC, Blokhuis JH, Gorbalenya AE, Snijder EJ.** 2006. Site-directed mutagenesis of the Nidovirus replicative endoribonuclease NendoU exerts pleiotropic effects on the arterivirus life cycle. J Virol **80:**1653-1661.
142. **Nedialkova DD, Ulferts R, van den Born E, Lauber C, Gorbalenya AE, Ziebuhr J, Snijder EJ.** 2009. Biochemical characterization of arterivirus nonstructural protein 11 reveals the nidovirus-wide conservation of a replicative endoribonuclease. J Virol **83:**5671-5682.
143. **Laneve P, Altieri F, Fiori ME, Scaloni A, Bozzoni I, Caffarelli E.** 2003. Purification, cloning, and characterization of XendoU, a novel endoribonuclease involved in processing of intron-encoded small nucleolar RNAs in Xenopus laevis. J Biol Chem **278:**13026-13032.
144. **Shi Y, Li Y, Lei Y, Ye G, Shen Z, Sun L, Luo R, Wang D, Fu ZF, Xiao S, Peng G.** 2016. A Dimerization-Dependent Mechanism Drives the Endoribonuclease Function of Porcine Reproductive and Respiratory Syndrome Virus nsp11. J Virol **90:**4579-4592.
145. **Wang D, Fan J, Fang L, Luo R, Ouyang H, Ouyang C, Zhang H, Chen H, Li K, Xiao S.** 2015. The nonstructural protein 11 of porcine reproductive and respiratory syndrome virus inhibits NF-kappaB signaling by means of its deubiquitinating activity. Mol Immunol **68:**357-366.
146. **Su Y, Shi P, Zhang L, Lu D, Zhao C, Li R, Zhang L, Huang J.** 2018. The Superimposed Deubiquitination Effect of OTULIN and PRRSV Nsp11 Promoted the Multiplication of PRRSV. J Virol doi:10.1128/JVI.00175-18.
147. **Sun Y, Ke H, Han M, Chen N, Fang W, Yoo D.** 2016. Nonstructural Protein 11 of Porcine Reproductive and Respiratory Syndrome Virus Suppresses Both MAVS and RIG-I Expression as One of the Mechanisms to Antagonize Type I Interferon Production. PLoS One **11:**e0168314.
148. **Shi X, Wang L, Li X, Zhang G, Guo J, Zhao D, Chai S, Deng R.** 2011. Endoribonuclease activities of porcine reproductive and respiratory syndrome virus nsp11 was essential for nsp11 to inhibit IFN-beta induction. Mol Immunol **48:**1568-1572.
149. **Sun Y, Han M, Kim C, Calvert JG, Yoo D.** 2012. Interplay between interferon-mediated innate immunity and porcine reproductive and respiratory syndrome virus. Viruses **4:**424-446.
150. **Wang C, Shi X, Zhang X, Wang A, Wang L, Chen J, Deng R, Zhang G.** 2015. The Endoribonuclease Activity Essential for the Nonstructural Protein 11 of Porcine Reproductive and Respiratory Syndrome Virus to Inhibit NLRP3 Inflammasome-Mediated IL-1beta Induction. DNA Cell Biol **34:**728-735.

151. **Wootton SK, Yoo D.** 2003. Homo-oligomerization of the porcine reproductive and respiratory syndrome virus nucleocapsid protein and the role of disulfide linkages. J Virol **77:**4546-4557.
152. **Wootton SK, Rowland RR, Yoo D.** 2002. Phosphorylation of the porcine reproductive and respiratory syndrome virus nucleocapsid protein. J Virol **76:**10569-10576.
153. **Rowland RR, Kervin R, Kuckleburg C, Sperlich A, Benfield DA.** 1999. The localization of porcine reproductive and respiratory syndrome virus nucleocapsid protein to the nucleolus of infected cells and identification of a potential nucleolar localization signal sequence. Virus Res **64:**1-12.
154. **Hiscox JA.** 2002. The nucleolus--a gateway to viral infection? Arch Virol **147:**1077-1089.
155. **Hiscox JA.** 2003. The interaction of animal cytoplasmic RNA viruses with the nucleus to facilitate replication. Virus Res **95:**13-22.
156. **Rowland RR, Yoo D.** 2003. Nucleolar-cytoplasmic shuttling of PRRSV nucleocapsid protein: a simple case of molecular mimicry or the complex regulation by nuclear import, nucleolar localization and nuclear export signal sequences. Virus Res **95:**23-33.
157. **Sagong M, Lee C.** 2011. Porcine reproductive and respiratory syndrome virus nucleocapsid protein modulates interferon-beta production by inhibiting IRF3 activation in immortalized porcine alveolar macrophages. Arch Virol **156:**2187-2195.
158. **Wang R, Nan Y, Yu Y, Yang Z, Zhang YJ.** 2013. Variable interference with interferon signal transduction by different strains of porcine reproductive and respiratory syndrome virus. Vet Microbiol **166:**493-503.
159. **Luo R, Fang L, Jiang Y, Jin H, Wang Y, Wang D, Chen H, Xiao S.** 2011. Activation of NF-kappaB by nucleocapsid protein of the porcine reproductive and respiratory syndrome virus. Virus Genes **42:**76-81.
160. **Xiao Y, Ma Z, Wang R, Yang L, Nan Y, Zhang YJ.** 2016. Downregulation of protein kinase PKR activation by porcine reproductive and respiratory syndrome virus at its early stage infection. Vet Microbiol **187:**1-7.
161. **Wysocki M, Chen H, Steibel JP, Kuhar D, Petry D, Bates J, Johnson R, Ernst CW, Lunney JK.** 2012. Identifying putative candidate genes and pathways involved in immune responses to porcine reproductive and respiratory syndrome virus (PRRSV) infection. Anim Genet **43:**328-332.
162. **Zhang Q, Huang C, Yang Q, Gao L, Liu HC, Tang J, Feng WH.** 2016. MicroRNA-30c Modulates Type I IFN Responses To Facilitate Porcine Reproductive and Respiratory Syndrome Virus Infection by Targeting JAK1. J Immunol **196:**2272-2282.
163. **Chen J, Shi X, Zhang X, Wang A, Wang L, Yang Y, Deng R, Zhang GP.** 2017. MicroRNA 373 Facilitates the Replication of Porcine Reproductive and Respiratory Syndrome Virus by Its Negative Regulation of Type I Interferon Induction. J Virol **91**.
164. **Duan E, Wang D, Luo R, Luo J, Gao L, Chen H, Fang L, Xiao S.** 2014. Porcine reproductive and respiratory syndrome virus infection triggers HMGB1 release to promote inflammatory cytokine production. Virology **468-470:**1-9.
165. **Wang R, Yang L, Zhang Y, Li J, Xu L, Xiao Y, Zhang Q, Bai L, Zhao S, Liu E, Zhang YJ.** 2018. Porcine reproductive and respiratory syndrome virus induces HMGB1 secretion via activating PKC-delta to trigger inflammatory response. Virology **518:**172-183.
166. **Erlandsson Harris H, Andersson U.** 2004. Mini-review: The nuclear protein HMGB1 as a proinflammatory mediator. Eur J Immunol **34:**1503-1512.
167. **Forthal DN.** 2014. Functions of Antibodies. Microbiol Spectr **2:**AID-0019-2014.
168. **Pennock ND, White JT, Cross EW, Cheney EE, Tamburini BA, Kedl RM.** 2013. T cell responses: naive to memory and everything in between. Adv Physiol Educ **37:**273-283.

169. **Chowdhury D, Lieberman J.** 2008. Death by a thousand cuts: granzyme pathways of programmed cell death. Annu Rev Immunol **26:**389-420.
170. **Arce-Sillas A, Alvarez-Luquin DD, Tamaya-Dominguez B, Gomez-Fuentes S, Trejo-Garcia A, Melo-Salas M, Cardenas G, Rodriguez-Ramirez J, Adalid-Peralta L.** 2016. Regulatory T Cells: Molecular Actions on Effector Cells in Immune Regulation. J Immunol Res **2016:**1720827.
171. **Osorio FA, Galeota JA, Nelson E, Brodersen B, Doster A, Wills R, Zuckermann F, Laegreid WW.** 2002. Passive transfer of virus-specific antibodies confers protection against reproductive failure induced by a virulent strain of porcine reproductive and respiratory syndrome virus and establishes sterilizing immunity. Virology **302:**9-20.
172. **Lopez OJ, Oliveira MF, Garcia EA, Kwon BJ, Doster A, Osorio FA.** 2007. Protection against porcine reproductive and respiratory syndrome virus (PRRSV) infection through passive transfer of PRRSV-neutralizing antibodies is dose dependent. Clin Vaccine Immunol **14:**269-275.
173. **Meier WA, Galeota J, Osorio FA, Husmann RJ, Schnitzlein WM, Zuckermann FA.** 2003. Gradual development of the interferon-gamma response of swine to porcine reproductive and respiratory syndrome virus infection or vaccination. Virology **309:**18-31.
174. **Lopez OJ, Osorio FA.** 2004. Role of neutralizing antibodies in PRRSV protective immunity. Vet Immunol Immunopathol **102:**155-163.
175. **Reitter JN, Means RE, Desrosiers RC.** 1998. A role for carbohydrates in immune evasion in AIDS. Nat Med **4:**679-684.
176. **Ansari IH, Kwon B, Osorio FA, Pattnaik AK.** 2006. Influence of N-linked glycosylation of porcine reproductive and respiratory syndrome virus GP5 on virus infectivity, antigenicity, and ability to induce neutralizing antibodies. J Virol **80:**3994-4004.
177. **Liu M, Chen H, Luo F, Li P, Pan Q, Xia B, Qi Z, Ho WZ, Zhang XL.** 2007. Deletion of N-glycosylation sites of hepatitis C virus envelope protein E1 enhances specific cellular and humoral immune responses. Vaccine **25:**6572-6580.
178. **Pirzadeh B, Dea S.** 1997. Monoclonal antibodies to the ORF5 product of porcine reproductive and respiratory syndrome virus define linear neutralizing determinants. J Gen Virol **78 (Pt 8):**1867-1873.
179. **Ostrowski M, Galeota JA, Jar AM, Platt KB, Osorio FA, Lopez OJ.** 2002. Identification of neutralizing and nonneutralizing epitopes in the porcine reproductive and respiratory syndrome virus GP5 ectodomain. J Virol **76:**4241-4250.
180. **Plagemann PG, Rowland RR, Faaberg KS.** 2002. The primary neutralization epitope of porcine respiratory and reproductive syndrome virus strain VR-2332 is located in the middle of the GP5 ectodomain. Arch Virol **147:**2327-2347.
181. **Vu HL, Kwon B, Yoon KJ, Laegreid WW, Pattnaik AK, Osorio FA.** 2011. Immune evasion of porcine reproductive and respiratory syndrome virus through glycan shielding involves both glycoprotein 5 as well as glycoprotein 3. J Virol **85:**5555-5564.
182. **Costers S, Delputte PL, Nauwynck HJ.** 2006. Porcine reproductive and respiratory syndrome virus-infected alveolar macrophages contain no detectable levels of viral proteins in their plasma membrane and are protected against antibody-dependent, complement-mediated cell lysis. J Gen Virol **87:**2341-2351.
183. **Lunney JK, Ho CS, Wysocki M, Smith DM.** 2009. Molecular genetics of the swine major histocompatibility complex, the SLA complex. Dev Comp Immunol **33:**362-374.
184. **Du J, Ge X, Liu Y, Jiang P, Wang Z, Zhang R, Zhou L, Guo X, Han J, Yang H.** 2016. Targeting Swine Leukocyte Antigen Class I Molecules for Proteasomal Degradation by the nsp1alpha Replicase Protein of the Chinese Highly Pathogenic Porcine Reproductive and Respiratory Syndrome Virus Strain JXwn06. J Virol **90:**682-693.

185. **Cao QM, Subramaniam S, Ni YY, Cao D, Meng XJ.** 2016. The non-structural protein Nsp2TF of porcine reproductive and respiratory syndrome virus down-regulates the expression of Swine Leukocyte Antigen class I. Virology **491:**115-124.
186. **Wang X, Eaton M, Mayer M, Li H, He D, Nelson E, Christopher-Hennings J.** 2007. Porcine reproductive and respiratory syndrome virus productively infects monocyte-derived dendritic cells and compromises their antigen-presenting ability. Arch Virol **152:**289-303.
187. **Qi P, Liu K, Wei J, Li Y, Li B, Shao D, Wu Z, Shi Y, Tong G, Qiu Y, Ma Z.** 2017. Nonstructural Protein 4 of Porcine Reproductive and Respiratory Syndrome Virus Modulates Cell Surface Swine Leukocyte Antigen Class I Expression by Downregulating beta2-Microglobulin Transcription. J Virol **91**.
188. **Zimmerman JJ, Jacobs AC, Hermann JR, Munoz-Zanzi C, Prickett JR, Roof MB, Yoon KJ.** 2010. Stability of Porcine reproductive and respiratory syndrome virus at ambient temperatures. J Vet Diagn Invest **22:**257-260.
189. **Van Alstine WG, Kanitz CL, Stevenson GW.** 1993. Time and temperature survivability of PRRS virus in serum and tissues. J Vet Diagn Invest **5:**621-622.
190. **Charerntantanakul W.** 2012. Porcine reproductive and respiratory syndrome virus vaccines: Immunogenicity, efficacy and safety aspects. World J Virol **1:**23-30.
191. **Gonzalez-Navajas JM, Lee J, David M, Raz E.** 2012. Immunomodulatory functions of type I interferons. Nat Rev Immunol **12:**125-135.
192. **Takaoka A, Yanai H.** 2006. Interferon signalling network in innate defence. Cell Microbiol **8:**907-922.
193. **Iwasaki A, Medzhitov R.** 2015. Control of adaptive immunity by the innate immune system. Nat Immunol **16:**343-353.
194. **Stark GR, Darnell JE, Jr.** 2012. The JAK-STAT pathway at twenty. Immunity **36:**503-514.
195. **O'Shea JJ, Schwartz DM, Villarino AV, Gadina M, McInnes IB, Laurence A.** 2015. The JAK-STAT pathway: impact on human disease and therapeutic intervention. Annu Rev Med **66:**311-328.
196. **O'Shea JJ, Plenge R.** 2012. JAK and STAT signaling molecules in immunoregulation and immune-mediated disease. Immunity **36:**542-550.
197. **Kane A, Deenick EK, Ma CS, Cook MC, Uzel G, Tangye SG.** 2014. STAT3 is a central regulator of lymphocyte differentiation and function. Curr Opin Immunol **28:**49-57.
198. **Casanova JL, Holland SM, Notarangelo LD.** 2012. Inborn errors of human JAKs and STATs. Immunity **36:**515-528.
199. **Haan C, Kreis S, Margue C, Behrmann I.** 2006. Jaks and cytokine receptors--an intimate relationship. Biochem Pharmacol **72:**1538-1546.
200. **Heim MH, Kerr IM, Stark GR, Darnell JE, Jr.** 1995. Contribution of STAT SH2 groups to specific interferon signaling by the Jak-STAT pathway. Science **267:**1347-1349.
201. **Schindler C.** 1999. Cytokines and JAK-STAT signaling. Exp Cell Res **253:**7-14.
202. **Kuchipudi SV.** 2015. The Complex Role of STAT3 in Viral Infections. J Immunol Res **2015:**272359.
203. **Wack A, Terczynska-Dyla E, Hartmann R.** 2015. Guarding the frontiers: the biology of type III interferons. Nat Immunol **16:**802-809.
204. **Bluyssen HA, Levy DE.** 1997. Stat2 is a transcriptional activator that requires sequence-specific contacts provided by stat1 and p48 for stable interaction with DNA. J Biol Chem **272:**4600-4605.
205. **Fink K, Grandvaux N.** 2013. STAT2 and IRF9: Beyond ISGF3. JAKSTAT **2:**e27521.
206. **Bluyssen H.** 2015. STAT2-directed pathogen responses. Oncotarget **6:**28525-28526.

207. **Blaszczyk K, Olejnik A, Nowicka H, Ozgyin L, Chen YL, Chmielewski S, Kostyrko K, Wesoly J, Balint BL, Lee CK, Bluyssen HA.** 2015. STAT2/IRF9 directs a prolonged ISGF3-like transcriptional response and antiviral activity in the absence of STAT1. Biochem J **466:**511-524.
208. **Chen Z, Laurence A, Kanno Y, Pacher-Zavisin M, Zhu BM, Tato C, Yoshimura A, Hennighausen L, O'Shea JJ.** 2006. Selective regulatory function of Socs3 in the formation of IL-17-secreting T cells. Proc Natl Acad Sci U S A **103:**8137-8142.
209. **Villarino AV, Kanno Y, Ferdinand JR, O'Shea JJ.** 2015. Mechanisms of Jak/STAT signaling in immunity and disease. J Immunol **194:**21-27.
210. **Garbers C, Aparicio-Siegmund S, Rose-John S.** 2015. The IL-6/gp130/STAT3 signaling axis: recent advances towards specific inhibition. Curr Opin Immunol **34:**75-82.
211. **Ray JP, Marshall HD, Laidlaw BJ, Staron MM, Kaech SM, Craft J.** 2014. Transcription factor STAT3 and type I interferons are corepressive insulators for differentiation of follicular helper and T helper 1 cells. Immunity **40:**367-377.
212. **Park SJ, Nakagawa T, Kitamura H, Atsumi T, Kamon H, Sawa S, Kamimura D, Ueda N, Iwakura Y, Ishihara K, Murakami M, Hirano T.** 2004. IL-6 regulates in vivo dendritic cell differentiation through STAT3 activation. J Immunol **173:**3844-3854.
213. **Holland SM, DeLeo FR, Elloumi HZ, Hsu AP, Uzel G, Brodsky N, Freeman AF, Demidowich A, Davis J, Turner ML, Anderson VL, Darnell DN, Welch PA, Kuhns DB, Frucht DM, Malech HL, Gallin JI, Kobayashi SD, Whitney AR, Voyich JM, Musser JM, Woellner C, Schaffer AA, Puck JM, Grimbacher B.** 2007. STAT3 mutations in the hyper-IgE syndrome. N Engl J Med **357:**1608-1619.
214. **Minegishi Y, Saito M, Tsuchiya S, Tsuge I, Takada H, Hara T, Kawamura N, Ariga T, Pasic S, Stojkovic O, Metin A, Karasuyama H.** 2007. Dominant-negative mutations in the DNA-binding domain of STAT3 cause hyper-IgE syndrome. Nature **448:**1058-1062.
215. **Yu CR, Dambuza IM, Lee YJ, Frank GM, Egwuagu CE.** 2013. STAT3 regulates proliferation and survival of CD8+ T cells: enhances effector responses to HSV-1 infection, and inhibits IL-10+ regulatory CD8+ T cells in autoimmune uveitis. Mediators Inflamm **2013:**359674.
216. **Yajima T, Yasukawa H, Jeon ES, Xiong D, Dorner A, Iwatate M, Nara M, Zhou H, Summers-Torres D, Hoshijima M, Chien KR, Yoshimura A, Knowlton KU.** 2006. Innate defense mechanism against virus infection within the cardiac myocyte requiring gp130-STAT3 signaling. Circulation **114:**2364-2373.
217. **Kobayashi M, Kweon MN, Kuwata H, Schreiber RD, Kiyono H, Takeda K, Akira S.** 2003. Toll-like receptor-dependent production of IL-12p40 causes chronic enterocolitis in myeloid cell-specific Stat3-deficient mice. J Clin Invest **111:**1297-1308.
218. **Matsukawa A, Takeda K, Kudo S, Maeda T, Kagayama M, Akira S.** 2003. Aberrant inflammation and lethality to septic peritonitis in mice lacking STAT3 in macrophages and neutrophils. J Immunol **171:**6198-6205.
219. **El Kasmi KC, Holst J, Coffre M, Mielke L, de Pauw A, Lhocine N, Smith AM, Rutschman R, Kaushal D, Shen Y, Suda T, Donnelly RP, Myers MG, Jr., Alexander W, Vignali DA, Watowich SS, Ernst M, Hilton DJ, Murray PJ.** 2006. General nature of the STAT3-activated anti-inflammatory response. J Immunol **177:**7880-7888.
220. **Kuchipudi SV, Tellabati M, Sebastian S, Londt BZ, Jansen C, Vervelde L, Brookes SM, Brown IH, Dunham SP, Chang KC.** 2014. Highly pathogenic avian influenza virus infection in chickens but not ducks is associated with elevated host immune and pro-inflammatory responses. Vet Res **45:**118.

221. **Schindler C, Levy DE, Decker T.** 2007. JAK-STAT signaling: from interferons to cytokines. J Biol Chem **282:**20059-20063.
222. **Liang Y, Pan HF, Ye DQ.** 2014. Therapeutic potential of STAT4 in autoimmunity. Expert Opin Ther Targets **18:**945-960.
223. **Villarino A, Laurence A, Robinson GW, Bonelli M, Dema B, Afzali B, Shih HY, Sun HW, Brooks SR, Hennighausen L, Kanno Y, O'Shea JJ.** 2016. Signal transducer and activator of transcription 5 (STAT5) paralog dose governs T cell effector and regulatory functions. Elife **5**.
224. **Belkaid Y.** 2007. Regulatory T cells and infection: a dangerous necessity. Nat Rev Immunol **7:**875-888.
225. **Walford HH, Doherty TA.** 2013. STAT6 and lung inflammation. JAKSTAT **2:**e25301.
226. **Chen H, Sun H, You F, Sun W, Zhou X, Chen L, Yang J, Wang Y, Tang H, Guan Y, Xia W, Gu J, Ishikawa H, Gutman D, Barber G, Qin Z, Jiang Z.** 2011. Activation of STAT6 by STING is critical for antiviral innate immunity. Cell **147:**436-446.
227. **Morrison TE, Mauser A, Wong A, Ting JP, Kenney SC.** 2001. Inhibition of IFN-gamma signaling by an Epstein-Barr virus immediate-early protein. Immunity **15:**787-799.
228. **Parisien JP, Lau JF, Rodriguez JJ, Ulane CM, Horvath CM.** 2002. Selective STAT protein degradation induced by paramyxoviruses requires both STAT1 and STAT2 but is independent of alpha/beta interferon signal transduction. J Virol **76:**4190-4198.
229. **Morrison J, Laurent-Rolle M, Maestre AM, Rajsbaum R, Pisanelli G, Simon V, Mulder LC, Fernandez-Sesma A, Garcia-Sastre A.** 2013. Dengue virus co-opts UBR4 to degrade STAT2 and antagonize type I interferon signaling. PLoS Pathog **9:**e1003265.
230. **Laurent-Rolle M, Morrison J, Rajsbaum R, Macleod JML, Pisanelli G, Pham A, Ayllon J, Miorin L, Martinez C, tenOever BR, Garcia-Sastre A.** 2014. The interferon signaling antagonist function of yellow fever virus NS5 protein is activated by type I interferon. Cell Host Microbe **16:**314-327.
231. **Reid SP, Leung LW, Hartman AL, Martinez O, Shaw ML, Carbonnelle C, Volchkov VE, Nichol ST, Basler CF.** 2006. Ebola virus VP24 binds karyopherin alpha1 and blocks STAT1 nuclear accumulation. J Virol **80:**5156-5167.
232. **Reid SP, Valmas C, Martinez O, Sanchez FM, Basler CF.** 2007. Ebola virus VP24 proteins inhibit the interaction of NPI-1 subfamily karyopherin alpha proteins with activated STAT1. Journal of Virology **81:**13469-13477.
233. **Ramachandran A, Parisien JP, Horvath CM.** 2008. STAT2 is a primary target for measles virus V protein-mediated alpha/beta interferon signaling inhibition. J Virol **82:**8330-8338.
234. **Ulane CM, Rodriguez JJ, Parisien JP, Horvath CM.** 2003. STAT3 ubiquitylation and degradation by mumps virus suppress cytokine and oncogene signaling. J Virol **77:**6385-6393.
235. **Frieman M, Yount B, Heise M, Kopecky-Bromberg SA, Palese P, Baric RS.** 2007. Severe acute respiratory syndrome coronavirus ORF6 antagonizes STAT1 function by sequestering nuclear import factors on the rough endoplasmic reticulum/Golgi membrane. J Virol **81:**9812-9824.
236. **Grant A, Ponia SS, Tripathi S, Balasubramaniam V, Miorin L, Sourisseau M, Schwarz MC, Sanchez-Seco MP, Evans MJ, Best SM, Garcia-Sastre A.** 2016. Zika Virus Targets Human STAT2 to Inhibit Type I Interferon Signaling. Cell Host Microbe **19:**882-890.
237. **Stuart JH, Sumner RP, Lu Y, Snowden JS, Smith GL.** 2016. Vaccinia Virus Protein C6 Inhibits Type I IFN Signalling in the Nucleus and Binds to the Transactivation Domain of STAT2. PLoS Pathog **12:**e1005955.
238. **Ulane CM, Kentsis A, Cruz CD, Parisien JP, Schneider KL, Horvath CM.** 2005. Composition and assembly of STAT-targeting ubiquitin ligase complexes: paramyxovirus V protein carboxyl terminus is an oligomerization domain. J Virol **79:**10180-10189.

239. **Lieu KG, Brice A, Wiltzer L, Hirst B, Jans DA, Blondel D, Moseley GW.** 2013. The rabies virus interferon antagonist P protein interacts with activated STAT3 and inhibits Gp130 receptor signaling. J Virol **87:**8261-8265.
240. **Chen Z, Lawson S, Sun Z, Zhou X, Guan X, Christopher-Hennings J, Nelson EA, Fang Y.** 2010. Identification of two auto-cleavage products of nonstructural protein 1 (nsp1) in porcine reproductive and respiratory syndrome virus infected cells: nsp1 function as interferon antagonist. Virology **398:**87-97.
241. **Subramaniam S, Sur JH, Kwon B, Pattnaik AK, Osorio FA.** 2011. A virulent strain of porcine reproductive and respiratory syndrome virus does not up-regulate interleukin-10 levels in vitro or in vivo. Virus Res **155:**415-422.
242. **Cui W, Liu Y, Weinstein JS, Craft J, Kaech SM.** 2011. An interleukin-21-interleukin-10-STAT3 pathway is critical for functional maturation of memory CD8+ T cells. Immunity **35:**792-805.
243. **Siegel AM, Heimall J, Freeman AF, Hsu AP, Brittain E, Brenchley JM, Douek DC, Fahle GH, Cohen JI, Holland SM, Milner JD.** 2011. A critical role for STAT3 transcription factor signaling in the development and maintenance of human T cell memory. Immunity **35:**806-818.
244. **Avery DT, Deenick EK, Ma CS, Suryani S, Simpson N, Chew GY, Chan TD, Palendira U, Bustamante J, Boisson-Dupuis S, Choo S, Bleasel KE, Peake J, King C, French MA, Engelhard D, Al-Hajjar S, Al-Muhsen S, Magdorf K, Roesler J, Arkwright PD, Hissaria P, Riminton DS, Wong M, Brink R, Fulcher DA, Casanova JL, Cook MC, Tangye SG.** 2010. B cell-intrinsic signaling through IL-21 receptor and STAT3 is required for establishing long-lived antibody responses in humans. J Exp Med **207:**155-171.
245. **Deenick EK, Avery DT, Chan A, Berglund LJ, Ives ML, Moens L, Stoddard JL, Bustamante J, Boisson-Dupuis S, Tsumura M, Kobayashi M, Arkwright PD, Averbuch D, Engelhard D, Roesler J, Peake J, Wong M, Adelstein S, Choo S, Smart JM, French MA, Fulcher DA, Cook MC, Picard C, Durandy A, Klein C, Holland SM, Uzel G, Casanova JL, Ma CS, Tangye SG.** 2013. Naive and memory human B cells have distinct requirements for STAT3 activation to differentiate into antibody-secreting plasma cells. J Exp Med **210:**2739-2753.
246. **Montaner-Tarbes S, Borras FE, Montoya M, Fraile L, Del Portillo HA.** 2016. Serum-derived exosomes from non-viremic animals previously exposed to the porcine respiratory and reproductive virus contain antigenic viral proteins. Vet Res **47:**59.
247. **Garcia-Nicolas O, Auray G, Sautter CA, Rappe JC, McCullough KC, Ruggli N, Summerfield A.** 2016. Sensing of Porcine Reproductive and Respiratory Syndrome Virus-Infected Macrophages by Plasmacytoid Dendritic Cells. Front Microbiol **7:**771.
248. **Hu X, Chen J, Wang L, Ivashkiv LB.** 2007. Crosstalk among Jak-STAT, Toll-like receptor, and ITAM-dependent pathways in macrophage activation. J Leukoc Biol **82:**237-243.
249. **Renukaradhya GJ, Meng XJ, Calvert JG, Roof M, Lager KM.** 2015. Live porcine reproductive and respiratory syndrome virus vaccines: Current status and future direction. Vaccine **33:**4069-4080.
250. **Renukaradhya GJ, Meng XJ, Calvert JG, Roof M, Lager KM.** 2015. Inactivated and subunit vaccines against porcine reproductive and respiratory syndrome: Current status and future direction. Vaccine **33:**3065-3072.
251. **Reichelt R, Holzenburg A, Buhle EL, Jr., Jarnik M, Engel A, Aebi U.** 1990. Correlation between structure and mass distribution of the nuclear pore complex and of distinct pore complex components. J Cell Biol **110:**883-894.
252. **Greber UF, Fornerod M.** 2005. Nuclear import in viral infections. Curr Top Microbiol Immunol **285:**109-138.

253. **Pemberton LF, Paschal BM.** 2005. Mechanisms of receptor-mediated nuclear import and nuclear export. Traffic **6:**187-198.
254. **Greber UF, Fassati A.** 2003. Nuclear import of viral DNA genomes. Traffic **4:**136-143.
255. **Sloan KE, Gleizes PE, Bohnsack MT.** 2016. Nucleocytoplasmic Transport of RNAs and RNA-Protein Complexes. J Mol Biol **428:**2040-2059.
256. **Miyamoto Y, Yamada K, Yoneda Y.** 2016. Importin alpha: a key molecule in nuclear transport and non-transport functions. J Biochem **160:**69-75.
257. **Gorlich D, Henklein P, Laskey RA, Hartmann E.** 1996. A 41 amino acid motif in importin-alpha confers binding to importin-beta and hence transit into the nucleus. EMBO J **15:**1810-1817.
258. **Moroianu J, Blobel G, Radu A.** 1996. The binding site of karyopherin alpha for karyopherin beta overlaps with a nuclear localization sequence. Proc Natl Acad Sci U S A **93:**6572-6576.
259. **Goldfarb DS, Corbett AH, Mason DA, Harreman MT, Adam SA.** 2004. Importin alpha: a multipurpose nuclear-transport receptor. Trends Cell Biol **14:**505-514.
260. **O'Neill RE, Palese P.** 1995. NPI-1, the human homolog of SRP-1, interacts with influenza virus nucleoprotein. Virology **206:**116-125.
261. **Sekimoto T, Imamoto N, Nakajima K, Hirano T, Yoneda Y.** 1997. Extracellular signal-dependent nuclear import of Stat1 is mediated by nuclear pore-targeting complex formation with NPI-1, but not Rch1. EMBO J **16:**7067-7077.
262. **Fagerlund R, Melen K, Kinnunen L, Julkunen I.** 2002. Arginine/lysine-rich nuclear localization signals mediate interactions between dimeric STATs and importin alpha 5. J Biol Chem **277:**30072-30078.
263. **Kohler M, Ansieau S, Prehn S, Leutz A, Haller H, Hartmann E.** 1997. Cloning of two novel human importin-alpha subunits and analysis of the expression pattern of the importin-alpha protein family. FEBS Lett **417:**104-108.
264. **Kohler M, Speck C, Christiansen M, Bischoff FR, Prehn S, Haller H, Gorlich D, Hartmann E.** 1999. Evidence for distinct substrate specificities of importin alpha family members in nuclear protein import. Mol Cell Biol **19:**7782-7791.
265. **Ma J, Cao X.** 2006. Regulation of Stat3 nuclear import by importin alpha5 and importin alpha7 via two different functional sequence elements. Cell Signal **18:**1117-1126.
266. **Sun Z, Wu T, Zhao F, Lau A, Birch CM, Zhang DD.** 2011. KPNA6 (Importin {alpha}7)-mediated nuclear import of Keap1 represses the Nrf2-dependent antioxidant response. Mol Cell Biol **31:**1800-1811.
267. **Yano R, Oakes M, Yamaghishi M, Dodd JA, Nomura M.** 1992. Cloning and characterization of SRP1, a suppressor of temperature-sensitive RNA polymerase I mutations, in Saccharomyces cerevisiae. Mol Cell Biol **12:**5640-5651.
268. **Weis K, Mattaj IW, Lamond AI.** 1995. Identification of hSRP1 alpha as a functional receptor for nuclear localization sequences. Science **268:**1049-1053.
269. **Cuomo CA, Kirch SA, Gyuris J, Brent R, Oettinger MA.** 1994. Rch1, a protein that specifically interacts with the RAG-1 recombination-activating protein. Proc Natl Acad Sci U S A **91:**6156-6160.
270. **Cortes P, Ye ZS, Baltimore D.** 1994. RAG-1 interacts with the repeated amino acid motif of the human homologue of the yeast protein SRP1. Proc Natl Acad Sci U S A **91:**7633-7637.
271. **Kelley JB, Talley AM, Spencer A, Gioeli D, Paschal BM.** 2010. Karyopherin alpha7 (KPNA7), a divergent member of the importin alpha family of nuclear import receptors. BMC Cell Biol **11:**63.

272. **Hu J, Wang F, Yuan Y, Zhu X, Wang Y, Zhang Y, Kou Z, Wang S, Gao S.** 2010. Novel importin-alpha family member Kpna7 is required for normal fertility and fecundity in the mouse. J Biol Chem **285:**33113-33122.
273. **Laurila E, Vuorinen E, Savinainen K, Rauhala H, Kallioniemi A.** 2014. KPNA7, a nuclear transport receptor, promotes malignant properties of pancreatic cancer cells in vitro. Exp Cell Res **322:**159-167.
274. **Fagerlund R, Kinnunen L, Kohler M, Julkunen I, Melen K.** 2005. NF-{kappa}B is transported into the nucleus by importin {alpha}3 and importin {alpha}4. J Biol Chem **280:**15942-15951.
275. **Lombardo E, Ramirez JC, Garcia J, Almendral JM.** 2002. Complementary roles of multiple nuclear targeting signals in the capsid proteins of the parvovirus minute virus of mice during assembly and onset of infection. J Virol **76:**7049-7059.
276. **Vihinen-Ranta M, Wang D, Weichert WS, Parrish CR.** 2002. The VP1 N-terminal sequence of canine parvovirus affects nuclear transport of capsids and efficient cell infection. J Virol **76:**1884-1891.
277. **Ojala PM, Sodeik B, Ebersold MW, Kutay U, Helenius A.** 2000. Herpes simplex virus type 1 entry into host cells: reconstitution of capsid binding and uncoating at the nuclear pore complex in vitro. Mol Cell Biol **20:**4922-4931.
278. **Newcomb WW, Juhas RM, Thomsen DR, Homa FL, Burch AD, Weller SK, Brown JC.** 2001. The UL6 gene product forms the portal for entry of DNA into the herpes simplex virus capsid. J Virol **75:**10923-10932.
279. **Dohner K, Ramos-Nascimento A, Bialy D, Anderson F, Hickford-Martinez A, Rother F, Koithan T, Rudolph K, Buch A, Prank U, Binz A, Hugel S, Lebbink RJ, Hoeben RC, Hartmann E, Bader M, Bauerfeind R, Sodeik B.** 2018. Importin alpha1 is required for nuclear import of herpes simplex virus proteins and capsid assembly in fibroblasts and neurons. PLoS Pathog **14:**e1006823.
280. **Miller MD, Farnet CM, Bushman FD.** 1997. Human immunodeficiency virus type 1 preintegration complexes: studies of organization and composition. J Virol **71:**5382-5390.
281. **Le Rouzic E, Mousnier A, Rustum C, Stutz F, Hallberg E, Dargemont C, Benichou S.** 2002. Docking of HIV-1 Vpr to the nuclear envelope is mediated by the interaction with the nucleoporin hCG1. J Biol Chem **277:**45091-45098.
282. **Zaitseva L, Cherepanov P, Leyens L, Wilson SJ, Rasaiyaah J, Fassati A.** 2009. HIV-1 exploits importin 7 to maximize nuclear import of its DNA genome. Retrovirology **6:**11.
283. **Hutchinson EC, Fodor E.** 2013. Transport of the influenza virus genome from nucleus to nucleus. Viruses **5:**2424-2446.
284. **Resa-Infante P, Gabriel G.** 2013. The nuclear import machinery is a determinant of influenza virus host adaptation. Bioessays **35:**23-27.
285. **O'Neill RE, Jaskunas R, Blobel G, Palese P, Moroianu J.** 1995. Nuclear import of influenza virus RNA can be mediated by viral nucleoprotein and transport factors required for protein import. J Biol Chem **270:**22701-22704.
286. **Wang P, Palese P, O'Neill RE.** 1997. The NPI-1/NPI-3 (karyopherin alpha) binding site on the influenza a virus nucleoprotein NP is a nonconventional nuclear localization signal. J Virol **71:**1850-1856.
287. **Gabriel G, Herwig A, Klenk HD.** 2008. Interaction of polymerase subunit PB2 and NP with importin alpha1 is a determinant of host range of influenza A virus. PLoS Pathog **4:**e11.
288. **Gabriel G, Klingel K, Otte A, Thiele S, Hudjetz B, Arman-Kalcek G, Sauter M, Shmidt T, Rother F, Baumgarte S, Keiner B, Hartmann E, Bader M, Brownlee GG, Fodor E, Klenk**

HD. 2011. Differential use of importin-alpha isoforms governs cell tropism and host adaptation of influenza virus. Nat Commun **2:**156.
289. **Resa-Infante P, Thieme R, Ernst T, Arck PC, Ittrich H, Reimer R, Gabriel G.** 2014. Importin-alpha7 is required for enhanced influenza A virus replication in the alveolar epithelium and severe lung damage in mice. J Virol **88:**8166-8179.
290. **Tarendeau F, Boudet J, Guilligay D, Mas PJ, Bougault CM, Boulo S, Baudin F, Ruigrok RW, Daigle N, Ellenberg J, Cusack S, Simorre JP, Hart DJ.** 2007. Structure and nuclear import function of the C-terminal domain of influenza virus polymerase PB2 subunit. Nat Struct Mol Biol **14:**229-233.
291. **Wulan WN, Heydet D, Walker EJ, Gahan ME, Ghildyal R.** 2015. Nucleocytoplasmic transport of nucleocapsid proteins of enveloped RNA viruses. Front Microbiol **6:**553.
292. **Lee C, Hodgins D, Calvert JG, Welch SK, Jolie R, Yoo D.** 2006. Mutations within the nuclear localization signal of the porcine reproductive and respiratory syndrome virus nucleocapsid protein attenuate virus replication. Virology **346:**238-250.
293. **Neufeldt CJ, Joyce MA, Levin A, Steenbergen RH, Pang D, Shields J, Tyrrell DL, Wozniak RW.** 2013. Hepatitis C virus-induced cytoplasmic organelles use the nuclear transport machinery to establish an environment conducive to virus replication. PLoS Pathog **9:**e1003744.
294. **Paul D, Hoppe S, Saher G, Krijnse-Locker J, Bartenschlager R.** 2013. Morphological and biochemical characterization of the membranous hepatitis C virus replication compartment. J Virol **87:**10612-10627.
295. **Bonamassa B, Ciccarese F, Antonio VD, Contarini A, Palu G, Alvisi G.** 2015. Hepatitis C virus and host cell nuclear transport machinery: a clandestine affair. Front Microbiol **6:**619.
296. **Reid SP, Valmas C, Martinez O, Sanchez FM, Basler CF.** 2007. Ebola virus VP24 proteins inhibit the interaction of NPI-1 subfamily karyopherin alpha proteins with activated STAT1. J Virol **81:**13469-13477.
297. **Chen J, Wu M, Zhang X, Zhang W, Zhang Z, Chen L, He J, Zheng Y, Chen C, Wang F, Hu Y, Zhou X, Wang C, Xu Y, Lu M, Yuan Z.** 2013. Hepatitis B virus polymerase impairs interferon-alpha-induced STA T activation through inhibition of importin-alpha5 and protein kinase C-delta. Hepatology **57:**470-482.
298. **Gagne B, Tremblay N, Park AY, Baril M, Lamarre D.** 2017. Importin beta1 targeting by hepatitis C virus NS3/4A protein restricts IRF3 and NF-kappaB signaling of IFNB1 antiviral response. Traffic **18:**362-377.
299. **Borden EC, Sen GC, Uze G, Silverman RH, Ransohoff RM, Foster GR, Stark GR.** 2007. Interferons at age 50: past, current and future impact on biomedicine. Nat Rev Drug Discov **6:**975-990.
300. **Nan Y, Nan G, Zhang YJ.** 2014. Interferon induction by RNA viruses and antagonism by viral pathogens. Viruses **6:**4999-5027.
301. **Nan Y, Wu C, Zhang YJ.** 2017. Interplay between Janus Kinase/Signal Transducer and Activator of Transcription Signaling Activated by Type I Interferons and Viral Antagonism. Front Immunol **8:**1758.
302. **Rusinova I, Forster S, Yu S, Kannan A, Masse M, Cumming H, Chapman R, Hertzog PJ.** 2013. Interferome v2.0: an updated database of annotated interferon-regulated genes. Nucleic Acids Res **41:**D1040-1046.
303. **Adams MJ, Lefkowitz EJ, King AMQ, Harrach B, Harrison RL, Knowles NJ, Kropinski AM, Krupovic M, Kuhn JH, Mushegian AR, Nibert M, Sabanadzovic S, Sanfacon H, Siddell SG, Simmonds P, Varsani A, Zerbini FM, Gorbalenya AE, Davison AJ.** 2017. Changes to taxonomy and the International Code of Virus Classification and Nomenclature

ratified by the International Committee on Taxonomy of Viruses (2017). Arch Virol **162:**2505-2538.
304. **Mardassi H, Mounir S, Dea S.** 1995. Molecular analysis of the ORFs 3 to 7 of porcine reproductive and respiratory syndrome virus, Quebec reference strain. Arch Virol **140:**1405-1418.
305. **Rossow KD, Collins JE, Goyal SM, Nelson EA, Christopher-Hennings J, Benfield DA.** 1995. Pathogenesis of porcine reproductive and respiratory syndrome virus infection in gnotobiotic pigs. Vet Pathol **32:**361-373.
306. **Buddaert W, Van Reeth K, Pensaert M.** 1998. In vivo and in vitro interferon (IFN) studies with the porcine reproductive and respiratory syndrome virus (PRRSV). Adv Exp Med Biol **440:**461-467.
307. **Wang R, Zhang YJ.** 2014. Antagonizing interferon-mediated immune response by porcine reproductive and respiratory syndrome virus. Biomed Res Int **2014:**315470.
308. **Luo R, Xiao S, Jiang Y, Jin H, Wang D, Liu M, Chen H, Fang L.** 2008. Porcine reproductive and respiratory syndrome virus (PRRSV) suppresses interferon-beta production by interfering with the RIG-I signaling pathway. Mol Immunol **45:**2839-2846.
309. **Yang L, Wang R, Ma Z, Xiao Y, Nan Y, Wang Y, Lin S, Zhang YJ.** 2017. Porcine Reproductive and Respiratory Syndrome Virus Antagonizes JAK/STAT3 Signaling via nsp5, Which Induces STAT3 Degradation. J Virol **91**.
310. **Patel D, Opriessnig T, Stein DA, Halbur PG, Meng XJ, Iversen PL, Zhang YJ.** 2008. Peptide-conjugated morpholino oligomers inhibit porcine reproductive and respiratory syndrome virus replication. Antiviral Res **77:**95-107.
311. **Yuan S, Nelsen CJ, Murtaugh MP, Schmitt BJ, Faaberg KS.** 1999. Recombination between North American strains of porcine reproductive and respiratory syndrome virus. Virus Res **61:**87-98.
312. **Conzelmann KK, Visser N, Van Woensel P, Thiel HJ.** 1993. Molecular characterization of porcine reproductive and respiratory syndrome virus, a member of the arterivirus group. Virology **193:**329-339.
313. **Nan Y, Wang R, Shen M, Faaberg KS, Samal SK, Zhang YJ.** 2012. Induction of type I interferons by a novel porcine reproductive and respiratory syndrome virus isolate. Virology **432:**261-270.
314. **Zhang YJ, Stein DA, Fan SM, Wang KY, Kroeker AD, Meng XJ, Iversen PL, Matson DO.** 2006. Suppression of porcine reproductive and respiratory syndrome virus replication by morpholino antisense oligomers. Vet Microbiol **117:**117-129.
315. **Zhang YJ, Wang KY, Stein DA, Patel D, Watkins R, Moulton HM, Iversen PL, Matson DO.** 2007. Inhibition of replication and transcription activator and latency-associated nuclear antigen of Kaposi's sarcoma-associated herpesvirus by morpholino oligomers. Antiviral Res **73:**12-23.
316. **Guo R, Katz BB, Tomich JM, Gallagher T, Fang Y.** 2016. Porcine Reproductive and Respiratory Syndrome Virus Utilizes Nanotubes for Intercellular Spread. J Virol **90:**5163-5175.
317. **Yang L, Wang R, Yang S, Ma Z, Lin S, Nan Y, Li Q, Tang Q, Zhang YJ.** 2018. Karyopherin alpha6 Is Required for the Replication of Porcine Reproductive and Respiratory Syndrome Virus and Zika Virus. J Virol **In press**.
318. **Zhang Y, Sharma RD, Paul PS.** 1998. Monoclonal antibodies against conformationally dependent epitopes on porcine reproductive and respiratory syndrome virus. Vet Microbiol **63:**125-136.

319. **Ma Z, Yu Y, Xiao Y, Opriessnig T, Wang R, Yang L, Nan Y, Samal SK, Halbur PG, Zhang YJ.** 2016. Sustaining Interferon Induction by a High-Passage Atypical Porcine Reproductive and Respiratory Syndrome Virus Strain. Sci Rep **6:**36312.
320. **Blaszczyk K, Nowicka H, Kostyrko K, Antonczyk A, Wesoly J, Bluyssen HA.** 2016. The unique role of STAT2 in constitutive and IFN-induced transcription and antiviral responses. Cytokine Growth Factor Rev **29:**71-81.
321. **Zhang M, Li X, Deng Z, Chen Z, Liu Y, Gao Y, Wu W, Chen Z.** 2017. Structural Biology of the Arterivirus nsp11 Endoribonucleases. J Virol **91**.
322. **Ramana CV, Chatterjee-Kishore M, Nguyen H, Stark GR.** 2000. Complex roles of Stat1 in regulating gene expression. Oncogene **19:**2619-2627.
323. **Hofer MJ, Li W, Manders P, Terry R, Lim SL, King NJ, Campbell IL.** 2012. Mice deficient in STAT1 but not STAT2 or IRF9 develop a lethal CD4+ T-cell-mediated disease following infection with lymphocytic choriomeningitis virus. J Virol **86:**6932-6946.
324. **Su Y, Shi P, Zhang L, Lu D, Zhao C, Li R, Zhang L, Huang J.** 2018. The Superimposed Deubiquitination Effect of OTULIN and PRRSV Nsp11 Promoted the Multiplication of PRRSV. J Virol **In press**.
325. **Qureshi SA, Leung S, Kerr IM, Stark GR, Darnell JE, Jr.** 1996. Function of Stat2 protein in transcriptional activation by alpha interferon. Mol Cell Biol **16:**288-293.
326. **Li X, Leung S, Kerr IM, Stark GR.** 1997. Functional subdomains of STAT2 required for preassociation with the alpha interferon receptor and for signaling. Mol Cell Biol **17:**2048-2056.
327. **Martinez-Moczygemba M, Gutch MJ, French DL, Reich NC.** 1997. Distinct STAT structure promotes interaction of STAT2 with the p48 subunit of the interferon-alpha-stimulated transcription factor ISGF3. J Biol Chem **272:**20070-20076.
328. **Brierley MM, Fish EN.** 2005. Stats: multifaceted regulators of transcription. J Interferon Cytokine Res **25:**733-744.
329. **Melen K, Kinnunen L, Julkunen I.** 2001. Arginine/lysine-rich structural element is involved in interferon-induced nuclear import of STATs. J Biol Chem **276:**16447-16455.
330. **Gupta S, Yan H, Wong LH, Ralph S, Krolewski J, Schindler C.** 1996. The SH2 domains of Stat1 and Stat2 mediate multiple interactions in the transduction of IFN-alpha signals. EMBO J **15:**1075-1084.
331. **Wojciak JM, Martinez-Yamout MA, Dyson HJ, Wright PE.** 2009. Structural basis for recruitment of CBP/p300 coactivators by STAT1 and STAT2 transactivation domains. EMBO J **28:**948-958.
332. **Banninger G, Reich NC.** 2004. STAT2 nuclear trafficking. J Biol Chem **279:**39199-39206.
333. **Dong J, Xu S, Wang J, Luo R, Wang D, Xiao S, Fang L, Chen H, Jiang Y.** 2015. Porcine reproductive and respiratory syndrome virus 3C protease cleaves the mitochondrial antiviral signalling complex to antagonize IFN-beta expression. J Gen Virol **96:**3049-3058.
334. **Holtkamp DJ, Kliebenstein JB, Neumann EJ, Zimmerman J, Rotto H, Yoder TK, Wang C, Yeske P, Mowrer C, Haley C.** 2013. Assessment of the economic impact of porcine reproductive and respiratory syndrome virus on U.S. pork producers. J Swine Health Prod **21:**72-84.
335. **Faaberg KS, Balasuriya UB, Brinton MA, Gorbalenya AE, Leung FC-C, Nauwynck H, Snijder EJ, Stadejek T, Yang H, Yoo D.** 2012. Family Arteriviridae. *In* King AMQ, Adams MJ, Carstens EB, Lefkowitz EJ (ed), Virus taxonomy: classification and nomenclature of viruses: Ninth Report of the International Committee on Taxonomy of Viruses. Elsevier Academic Press, San Diego.

336. **Rossow KD, Collins JE, Goyal SM, Nelson EA, Christopher Hennings J, Benfield DA.** 1995. Pathogenesis of porcine reproductive and respiratory syndrome virus infection in gnotobiotic pigs. Vet Pathol **32:**361-373.
337. **Kim HS, Kwang J, Yoon IJ, Joo HS, Frey ML.** 1993. Enhanced replication of porcine reproductive and respiratory syndrome (PRRS) virus in a homogeneous subpopulation of MA-104 cell line. Archives of Virology **133:**477-483.
338. **Labarque GG, Nauwynck HJ, Van Reeth K, Pensaert MB.** 2000. Effect of cellular changes and onset of humoral immunity on the replication of porcine reproductive and respiratory syndrome virus in the lungs of pigs. Journal of General Virology **81:**1327-1334.
339. **Albina E, Carrat C, Charley B.** 1998. Interferon-alpha response to swine arterivirus (PoAV), the porcine reproductive and respiratory syndrome virus. J Interferon Cytokine Res **18:**485-490.
340. **Ikeda M, Mori K, Ariumi Y, Dansako H, Kato N.** 2009. Oncostatin M synergistically inhibits HCV RNA replication in combination with interferon-alpha. FEBS Lett **583:**1434-1438.
341. **Larrea E, Aldabe R, Gonzalez I, Segura V, Sarobe P, Echeverria I, Prieto J.** 2009. Oncostatin M enhances the antiviral effects of type I interferon and activates immunostimulatory functions in liver epithelial cells. J Virol **83:**3298-3311.
342. **Meng XJ, Paul PS, Halbur PG.** 1994. Molecular cloning and nucleotide sequencing of the 3'-terminal genomic RNA of the porcine reproductive and respiratory syndrome virus. Journal of General Virology **75 (Pt 7):**1795-1801.
343. **Collins JE, Benfield DA, Christianson WT, Harris L, Hennings JC, Shaw DP, Goyal SM, McCullough S, Morrison RB, Joo HS, Gorcyca D, Chladek D.** 1992. Isolation of swine infertility and respiratory syndrome virus (isolate ATCC VR-2332) in North America and experimental reproduction of the disease in gnotobiotic pigs. J Vet Diagn Invest **4:**117-126.
344. **Zhang YJ, Stein DA, Fan SM, Wang KY, Kroeker AD, Meng XJ, Iversen PL, Matson DO.** 2006. Suppression of porcine reproductive and respiratory syndrome virus replication by morpholino antisense oligomers. Vet Microbiol **117:**117-129.
345. **Petiot A, Ogier-Denis E, Blommaart EF, Meijer AJ, Codogno P.** 2000. Distinct classes of phosphatidylinositol 3'-kinases are involved in signaling pathways that control macroautophagy in HT-29 cells. J Biol Chem **275:**992-998.
346. **Nan Y, Ma Z, Wang R, Yu Y, Kannan H, Fredericksen B, Zhang YJ.** 2014. Enhancement of interferon induction by ORF3 product of hepatitis E virus. J Virol **88:**8696-8705.
347. **Timofeeva OA, Plisov S, Evseev AA, Peng S, Jose-Kampfner M, Lovvorn HN, Dome JS, Perantoni AO.** 2006. Serine-phosphorylated STAT1 is a prosurvival factor in Wilms' tumor pathogenesis. Oncogene **25:**7555-7564.
348. **Zhong Z, Wen Z, Darnell JE, Jr.** 1994. Stat3 and Stat4: members of the family of signal transducers and activators of transcription. Proc Natl Acad Sci U S A **91:**4806-4810.
349. **Horvath CM, Wen Z, Darnell JE, Jr.** 1995. A STAT protein domain that determines DNA sequence recognition suggests a novel DNA-binding domain. Genes Dev **9:**984-994.
350. **Besser D, Bromberg JF, Darnell JE, Jr., Hanafusa H.** 1999. A single amino acid substitution in the v-Eyk intracellular domain results in activation of Stat3 and enhances cellular transformation. Mol Cell Biol **19:**1401-1409.
351. **Patel D, Stein DA, Zhang YJ.** 2009. Morpholino oligomer-mediated protection of porcine pulmonary alveolar macrophages from arterivirus-induced cell death. Antivir Ther **14:**899-909.
352. **Cottam EM, Maier HJ, Manifava M, Vaux LC, Chandra-Schoenfelder P, Gerner W, Britton P, Ktistakis NT, Wileman T.** 2011. Coronavirus nsp6 proteins generate autophagosomes from the endoplasmic reticulum via an omegasome intermediate. Autophagy **7:**1335-1347.

353. **Yang L, Wang R, Ma Z, Wang Y, Zhang Y.** 2015. Inducing Autophagic Cell Death by nsp5 of Porcine Reproductive and Respiratory Syndrome Virus. Austin Virol and Retrovirology **2015:**1014.
354. **Caron JM, Jones AL, Kirschner MW.** 1985. Autoregulation of tubulin synthesis in hepatocytes and fibroblasts. J Cell Biol **101:**1763-1772.
355. **Krogh A, Larsson B, von Heijne G, Sonnhammer EL.** 2001. Predicting transmembrane protein topology with a hidden Markov model: application to complete genomes. J Mol Biol **305:**567-580.
356. **Mosser DM, Edwards JP.** 2008. Exploring the full spectrum of macrophage activation. Nat Rev Immunol **8:**958-969.
357. **Chung HK, Chae C.** 2003. Expression of interleukin-10 and interleukin-12 in piglets experimentally infected with porcine reproductive and respiratory syndrome virus (PRRSV). J Comp Pathol **129:**205-212.
358. **Suradhat S, Thanawongnuwech R.** 2003. Upregulation of interleukin-10 gene expression in the leukocytes of pigs infected with porcine reproductive and respiratory syndrome virus. J Gen Virol **84:**2755-2760.
359. **Halbur PG, Paul PS, Frey ML, Landgraf J, Eernisse K, Meng XJ, Lum MA, Andrews JJ, Rathje JA.** 1995. Comparison of the pathogenicity of two US porcine reproductive and respiratory syndrome virus isolates with that of the Lelystad virus. Vet Pathol **32:**648-660.
360. **Perry E, Tsruya R, Levitsky P, Pomp O, Taller M, Weisberg S, Parris W, Kulkarni S, Malovani H, Pawson T, Shpungin S, Nir U.** 2004. TMF/ARA160 is a BC-box-containing protein that mediates the degradation of Stat3. Oncogene **23:**8908-8919.
361. **Fried H, Kutay U.** 2003. Nucleocytoplasmic transport: taking an inventory. Cell Mol Life Sci **60:**1659-1688.
362. **Vasu SK, Forbes DJ.** 2001. Nuclear pores and nuclear assembly. Curr Opin Cell Biol **13:**363-375.
363. **Mosammaparast N, Pemberton LF.** 2004. Karyopherins: from nuclear-transport mediators to nuclear-function regulators. Trends Cell Biol **14:**547-556.
364. **Chook YM, Blobel G.** 2001. Karyopherins and nuclear import. Curr Opin Struct Biol **11:**703-715.
365. **Stewart M.** 2007. Molecular mechanism of the nuclear protein import cycle. Nat Rev Mol Cell Biol **8:**195-208.
366. **Pumroy RA, Cingolani G.** 2015. Diversification of importin-alpha isoforms in cellular trafficking and disease states. Biochem J **466:**13-28.
367. **McBride KM, Banninger G, McDonald C, Reich NC.** 2002. Regulated nuclear import of the STAT1 transcription factor by direct binding of importin-alpha. EMBO J **21:**1754-1763.
368. **Reich NC, Liu L.** 2006. Tracking STAT nuclear traffic. Nat Rev Immunol **6:**602-612.
369. **Nelson LM, Rose RC, LeRoux L, Lane C, Bruya K, Moroianu J.** 2000. Nuclear import and DNA binding of human papillomavirus type 45 L1 capsid protein. J Cell Biochem **79:**225-238.
370. **Bertram S, Thiele S, Dreier C, Resa-Infante P, Preuss A, van Riel D, Mok CK, Schwalm F, Peiris JS, Klenk HD, Gabriel G.** 2017. H7N9 Influenza A Virus Exhibits Importin-alpha7-Mediated Replication in the Mammalian Respiratory Tract. Am J Pathol **187:**831-840.
371. **Resa-Infante P, Paterson D, Bonet J, Otte A, Oliva B, Fodor E, Gabriel G.** 2015. Targeting Importin-alpha7 as a Therapeutic Approach against Pandemic Influenza Viruses. J Virol **89:**9010-9020.
372. **Faaberg KS, Balasuriya UB, Brinton MA, Gorbalenya AE, Leung FC-C, Nauwynck H, Snijder EJ, Stadejek T, Yang H, Yoo D.** 2012. Family Arteriviridae, p 796-805. *In* King AMQ, Adams MJ, Carstens EB, Lefkowitz EJ (ed), Virus taxonomy: classification and nomenclature of

viruses: Ninth Report of the International Committee on Taxonomy of Viruses. Elsevier Academic Press, San Diego.
373. **Mlakar J, Korva M, Tul N, Popovic M, Poljsak-Prijatelj M, Mraz J, Kolenc M, Resman Rus K, Vesnaver Vipotnik T, Fabjan Vodusek V, Vizjak A, Pizem J, Petrovec M, Avsic Zupanc T.** 2016. Zika Virus Associated with Microcephaly. N Engl J Med **374:**951-958.
374. **Panchaud A, Stojanov M, Ammerdorffer A, Vouga M, Baud D.** 2016. Emerging Role of Zika Virus in Adverse Fetal and Neonatal Outcomes. Clin Microbiol Rev **29:**659-694.
375. **Plourde AR, Bloch EM.** 2016. A Literature Review of Zika Virus. Emerg Infect Dis **22:**1185-1192.
376. **Lazear HM, Diamond MS.** 2016. Zika Virus: New Clinical Syndromes and Its Emergence in the Western Hemisphere. J Virol **90:**4864-4875.
377. **Meng XJ, Paul PS, Halbur PG, Lum MA.** 1996. Characterization of a high-virulence US isolate of porcine reproductive and respiratory syndrome virus in a continuous cell line, ATCC CRL11171. J Vet Diagn Invest **8:**374-381.
378. **Benfield DA, Nelson E, Collins JE, Harris L, Goyal SM, Robison D, Christianson WT, Morrison RB, Gorcyca D, Chladek D.** 1992. Characterization of swine infertility and respiratory syndrome (SIRS) virus (isolate ATCC VR-2332). Journal of Veterinary Diagnostic Investigation **4:**127-133.
379. **Lanciotti RS, Lambert AJ, Holodniy M, Saavedra S, Signor Ldel C.** 2016. Phylogeny of Zika Virus in Western Hemisphere, 2015. Emerg Infect Dis **22:**933-935.
380. **Yang L, Wang R, Ma Z, Xiao Y, Nan Y, Wang Y, Lin S, Zhang YJ.** 2017. Porcine Reproductive and Respiratory Syndrome Virus Antagonizes JAK/STAT3 Signaling via nsp5, Which Induces STAT3 Degradation. J Virol **91:**e02087-02016.
381. **Ran FA, Hsu PD, Wright J, Agarwala V, Scott DA, Zhang F.** 2013. Genome engineering using the CRISPR-Cas9 system. Nat Protoc **8:**2281-2308.
382. **Cong L, Ran FA, Cox D, Lin S, Barretto R, Habib N, Hsu PD, Wu X, Jiang W, Marraffini LA, Zhang F.** 2013. Multiplex genome engineering using CRISPR/Cas systems. Science **339:**819-823.
383. **Matsuda T, Cepko CL.** 2004. Electroporation and RNA interference in the rodent retina in vivo and in vitro. Proc Natl Acad Sci U S A **101:**16-22.
384. **Kannan H, Fan S, Patel D, Bossis I, Zhang YJ.** 2009. The hepatitis E virus open reading frame 3 product interacts with microtubules and interferes with their dynamics. J Virol **83:**6375-6382.
385. **Henchal EA, Gentry MK, McCown JM, Brandt WE.** 1982. Dengue virus-specific and flavivirus group determinants identified with monoclonal antibodies by indirect immunofluorescence. Am J Trop Med Hyg **31:**830-836.
386. **Wang R, Xiao Y, Opriessnig T, Ding Y, Yu Y, Nan Y, Ma Z, Halbur PG, Zhang YJ.** 2013. Enhancing neutralizing antibody production by an interferon-inducing porcine reproductive and respiratory syndrome virus strain. Vaccine **31:**5537-5543.
387. **Faye O, Faye O, Diallo D, Diallo M, Weidmann M, Sall AA.** 2013. Quantitative real-time PCR detection of Zika virus and evaluation with field-caught mosquitoes. Virol J **10:**311.
388. **Han M, Ke H, Zhang Q, Yoo D.** 2017. Nuclear imprisonment of host cellular mRNA by nsp1beta protein of porcine reproductive and respiratory syndrome virus. Virology **505:**42-55.
389. **Gustin KE, Sarnow P.** 2001. Effects of poliovirus infection on nucleo-cytoplasmic trafficking and nuclear pore complex composition. EMBO J **20:**240-249.
390. **Fernandez-Garcia MD, Meertens L, Bonazzi M, Cossart P, Arenzana-Seisdedos F, Amara A.** 2011. Appraising the roles of CBLL1 and the ubiquitin/proteasome system for flavivirus entry and replication. J Virol **85:**2980-2989.

391. **Chen J, Xu X, Tao H, Li Y, Nan H, Wang Y, Tian M, Chen H.** 2017. Structural Analysis of Porcine Reproductive and Respiratory Syndrome Virus Non-structural Protein 7alpha (NSP7alpha) and Identification of Its Interaction with NSP9. Front Microbiol **8:**853.
392. **Dong S, Liu L, Wu W, Armstrong SD, Xia D, Nan H, Hiscox JA, Chen H.** 2016. Determination of the interactome of non-structural protein12 from highly pathogenic porcine reproductive and respiratory syndrome virus with host cellular proteins using high throughput proteomics and identification of HSP70 as a cellular factor for virus replication. J Proteomics **146:**58-69.
393. **Yu Y, Wang R, Nan Y, Zhang L, Zhang Y.** 2013. Induction of STAT1 phosphorylation at serine 727 and expression of proinflammatory cytokines by porcine reproductive and respiratory syndrome virus. PLoS One **8:**e61967.
394. **Manns MP, Buti M, Gane E, Pawlotsky JM, Razavi H, Terrault N, Younossi Z.** 2017. Hepatitis C virus infection. Nat Rev Dis Primers **3:**17006.
395. **Duarte M, Gelfi J, Lambert P, Rasschaert D, Laude H.** 1993. Genome organization of porcine epidemic diarrhoea virus. Adv Exp Med Biol **342:**55-60.
396. **Jung K, Saif LJ.** 2015. Porcine epidemic diarrhea virus infection: Etiology, epidemiology, pathogenesis and immunoprophylaxis. Vet J **204:**134-143.
397. **Xiong A, Yang Z, Shen Y, Zhou J, Shen Q.** 2014. Transcription Factor STAT3 as a Novel Molecular Target for Cancer Prevention. Cancers (Basel) **6:**926-957.